AN ABSTRACT OF THE DISSERTATION OF

Mostafa E. Abugrain for the degree of Doctor of Philosophy in Pharmacy presented on June 8, 2015.

Title: Biosynthesis and Rational Design of Novel Pactamycin Analogs

Abstract approved:

_____

Taifo Mahmud

Pactamycin, a potent antitumor antibiotic produced by the soil bacterium *Streptomyces pactum,* is a structurally unique aminocyclopentitol-containing natural product. It consists of a highly functionalized cyclopentitol core unit, two aromatic rings [3-aminoacetophenone (3AAP) and 6-methylsalicylic acid (6MSA)], and a 1,1-dimethylurea moiety. Despite its potent biological activity, the development of this antibiotic was hampered by its high-toxicity profile. Earlier efforts to modulate its pharmacological properties by modifying the chemical structure using conventional synthetic chemistry were hampered by the complexity of the molecule, requiring alternative strategies for structure modifications, e.g., biosynthetic approaches. This dissertation describes an investigation of pactamycin biosynthesis in *S. pactum* and the development of new pactamycin analogs using biosynthetic approaches.

Earlier studies have shown that the aminocyclopentitol unit of pactamycin is derived from glucose, possibly via *N*-acetylglucosamine (GlcNAc), whereas the 3AAP unit is derived from 3-aminobenzoic acid (3ABA). Although direct involvement of glucose and 3ABA in pactamycin has previously been established, the processes underlying their conversions to the aminocyclopentitol and 3AAP moieties were unknown. Using a combination of gene inactivation, chemical complementation, and biochemical studies, we demonstrated that 3ABA is processed by a set of discrete polyketide synthase (PKS) proteins, i.e., an adenosine monophosphate-forming acyl-coenzyme A (AMP-forming acyl-CoA) synthetase (PtmS), an acyl carrier protein (ACP) (PtmI), and a β-ketoacyl-ACP synthase (PtmK), to produce 3-[3-aminophenyl]3-oxopropionyl-ACP (3AP-3OP-ACP). We also found that the hydrolase PtmO is responsible for the cleavage of a β-ketoacyl product from ACP, which then undergoes a spontaneous decarboxylation. This study also revealed that neither free 3AAP nor its glycosylated form are directly involved in pactamycin biosynthesis.

One of the most intriguing aspects of pactamycin biosynthesis is its high degree of tailoring modifications, e.g., *N*-carbamoylation, *N*-methylation, *C*-methylation, hydroxylation, an 6MSA attachment, which are all confined within the highly compacted core structure. Due to the promiscuity of some of the tailoring enzymes in the pactamycin pathway, the sequence or the timing of the tailoring processes were previously unclear. However, using a multiple gene inactivation strategy, we were able to establish the tailoring steps involved in pactamycin biosynthesis. Additionally,

we produced two novel pactamycin analogs, TM-101 and TM-102. TM-101 was generated from a triple knockout mutant of *ptmH* (a radical *S*-adenosylmethionine (SAM) *C*-methyltransferase gene), *ptmD* (*N*-methyltransferase), and *ptmQ* (a PKS), whereas TM-102 was generated from a Δ*ptmD*/*ΔptmQ d*ouble knockout mutant. The chemical structures of TM-101 and TM-102 were elucidated by MS, ^{1}H NMR, ^{13}C NMR, COSY, HMBC, and HSQC. Both compounds showed antimalarial activity but lacked significant antibacterial activity and were less toxic than pactamycin toward mammalian cells.

Previous studies have also shown that the type I iterative PKS PtmQ is a 6MSA synthase that supplies 6MSA for pactamycin biosynthesis. However, the enzyme that is responsible for the attachment of 6MSA to the aminocyclitol unit was unknown. Through genetic and biochemical characterization, we discovered that PtmR, a β-ketoacyl-acyl carrier transferase (ACP) synthase (KAS) III-like protein, is responsible for the direct transfer of the 6-methylsalicylyl moiety from PtmQ to the aminocyclopentitol unit. The enzyme also recognizes a wide array of synthetically prepared acyl-*N*-acetylcysteamines (acyl-NACs) as substrates to generate a suit of new pactamycin derivatives with diverse functionalities.

Biosynthesis and Rational Design of Novel Pactamycin Analogs

By

Mostafa Abugrain

A DISSERTATION

submitted to

Oregon State University

in partial fulfillment of
the requirements for the
degree of

Doctor of Philosophy

Presented June 8, 2015
Commencement June 2015

Doctor of Philosophy dissertation of Mostafa Abugrain presented on June 8, 2015

APPROVED:

Major Professor, representing Pharmacy

Dean of the College of Pharmacy

Dean of the Graduate School

I understand that my dissertation will become part of the permanent collection of Oregon State University libraries. My signature below authorizes release of my dissertation any reader upon request.

Mostafa E. Abugrain, Author

ACKNOWLEDGEMENTS

There are many people that have supported me during my research endeavors. First and foremost, I would like to thank my wife, Majda, for her amazing support and patience. She deserves most of the credit for this work, and without her support I could not have made it. My daughters Malak, Maysaloon, Maysam and Muntaha have shown a remarkable understanding of my long hours and my anxiety at stressful times. I would like to thank my parents for teaching me the value of hard work.

I would like to acknowledge my major advisor, Prof. Taifo Mahmud, for his guidance and support. He has encouraged me when plans fail and works tirelessly to find solutions to difficult problems. I have had the privilege to work with some great individuals in the Taifo Mahmud lab, only a few of which I can thank here. I would like to thank Dr. Wanli Lu, Dr. Niran Roongsawang, and Dr. Takuya Ito for the early studies on pactamycin. I would like to thank Eva Wan-Knight and Kwun Wah Wen for technical assistance, Michael J. Calcutt for providing the pactamycin resistance gene sequence, and Andrea deBarber for the HR-ESI-MS analysis. I would like also to thank Corey Brumsted and Andrew Osborn for their contributions to this work.

I would like to thank my committee members Dr. Barbara Taylor, Dr. Mark Zabriskie, Dr. Chrissa Kioussi, and Dr. Kerry MacPhail for their time, guidance, suggestions, and valuable insights. Finally, I would like to thank OSU Department of Pharmaceutical Sciences for the fantastic opportunity to pursue my Ph.D. I acknowledge the OSU College of Pharmacy for funding my research.

CONTRIBUTION OF AUTHORS

Dr. Taifo Mahmud designed research. Mostafa Abugrain performed research. Dr. Taifo Mahmud and Mostafa Abugrain analyzed data and wrote the manuscripts.

Chapter 2: Mostafa Abugrain performed all experiments related to *ptmS, ptmI*, *ptmO*, and *ptmK* gene inactivations as well as inactivation of these genes in the PtmH mutant and enzymatic assay of PtmS and PtmO. Corey Brumsted synthesized 3-[3-aminophenyl]3-oxopropionyl-SNAC.

Chapter 3: Mostafa Abugrain repeats the gene disruption of PtmD / PtmQ double mutant, PtmD/ptmH/ptmQ triple mutants, PtmD/PtmQ/PtmT triple mutants and PtmD/PtmH/ptmQ/PtmT mutant. PtmD/PtmH mutant was done by Wanli Lu. Mostafa Abugrain did all the work related to the isolation and purification of TM-101 and TM-102, elucidated their chemical structures, and did the antibacterial assay, as well as cloned and expressed the *ptmD* gene. Dr. Jane Ishmael did the cytotoxicity assay. Dr. Jane X. Kelly and Yuexin Li from Portland VA Medical Center did the antimalarial assay.

Chapter 4: Mostafa Abugrain performed all experiments related to *ptmR*, *ptmS, ptmI*, *ptmJ, ptmO*, and *ptmK* gene inactivations as well as inactivation of these genes in the PtmH mutant, enzymatic assay of PtmR, and identification of the role of PtmR. Corey Brumsted synthesized 6-methylsalicylic acid thioester. Andrew Osborn inactivated the *orfX2* gene.

TABLE OF CONTENTS

TABLE OF CONTENTS (Continued)

Page

TABLE OF CONTENTS (Continued)

Page

TABLE OF CONTENTS (Continued)

Page

TABLE OF CONTENTS (Continued)

Page

TABLE OF CONTENTS (Continued)

Page

LIST OF FIGURES

Figure Page

LIST OF FIGURES (Continued)

LIST OF FIGURES (Continued)

LIST OF FIGURES (Continued)

LIST OF FIGURES (Continued)

LIST OF FIGURES (Continued)

LIST OF FIGURES (Continued)

LIST OF FIGURES (Continued)

LIST OF TABLES

LIST OF ABBREVIATIONS

3AAP	3-aminoacetophenone
3ABA	3-aminobenzoic acid
3AP-3OP	3-[3-aminophenyl]3-oxopropionyl
6MSA	6-methylsalicylic acid
ACP	acyl carrier protein
AHBA	3-amino-5-hydroxybenzoic acid
AMP	adenosine monophosphate
AT	acyltransferase
CoA	coenzyme A
FA	fatty acid
FAS	fatty acid synthase
GlcN	glucosamine
GlcNAc	*N*-acetylglucosamine
IC_{50}	half maximal inhibitory concentration
IPTG	isopropyl β-D-thiogalactopyranoside
LD_{50}	median lethal dose
NAC	*N*-acetylcysteamine
NRPS	non-ribosomal peptide synthetase
ORF	open reading frame
PKS	polyketide synthase
UDP-GlcNAc	Uridine Diphosphate N-acetylglucosamine

DEDICATION

To my wife and daughters

Chapter 1 : General Introduction

Mostafa E. Abugrain

1.1 The Importance of Natural Products

Secondary metabolites such as pigments, antibiotics, and other bioactive molecules are organic compounds with diverse chemical structures and physiological functions. They are mainly produced by the secondary metabolic pathways in the producing organism and are not directly required for the growth and the survival of the organism in a given environment, differing from primary metabolites, which are essential and crucial for the organism's survival. Numerous bioactive natural products have been used as clinical therapeutic agents, such as antibiotics (e.g., erythromycin, penicillin, and tetracycline), anticancer agents (e.g., doxorubicin and taxol), antimalarial agents (e.g., artemisinin and quinine), antiparasitics (e.g., avermectin), hypolipidemic agents (e.g., lovastatin), and immunosuppressants (e.g., cyclosporine and rapamycin).

Historically, the majority of these drugs have been either directly derived from or inspired by natural products (Li and Vederas, 2009). Fourteen antiparasitic agents were developed between 1981 and 2006, of which five were natural product derivatives, four were natural product mimics, two were pure natural products, and two were derived from natural product pharmacophores. Moreover, among a hundred small-molecule anticancer drugs developed during 1981 and 2006, twenty-five were natural product derivatives, eighteen were natural product mimics, and nine were pure natural products (Newman and Cragg, 2007). Thus, bioactive natural products make a significant contribution toward drug discovery. However, recently the discovery of new bioactive natural products by the pharmaceutical industry has declined as

companies rely on the high-throughput screening of synthetic libraries instead (Li and Vederas, 2009). Comparing the chemical space occupied by combinatorial compounds to natural product and drug databases (Figure 1.1), it can be seen that natural products display a large-scale structural diversity and represent a larger chemical space than synthetic compounds, which only occupy a limited chemical space. The chemical space pattern of the natural product database and drug database display more similarities than combinatorial compounds (Ortholand and Ganesan, 2004).

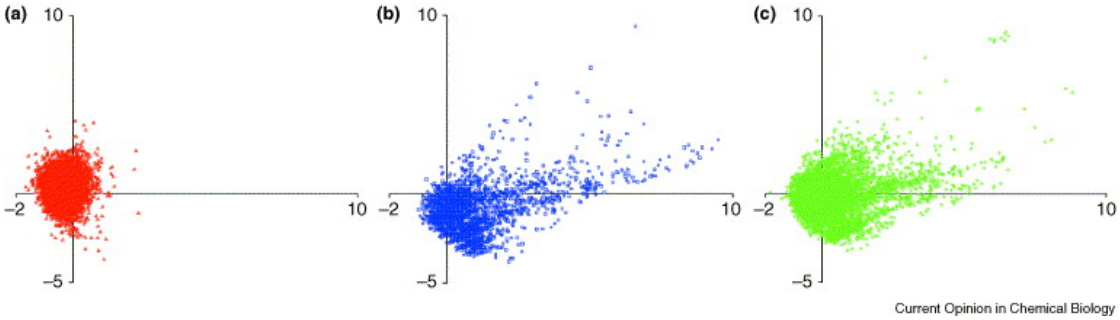

Figure 1.1 Representation of the chemical space occupied by combinatorial compounds **(a),** natural product database **(b)** and drug database **(c)**. "Reprinted from Current Opinion in Chemical Biology, 8, Ortholand J. -Y.; Ganesan A., Natural product and combinatorial chemistry: back to the future, 271-280, Copyright (2004), with permission from Elsevier."

During the last 40 years, it has become more difficult to isolate new natural products with new biological activities; therefore, the discovery rate of novel drugs has dropped considerably. The major question of interest is: Are there feasible strategies to modify the chemical potential of small-molecule natural products?

1.2 The Generation of "Nonnatural Natural" Products

Drug discovery from natural resources has largely depended on bioactivity-guided isolation methods. However, the current methodologies for identification, isolation,

and structural elucidation of bioactive natural products are highly-priced, labor-intensive, and time-consuming (Dias et al., 2012). Furthermore, the structural modifications through total synthesis or semi-synthesis of many bioactive natural products are demanding and laborious due to their structural complexity. However, new approaches have emerged during the past two decades to generate new analogs or "nonnatural" natural products through genetic manipulation. The generation of new analogs is important not only to improve the bioavailability and reduce the toxicity of certain bioactive compounds but also for use as a powerful tool to study mechanisms of action and structure-activity relationships (Goss et al., 2012). The biosynthesis of secondary metabolites is a multistep process. The genetic information needed to encode proteins for the production of bacterial secondary metabolites is typically clustered together, and, recently, many of the gene clusters responsible for the biosynthesis of secondary metabolites have been discovered.

The rapid development of DNA sequencing techniques has increased the availability of genome sequence data and accelerated functional investigations of biosynthetic pathways of secondary metabolites (Weber et al., 2015). Extensive biosynthetic studies have demonstrated that new derivatives can be generated by the selective inactivation of structural genes that are involved in downstream processes or individual domains within multi-domain modular megasynthases (Li and Vederas, 2009). The generation of new analogs can also be performed by mutational biosynthesis, also known as mutasynthesis, by inactivating the key biosynthetic

components at the gene level to generate mutant strains, which disable the production of the parent secondary metabolites, and then feeding the deficient mutant with a variety of alternative biosynthetic intermediates that act as artificial building blocks to produce novel secondary hybrids between the artificial building blocks and the original natural compounds. Mutasynthesis was first established in 1969 during the production of neomycin analogs (Shier et al., 1969). *Streptomyces fradiae*, a neomycin producer strain, was randomly mutated with nitrosoguanidine, and the mutated strain was unable to produce the natural precursor deoxystreptamine. The deoxystreptamine-deficient mutants were identified. The selected mutant colonies were complemented with deoxystreptamine in the presence of *Bacillus subtilus*. The mutant strains were able to use deoxystreptamine and rescue the production of neomycin, and, as a result, the growth of *Bacillus subtilus* was inhibited (Figure 1.2). Additionally, other related aminocyclitols such as epistreptamine and streptamine were complemented to deoxystreptamine-deficient mutants. The related aminocyclitols were incorporated and produced novel hybrimycins (Rinehart, 1977).

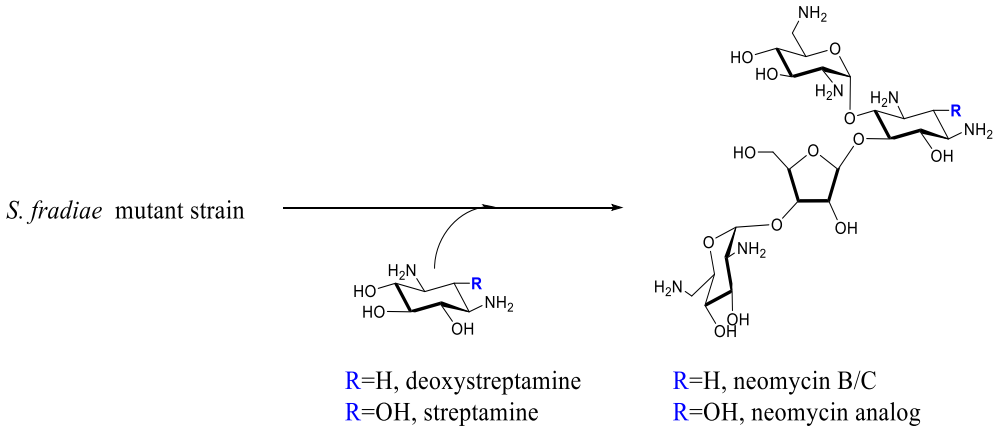

Figure 1.2 Mutational biosynthesis of new neomycin analogs using deoxystreptamine-deficient mutants.

Since then, this technique has been applied to other aminoglycoside antibiotics, such as butirosin (Takeda et al., 1978), and many other classes of natural products including aminocoumarin antibiotics (e.g., pyochelin) (Ankenbauer et al., 1991), non-ribosomal peptide synthetases (NRPSs) (Weist et al., 2002), nucleoside antibiotics (e.g., nikkomycin) (Bormann et al., 1999), and polyketide synthase (PKS) (Boddy et al., 2004; Gregory et al., 2005). Mutasynthesis is used to generate novel analogs of many bioactive natural products. Novel fluorinated pactamycin derivatives, fluorinated TM-25 and TM-26, were generated in our laboratory. We used a mutant strain of *Streptomyces pactum, ΔptmT/ΔptmH*, in which the biosynthesis of the precursor 3-aminobenzoic acid (3ABA) was blocked. The mutant was grown, and a synthetic precursor, 3-amino-5-fluorobenzoic acid, was fed to the culture. A new pactamycin analog containing a fluorinated aminoacetophenone moiety was produced (Almabruk et al., 2013) (Figure 1.3).

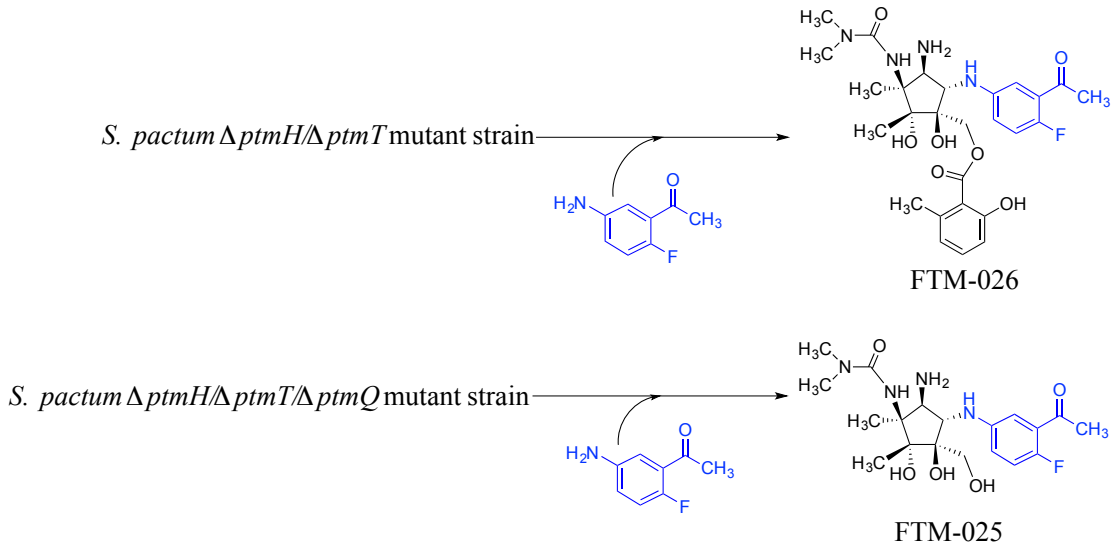

Figure 1.3 Mutational biosynthesis of new pactamycin analogs using the *ΔptmT/ΔptmH* and *ΔptmH/ΔptmT/ΔptmQ* mutant strains. The mutant strains lack the ability to synthesize 3ABA.

1.3 *Streptomyces* and Drug Discovery

Microorganisms are a prolific source of structurally-diverse bioactive metabolites and have produced some of the most essential drugs in the pharmaceutical industry. The bacterial genus *Streptomyces* is the largest genus of all actinomycetes with over 500 known species (Kampfer, 2006). *Streptomyces* are Gram-positive soil bacteria characterized by a high GC content (>55%), complex morphological development, and a high production rate of secondary metabolites that are biologically active and structurally diverse. Antibiotics are the common secondary metabolites produced by certain *Streptomyces* species. In fact, they are the source of approximately 75% of commercially and medically useful compounds, have provided more than half of the naturally occurring antibiotics discovered to date, and continue to be screened to discover useful compounds (Miyadoh, 1993). The natural products of *Streptomyces* have enormous biological activities and applications including a wide array of antibiotics (e.g., aminoglycosides, cephalosporins, macrolides, and tetracyclines) (Bérdy, 2005), anticancer drugs (e.g., aclarubicin, adriamycin, anthracyclines, daunomycin, and doxorubicin) (Olano et al., 2009), and immunosuppressive agents (e.g., rapamycin) (Gummert et al., 1999).

1.4 Classes of Natural Products

1.4.1 Introduction

Natural products can be broadly divided into different categories with distinct biosynthetic pathways: isoprenoids or terpenes, alkaloids, non-ribosomal peptides, polyketides, aminocyclopentitol-containing compounds, etc.

1.4.2 Isoprenoids

Isoprenoids or terpenoids are one of the oldest and largest families of natural products with approximately 25,000 structures reported in the literature (Sacchettini and Poulter, 1997). The basic building block of all isoprenoids is isoprene unit (C_5) hydrocarbon. These units are assembled and modified to form the basic skeleton. Terpenoids can be classified according to the number of isoprene units in the molecule such as monoterpenes (2 isoprene units or C_{10}), sesquiterpenes (3 isoprene units or C_{15}), diterpenenes (4 isoprene units or C_{20}), and triterpenes (6 isoprene units or C_{30}). There are two known pathways for the biosynthesis of terpenoids. The first one is the mevalonate pathway (MVA), which is common in animals, bacteria, fungi, and plants. The second one is the non-mevalonate or methylerythritol phosphate pathway (MEP), a more recently discovered pathway in apicomplexan parasites, plants, and many species of bacteria (Hunter, 2001).

1.4.3 Alkaloids

Alkaloids are a highly diverse group of natural products containing basic nitrogen in their structures, derived mostly from amino acids, and found in approximately 20% of plant species (Ziegler and Facchini, 2008). Traditionally, plants are the main source of alkaloids; however, a tremendous number of valuable alkaloids have been isolated from insects, other invertebrates, marine organisms, and microorganisms (Roberts and Wink, 1998). Alkaloids have wide range of medical applications such as antiarrhythmics (e.g., quinidine), anticancer agents (e.g., camptothecin, taxol, and vincablastin), antihypertensive agents (e.g., reserpine), antimalarial agents (e.g.,

quinine), cough-suppressants (e.g., noscapine), local anaesthetic agents (e.g. cocaine), and strong analgesics (e.g., morphine) (Figure 1.4). Alkaloids can be classified chemically as diterpenoid alkaloids, indole alkaloids, isoprenoid alkaloids, phenylalkylamine alkaloids, piperidines alkaloids, purine alkaloids, pyridines alkaloids, pyrrolidine alkaloids, and tropane alkaloids.

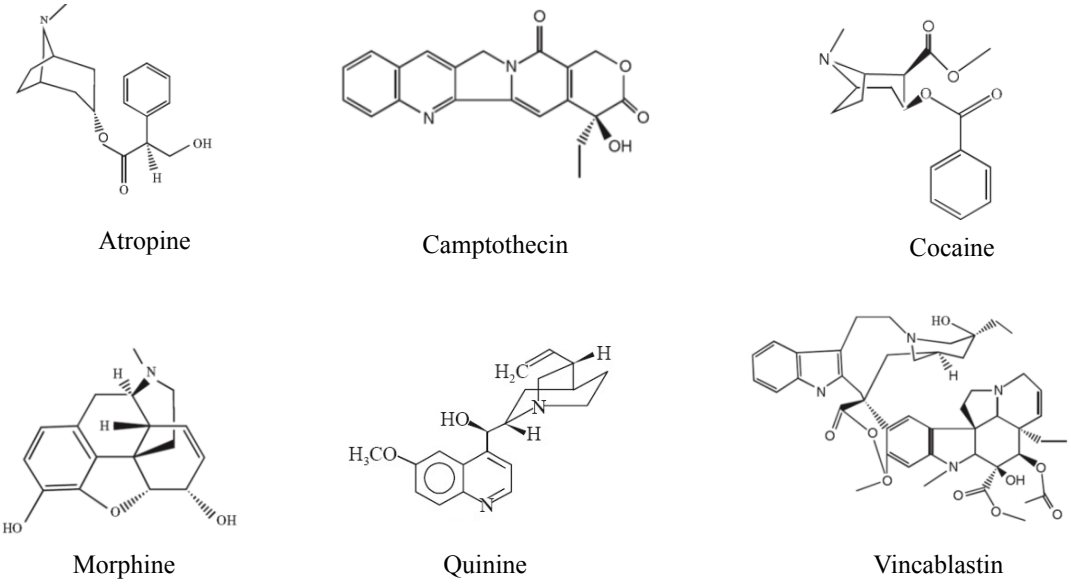

Figure 1.4 Examples of important alkaloid natural products.

1.4.4 Non-Ribosomal Peptides

Many bacteria and fungi produce peptides with broad structural and biological activities, (Figure 1.5), and are derived from both proteinogenic and non-proteinogenic amino acids by multi-domain multimodular enzymes called non-ribosomal peptide synthetases (NRPSs). The fungal NRPS penicillin has saved innumerable lives and has been used intensively to treat bacterial infection. The relatively recently-approved

antibiotic daptomycin represents the first antibiotic in a new structural class of non-ribosomal lipopeptides (Raja et al., 2003).

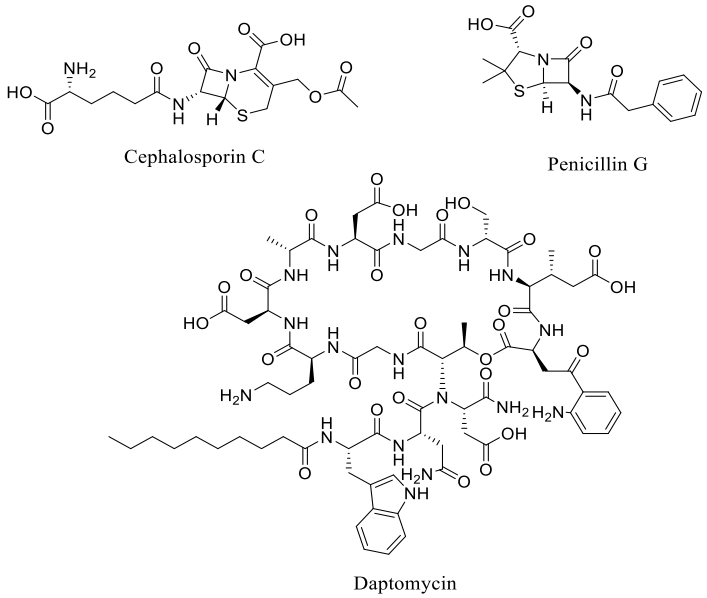

Figure 1.5 Clinically important NRPS-derived natural products.

1.4.5 Polyketides

Polyketides are a diverse group of secondary metabolites with around 10,000 known structures. Polyketides are produced by both prokaryotic bacteria and eukaryotic fungi and plants. Although polyketides have a simple biosynthetic pathway from simple acetate units, they can form complex natural products with a wide range of functional and structural diversity. More importantly, they boast a wealth of biological activities, which can be used either directly as clinical drugs or indirectly as an inspiration for the development of more potent compounds. The remarkable, medicinally-important polyketides include antibacterials (e.g., erythromycin) (Staunton, 1997), anticancer agents (e.g., doxorubicin) (Singh, 2010), antifungal drugs (e.g., strobilurin B)

(Coleman, 2006), and hypolipidemic agents (e.g., lovastatin) (Manzoni, 2002) (Figure 1.6).

Similar to fatty acid synthases (FASs), PKSs catalyze the condensation of activated acetyl-coenzyme A (acetyl-CoA) and malonyl-CoA to form β-ketoacetyl polymers linked to the enzyme by thioester bonds (Fujii et al., 2001). PKSs can be classified into different types based on their number of subunits (a singular or multiple) and their mode of synthesis (linear or iterative). Type I PKSs are large enzymes comprised of multiple functional domains, and each enzyme catalyzes a distinct reaction in the process of polyketide assembly. Type I PKSs are further classified as modular or iterative. Type II PKSs are a complex set of monodomain proteins with separate enzymatic activities, and all known examples are classified as iterative. Type III PKSs are characterized by a single active site where they catalyze polyketide chain extension and cyclization without the use of an acyl carrier protein (ACP) domain. Type III PKSs have been extensively studied, especially in plants, but have also been found in bacteria and fungi (Moore and Hopke, 2001; Austin and Noel 2003; Saxena et al., 2003; Seshime et al., 2005).

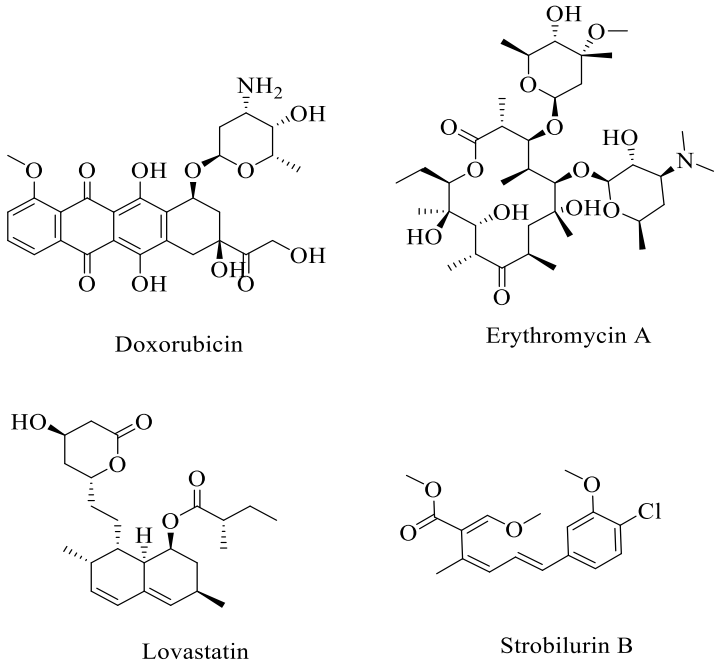

Figure 1.6 Examples of medicinally important polyketides.

1.4.6 Aminocyclopentitol Natural Products

Aminocyclopentitol-containing natural products represent a family of sugar-derived microbial secondary metabolites (Figure 1.7) (Flatt and Mahmud, 2007). Their biological activities and unique structures have been attractive objects of investigation, even though they are rare in nature. There are a number of bioactive natural products containing aminocyclopentitol sub-structures such as adecypenol, allosamidin, epoxyqueusin, mannostatin A, neplanocin A, pactamycin, queuosine, trehazolin, and the carbocyclic nucleosides-aristeromycin. The aminocyclopentitol neuraminidase inhibitor BCX-1812 is in clinical development to treat influenza and is inspired by aminocyclopentitol-containing natural product.

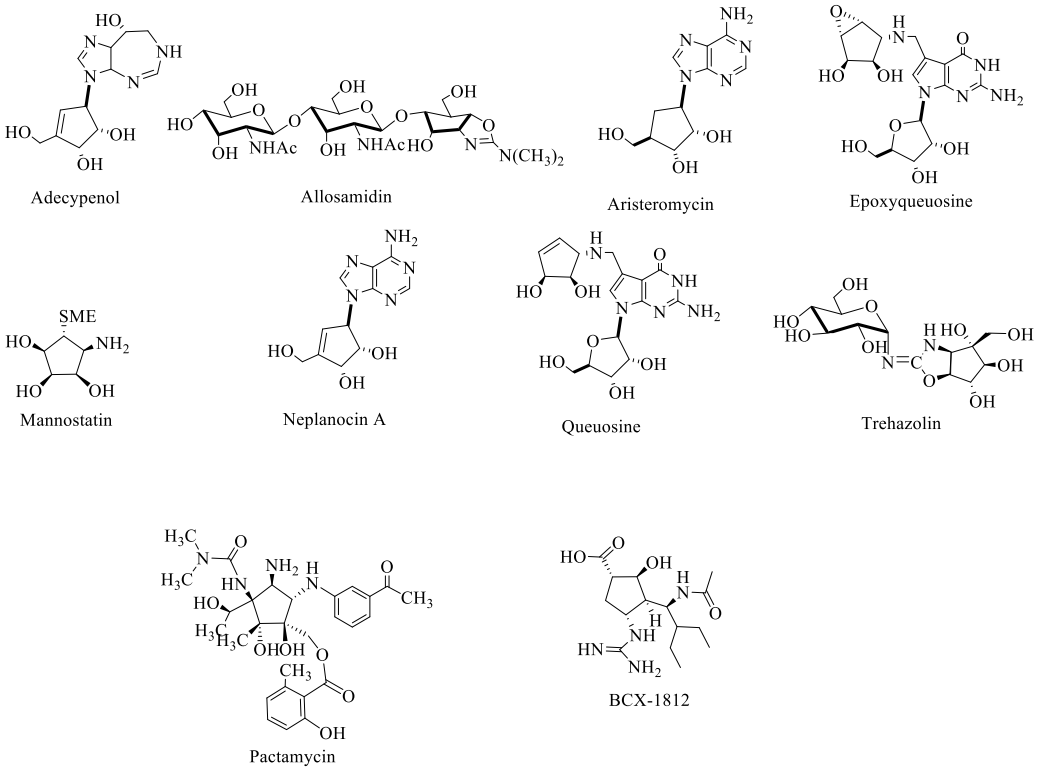

Figure 1.7 Examples of bioactive natural products containing aminocyclopentitol sub-structures.

1.5 Pactamycin

1.5.1 The History and Significance of Pactamycin

Pactamycin is a promising bioactive natural product belonging to the aminocyclopentitol family of natural products. Pactamycin is a structurally-unique, microbial-derived antitumor antibiotic isolated by scientists at the former Upjohn Company in 1961 (Bhuyan, 1962; Bhuyan et al., 1961) from a culture broth of the soil bacterium *Streptomyces pactum* var. *pactum*. A number of structurally related pactamycin derivatives have been isolated from *S. pactum* and other *Streptomyces*

species (Figure 1.8). In 1964, 7-deoxypactamycin (cranomycin), a pactamycin analog, was isolated from *Streptomyces* SE-801 by scientists at the Meiji Seika Kaisha Company (Hara et al., 1964; Kondo et al., 1964). In 1970, pactamycate, a cyclic derivative of pactamycin, was first isolated by Upjohn scientists (Wiley et al., 1970). In 1980, other pactamycin analogs including 7-deoxypactalactam, 7-deoxypactamycin, 8″-hydroxypactamycin, 8″-hydroxy-7-deoxypactamycin, 8″-hydroxypactamycate, and pactalactam were isolated from *S. pactum* (Rinehart et al., 1980). In 1986, two independent studies reported that 7-deoxypactamycin and 8″-hydroxypactamycin were both re-isolated from *Streptomyces* sp. (SIPI-A3-0121) and *Streptomyces* sp. (WP-4371) (Dobashi et al., 1986; Hurley et al., 1986). Recently, a new pactamycin, de-6MSA-7-deoxypactamycin (jogyamycin), was isolated from the culture of *Streptomyces* sp. (WM-JG-16.2) (Iwatsuki et al., 2012). Pactamycin consists of a five-member ring aminocyclitol unit that is rich in stereogenic centers, two aromatic rings (6-methylsalicylic acid (6MSA) and 3-aminoacetophenone (3AAP)), and a 1,1-dimethylurea moiety (Rinehart et al., 1980; Weller et al., 1978). Pactamycin is one the most densely functionalized naturally occurring aminocyclopentitols.

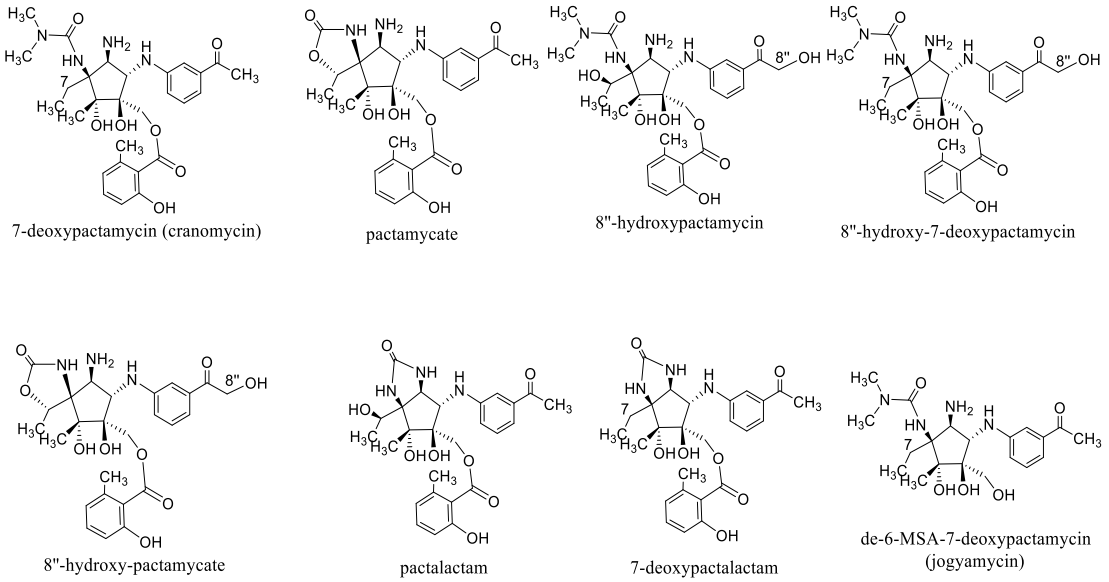

Figure 1.8 Chemical structures of pactamycin analogs.

1.5.2 Biological Significance

Pactamycin is a densely functionalized structure and exhibits potent antimicrobial, antiprotozoal, antitumor, and antiviral activities (Bhuyan, 1962; Otoguro et al., 2010; Taber et al., 1971; White, 1962). Pactamycin affects cell growth in all three phylogenetic kingdoms: eukarya, bacteria, and archaea. Pactamycin also has broad-spectrum antibacterial activities against both Gram-positive and Gram-negative bacteria as well as antifungal activities (Bhuyan et al., 1961). The antimicrobial activities of pactamycin, 7-deoxypactamycin, and 8″-hydroxypactamycin were measured using the agar diffusion method. Pactamycin and the other two pactamycin analogs are equally active against a number of Gram-positive and Gram-negative bacteria as shown in Table 1.1 (Bhuyan et al., 1961; Dobashi et al., 1986; Kondo et al., 1964). However, no antimicrobial activities have been reported with pactamycate or pactalactam-related compounds (Rinehart et al., 1980).

Table 1.1 Antimicrobial spectra of pactamycin, 7-deoxypactamycin and 8"-hydroxypactamycin (MIC in μg/mL).

Test organism	Gram	Pactamycin	7-deoxy-pactamycin	8"-Hydroxy-pactamycin	Ref.
Bacillus subtilis UC-28	+	0.8			(Bhuyan et al., 1961)
Staphylococcus aureus OSU-284	+	0.2			
S.aureus ATCC 151	+	0.05			
Streptococcus pyogenes C 203	+	1.6			
Streptococcus faecalis ATCC 6057	+	1.6			
Viridans group UC 155	+	3.2			
Escherichia coli ATCC 26	-	6.5			
Klebsiella pneumoniae U of Calif. A-D	-	0.8			
Pasteurella multocida Lederle P-449	-	0.012			
Proteus vulgaris ATCC 6380	-	110			
Salmonella typhosa MSDH TG 3	-	55			
Salmonella pullorum 75	-	1.6			
Pseudomonas aeruginosa ATCC 9027	-	110			
B. subtilis ATCC 6633	+		<0.06		(Kondo et al., 1964)
B. subtilis NRRL B558	+		<0.06		
Bacillus cereus	+		>4.0		
S. aureus 209P	+		0.25		
S. aureus resistant to erythromycin	+		0.5		
Sarcina lutea	+		<0.06		
Mycobacterium 607	+		4		
Mycobacterium phlei	+		4		
Klebsiella pneumonia	-		>40		
Salmonella typhosa	-		>40		
Salmonella paratyphi A	-		>40		
Salmonella paratyphi B	-		>40		
Shigella dysenteriae	-		>40		
E. coli	-		>40		
Xanthomonas oryzae	-		0.01		
Xanthomonas pruni	-		0.16		
Xanthomonas citri	-		0.08		
Erwinia aroideae	-		5		
S. aureus FDA 209P	+	0.1	0.2	0.2	(Dobashi

					et al., 1986)
S. aureus Smith	+	0.39	0.39	0.39	
Micrococcus luteus PCI 1001	+	0.1	0.025	0.1	
Bacillus anthracis	+	50	25	50	
B. subtilis PCI 219	+	0.39	0.1	0.2	
B. subtilis NRRL B-558	+	0.1	0.1	0.2	
E. coli NIHJ	-	1.56	1.56	1.56	
E. coli K-12	-	25	25	12.5	
E. coli K-12 ML 1629	-	25	25	12.5	
Shigella dysenteriae JS 11910	-	1.56	0.78	1.56	
Shigella flexneri 4b JS 11811	-	6.25	12.5	6.25	
Shigella sonnei JS 11746	-	12.5	12.5	6.25	
Salmonella typhi T-63	-	50	50	12.5	
Salmonella enteritidis 1891	-	3.12	1.56	1.56	
Proteus vulgaris OX 19	-	12.5	12.5	6.25	
Serratia marcescens	-	25	50	25	

In addition to antimicrobial activities, pactamycin showed strong anticancer activity *in vitro* against several cell lines. The half maximal inhibitory concentration (IC_{50}) against KB human epidermoid carcinoma cells was 0.003 μg/mL (Bhuyan, 1962). The IC_{50} values of 8"-hydroxypactamycin and 7-deoxypactamycin against L1210 mouse lymphocytic leukemia cells were 0.027 μg/mL and 0.026 μg/mL, respectively (Dobashi et al., 1986). *In vivo* experiments in mice and hamsters demonstrated that pactamycin was active against multiple tumors. As shown in Table 1.2, pactamycin can either inhibit the growth of the solid tumors or increase the survival time of leukemic animals at doses ranging from 0.5 to 2 mg/kg (Bhuyan, 1962; Bhuyan et al., 1961).

Table 1.2 The antitumor activities of pactamycin.

Tumor	Organic Tissue	Dose (mg/kg)	Inhibition (%)	Toxicity
Ehrlich carcinoma	Breast	1	39	±
Glioma-26	neuroectodermal	1	35	±
Ca-755	Breast	2	30	±
Iglesias adrenal tumor	adrenal	1	47	±
Crabb hamster sarcoma	connective tissue	0.5	39	±
Forner adenocarcinoma of small bowel	small-bowel	1	25	+
Rous sarcoma	connective tissue	0.5	30	+
L-1210 G	Blood	2	40*	?
Human melanoma (ME-1) in hamsters	Skin	1.5	58	-
Human choriocarcinoma in hamsters	Uterus	0.75	90	-

*Increase in survival time.

In 2010, Omura and co-workers demonstrated the activity of certain compounds, isolated from soil bacteria as well as coming from the antibiotic libraries of the Kitasato Institute, against protozoan pathogens (trypanosoma and malaria strains K1 and FCR3) (Otoguro et al., 2010). The researchers found that 7-deoxypactamycin showed the highest activity against both drug-resistant K1 and drug-susceptible FCR3 strains of *Plasmodium falciparum.* The IC_{50} value was 0.4 nM against both strains, which was almost 30-fold greater than that shown by artemisinin. The selectivity index of 7-deoxypactamycin was 70, showing that it is a promising compound that needs further investigation. The IC_{50} values of pactamycin were 14.2 nM and 16.8 nM against the *P. falciparum* K1 and FCR3 strains, respectively, which were still comparable with those of artemisinin (Otoguro et al., 2010). The newly isolated de-6MSA-7-deoxypactamycin (jogyamycin) also showed potent antimalarial activity,

with an IC_{50} value of 1.5 nM against *P. falciparum* K1, which was 13.5-fold stronger than artemisinin (Iwatsuki et al., 2012).

1.5.3 Pactamycin Toxicities

Pactamycin and its analogs have demonstrated strong antitumor activities. However, the high toxicity levels of these compounds have restricted their further development as chemotherapeutic agents. *In vitro* cytotoxicity assessment against the human diploid embryonic cell line MRC-5 of de-6MSA-7-deoxypactamycin, 7-deoxypactamycin, and pactamycin revealed IC_{50} values of 5.6, 29.5, and 95 nM, respectively, indicating that de-6MSA-7-deoxypactamycin had the highest cytotoxicity (Iwatsuki et al., 2012). An *in vivo* pactamycin toxicity assessment was performed in dogs, rats, and mice with intravenous median lethal dose (LD_{50}) values of 0.75, 1.4, and 15.6 mg/kg, respectively. The oral LD_{50} in mice was 10.7 mg/kg. The results indicated that dogs were the most sensitive, followed by rats and mice (Bhuyan et al., 1961). 7-Deoxypactamycin resulted in higher *in vivo* toxicity than other analogs. The intraperitoneal, intravenous, and oral LD_{50} in mice were 0.76, 0.84, and 8.6 mg/kg, respectively. The percutaneous LD_{50} in pigs was less than 10 mg/kg (Kondo et al., 1964). An additional mouse study revealed that the intraperitoneal LD_{100} values of 8"-hydroxypactamycin and 7-deoxypactamycin were 25 mg/kg and 1.57 mg/kg, respectively (Dobashi et al., 1986).

1.5.4 Mechanism of Action

Protein synthesis can be divided into four main steps: peptide initiation, elongation, termination, and recycling (Wilson, 2014). Ribosomes are the protein-synthesizing

factories and are one of the main antibiotic targets in a bacterial cell. Several antibiotics (e.g., streptomycins and tetracyclines) target and inhibit translational elongation processes by interfering with either the delivery of tRNAs to the ribosomal A-site or the subsequent translocation of the mRNA–tRNA. A minority of antibiotics, such as edeine, kasugamycin, and pactamycin, bind to the 30S subunit and inhibit translational initiation by preventing a stable interaction between the initiator tRNA and the start codon at the ribosomal P-site (Cohen et al., 1969; Wilson, 2014) (Figure 1.9). Pactamycin binds to both the 30S ribosomal subunit of bacteria and the 40S ribosomal subunit of eukaryotic cells (Wettenhall and Wool, 1974).

The activity of pactamycin as a potent inhibitor of translation in all three domains of life (eukarya, bacteria, and archaea) has been reported. This finding suggests that the inhibition mechanism of pactamycin is identical across the three phylogenetic kingdoms (Vazquez, 1979). Woodcock and co-workers have studied the interaction of several antibiotics including pactamycin with 16S rRNA by chemical probing of drug-ribosome complexes. They showed that pactamycin protects two universally conserved bases (G693 and C795) in 16S rRNA from chemical modification, which are the same bases that are typically shown to be protected by P-site-bound tRNA (Woodcock et al., 1991).

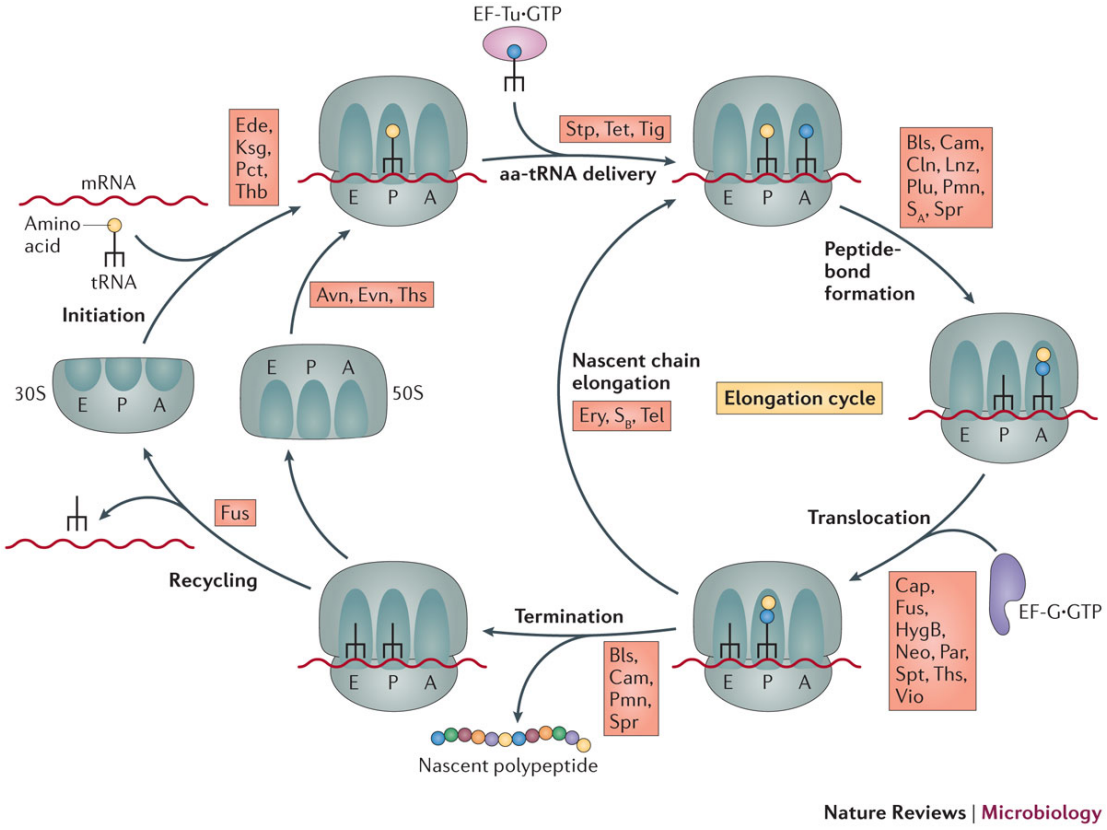

Figure 1.9 Antibiotic target sites during bacterial protein synthesis. Edeine (Ede), Kasugamycin (Ksg), Pactamycin (Pct), and Thermorubin (Thb) (Wilson, 2014).

In addition, mutating A694G, C795U, and C796U of 16S rRNA confers *Halobacterium halobium* resistance to pactamycin illustrating that the corresponding rRNA sites might be involved in pactamycin binding (Mankin, 1997). According to previous studies, pactamycin acts as a protein synthesis inhibitor by preventing the initiation step of protein synthesis, which could be attributed to conformational changes in the 30S subunit. Furthermore, X-ray crystallographic studies have showed key interactions between pactamycin and the ribosome (Figure 1.10). It has been proposed that the cyclopentitol ring of pactamycin mimics the RNA sugar-phosphate

backbone and interacts with C795 and C796 in H24a, while the two aromatic rings stack against each other on G693 at the tip of H23b, mimicking an RNA dinucleotide (Brodersen et al., 2000); see Figure 1.10. The analysis of the atomic structure of the 30S subunit suggested that pactamycin binds to the ribosomal E site rather than the P site as previously proposed (Carter et al., 2000). The two aromatic rings stay in the position normally occupied by the last two bases of the E site codon, which results in a remarkable distortion, leading to a displacement of the mRNA path.

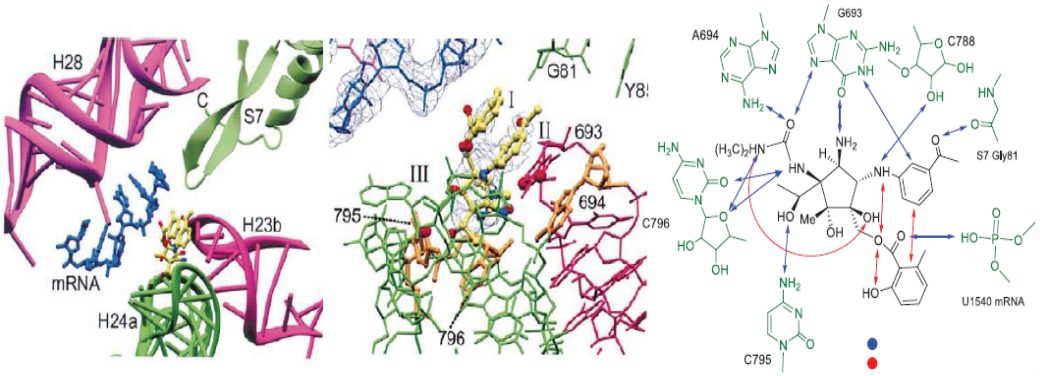

Figure 1.10 Diagram of pactamycin (in yellow) and its proposed interactions with 16S RNA (Brodersen et al., 2000).

1.5.5 Resistance Mechanisms

Organisms produce a variety of secondary metabolites to protect themselves against other invading organisms as a first line of defense. Some of these metabolites are toxic to the producing cells, especially when a metabolite target site is present in the producing organism. Therefore, a specific self-resistance mechanism must exist in the organism to prevent self-toxicity. Since pactamycin is a potent protein synthesis inhibitor, the producing strains are faced with self-toxicity. To avoid self-toxicity,

microorganisms have evolved a detoxification mechanism through either mutating the antibiotic binding sites, modifying the antibiotic itself to the inactive form *via* structure modification or degradation, or increasing efflux and preventing the accumulation of the antibiotics in the cell. A proposed mechanism for acquiring ribosomal resistance to pactamycin is through methylation of 16S RNA. Ribosomes from *S. pactum* were shown to be insensitive to pactamycin *in vitro*. The 4 kb pactamycin resistance determinant DNA fragment had been isolated from *S. pactum* and cloned in the *Streptomyces lividans* genome (Calcutt and Cundliffe, 1990a). The resulting *S. lividans* strain successfully became resistant to pactamycin. It was found that in *S. lividans* 16S rRNA, the A-941 residue (A-964 in *Escherichia coli* 16S rRNA) was converted to 1-methyladenosine, and as a result, the ribosomal ability to bind pactamycin was reduced or abolished. As mentioned in the Mechanism of Action section (1.5.4), pactamycin-resistant mutants of an archaeon *Halobacterium halobium* have been isolated. Three types of mutations were found in A694G, C795U, and C796U (*Escherichia coli* 16S rRNA numeration) in the 16S rRNA, conferring the pactamycin resistance (Mankin, 1997).

1.6 Pactamycin Biosynthesis

1.6.1 Biosynthetic Origin of Pactamycin

The biosynthetic origin of pactamycin had been studied by conventional feeding experiments with ^{14}C-labeled precursors followed by detection where the precursor was incorporated into pactamycin (Weller and Rinehart, 1978). The next feeding experiments were done with ^{13}C-labeled precursors, and the results showed that acetic

acid, glucose, and methionine are well-incorporated while other potential precursors are less well-incorporated. It has been suggested that the five-member ring aminocyclitol moiety of pactamycin is derived from glucose, whereas 6MSA is derived from acetic acid. The 3AAP moiety is derived from an unknown branch of the shikimate pathway (Rinehart et al., 1981). One of the intriguing features of pactamycin biosynthesis is that the compound is highly decorated with amino and methyl groups. Results from feeding experiments revealed that the two *N*-methyl carbons and three carbons (C-6, C-7, and C-8) on the cyclopentane ring are derived from the methyl group of methionine (Rinehart et al., 1981) (Figure 1.11).

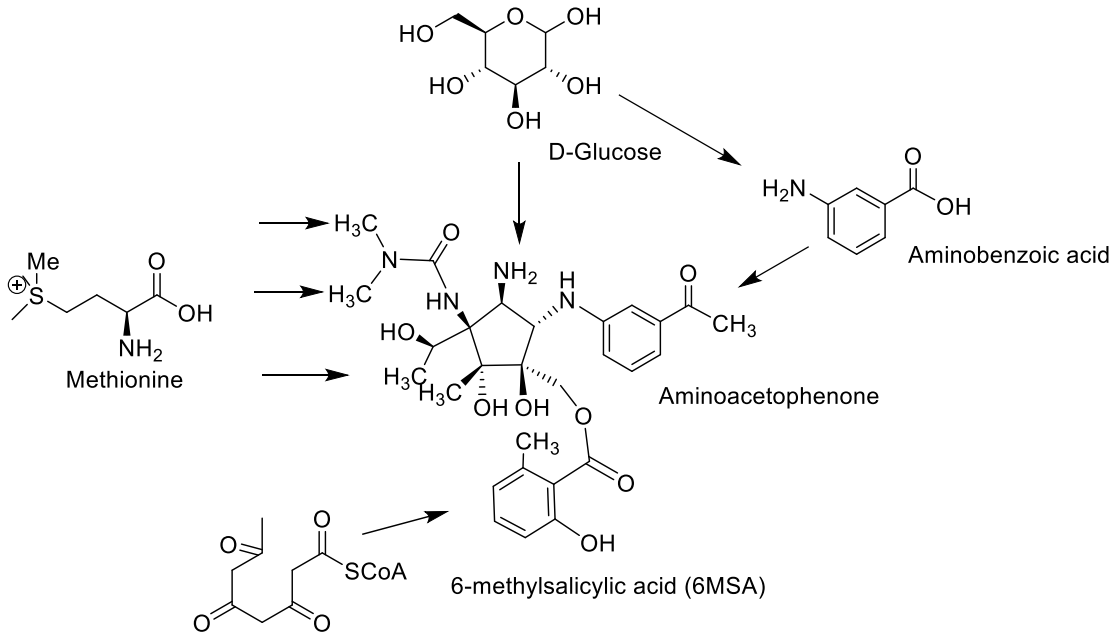

Figure 1.11 Biosynthetic origin of pactamycin (Rinehart et al., 1981).

1.6.2 The Pactamycin Biosynthetic Gene Cluster

While pactamycin is excluded from clinical use because of its cytotoxicity, it can serve as a promising lead compound for the development of new drugs to treat malaria and cancers. In order to manipulate the biosynthesis of pactamycin and create new analogs by rational design, it is important to identify the biosynthetic gene cluster to pactamycin biosynthesis. Functional analysis of the pactamycin biosynthetic gene cluster will provide important insights into the role of each gene within the cluster. Furthermore, *in vitro* characterization of the gene products will provide in-depth knowledge about the enzymes and the reaction mechanisms involved in pactamycin biosynthesis. Finally, a deeper understanding of the biosynthetic pathway will be used to facilitate the production of novel pactamycin analogs, which may be developed as new drug leads. Our group has identified the biosynthetic gene cluster of pactamycin within an 86 kb sequenced region of chromosomal DNA from *S. pactum* ATCC 27456 (Ito et al., 2009). Sequence analysis revealed the presence of 53 open reading frames (ORFs), some of which (*ptmA-Z*) are predicted to be involved in the biosynthesis of pactamycin (Figure 1.12 and Table 1.3). Kudo *et al*. have independently reported the biosynthetic gene cluster of pactamycin from *S. pactum* NBRC 13433, which turns out to be identical to the strain ATCC 27456. The previously reported 34 kb DNA sequence consists of 26 ORFs and is believed to be involved in the biosynthesis of pactamycin (Kudo et al., 2007). Our group also identified a number of additional genes upstream and downstream of the core cluster that may be involved in the transcriptional regulation of the pathway and/or in resistance.

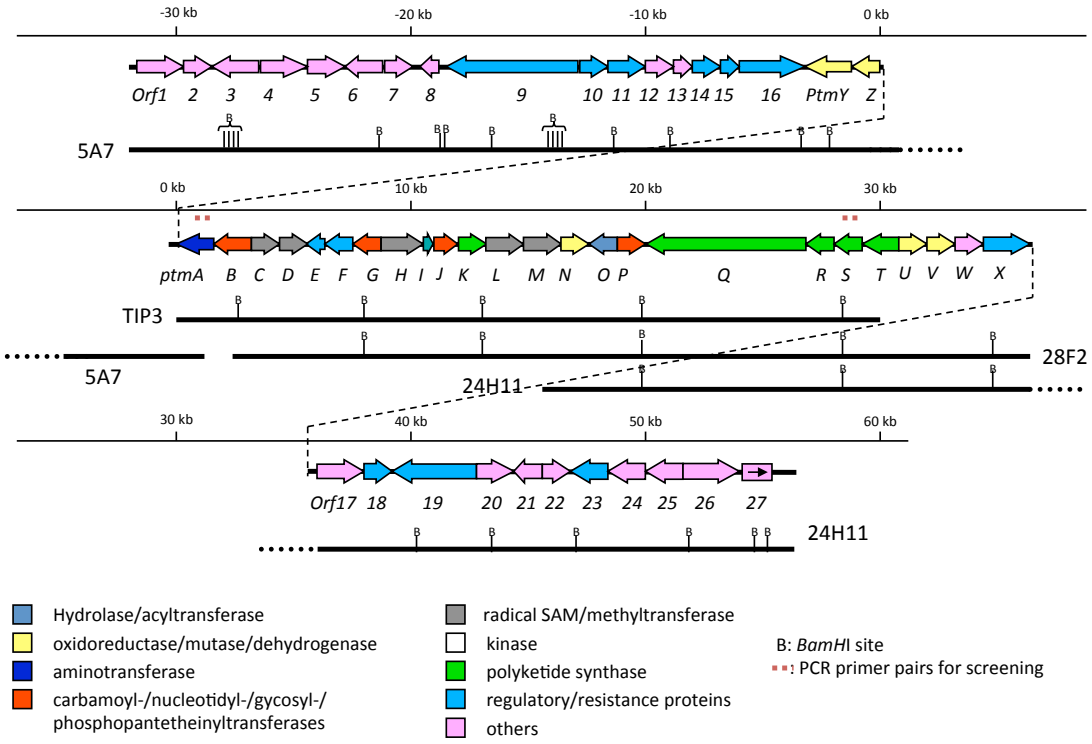

Figure 1.12 Genetic organization of the pactamycin biosynthetic gene cluster.

Table 1.3 The proposed function of genes in the *ptm* cluster and the flanking regions.

Protein	Aa	Proposed function (homologous protein and/or source organism)	Identi. %	Sim. %	Accession no.
Orf1	483	phosphoribosylformylglycinamidine synthase subunit [*S. coelicolor*]	86	92	NP_628260
Orf2	295	hypothetical protein SAV4137 [*S. avermitilis*]	59	68	NP_825314
Orf3	524	*N*-acetylgalactosamine-6-sulfate sulfatase [*Thermobifida fusca*]	53	65	YP_289414
Orf4	527	amidophosphoribosyltransferase [*S. coelicolor*]	89	96	NP_628267
Orf5	356	phosphoribosylaminoimidazole synthetase [*S. coelicolor*]	84	90	NP_628268
Orf6	364	valine dehydrogenase [*S. avermitilis*]	85	93	NP_825309
Orf7	272	hypothetical protein [*S. avermitilis*]	71	82	NP_825308
Orf8	211	hypothetical protein [*Bradyrhizobium japonicum*]	37	44	NP_767161
Orf9	1328	ATP-dependent helicase [*S. avermitilis*]	79	88	NP_825305

Orf10	328	integral membrane protein [*S. coelicolor*]	76	84	NP_625346
Orf11	575	putative sigma factor [*Saccharopolyspora erythraea*]	48	62	YP_001104010
Orf12	385	putative oxidoreductase [*Saccharopolyspora erythraea*]	49	60	YP_001103666
Orf13	156	hypothetical protein [*S. coelicolor*]	93	96	NP_628275
Orf14	255	translation initiation factor IF-2 [*Frankia alni*]	32	35	YP_715913
Orf15	150	translation initiation factor IF-2 [*S. avermitilis*]	40	40	NP_823727
ORF16	788	ATP-dependent RNA helicase [*S. avermitilis*]	69	76	NP_825300
PtmY	397	Cytochrome P450 monooxygenase (*S. tubercidicus*)	59	71	AAT45281
PtmZ	162	Glutathione peroxidase (*Mycobacterium vanbaalenii*)	60	72	YP_955911
PtmA	391	L-alanine:N-amidino-3-keto-*scyllo*-inosamine aminotransferase (StsC, *S. griceus*)	37	50	CAH94315
PtmB	570	Carbamoyltransferase (MmcS, *S. lavandulae*)	47	59	AAD32743
PtmC	367	Fe-S Radical SAM oxidoreductase (MitD, *S. lavandulae*)	32	50	AAD32720
PtmD	358	HemK family methyltransferase (*S. ambofaciens*)	35	49	CAJ88518
PtmE	178	Hypothetical protein SACE-5647 (*Saccharopolyspora erythreae*)	38	59	YP_001107758
PtmF	216	DNA-binding winged-HTH domain (*Silicibacter* sp.)	38	52	YP_611468
PtmG	378	Putative deacetylase (MitC, *S. lavandulae*)	38	46	AAD32721
PtmH	661	Radical SAM + B12 binding domain (*Salinispora arenicola*)	53	69	YP_001537758
PtmI	94	Putative ACP (*Clostridium perfringens*)	33	61	YP_473450
PtmJ	318	Glycosyltransferase (MitB, *S. lavandulae*)	34	43	AAD32722
PtmK	562	3-oxoacyl-(ACP) synthase (*Saccharopolyspora erythreae*)	44	55	YP_01102877
PtmL	575	Radical SAM + B12 binding domain (*Rhodospeudomonas palustris*)	32	47	YP_485691
PtmM	578	Radical SAM + B12 binding domain (*R. palustris*)	31	46	YP_485691

PtmN	351	Oxidoreductase (YcjS, *Escherichia coli*)	33	50	P77503
PtmO	257	Hydrolase or acyltransferase (*Rhodococcus* sp.)	40	52	YP_706151
PtmP	211	Phosphopantetheinyltransferase (PptA, *Silicibacter pomeroyi*)	43	55	YP_166099
PtmQ	1844	PKS (6MSA synthase) (ChlB1, *S. antibioticus*)	53	63	AAZ77673
PtmR	357	3-oxoacyl-(ACP) synthase (CalO4, *Micromonospora echinospora*)	41	59	AAM70354
PtmS	505	Acyl-CoA synthetase (HbmAI, *S. hygroscopicus*)	29	37	AAY28225
PtmT	444	Glutamate-1-semialdehyde aminotransferase (*Blastopirellula marina*)	41	57	ZP_01092129
PtmU	279	NAD^+-dependent oxidoreductase (SimJ1, *S. antibioticus*)	40	53	AAL15603
PtmV	226	Phosphoglycerate mutase (*Chlorflexus aurantiacus*)	37	53	YP_001636926
PtmW	271	Hypothetical protein SAV3686 (*S. avermitilis*)	46	55	NP_824863
PtmX	431	Integral membrane protein (*S. coelicolor*)	58	68	NP_628287

1.6.3 Proposed Biosynthetic Pathway to Pactamycin

The biosynthetic pathway of pactamycin has been proposed based on results of the isotope incorporation experiments, bioinformatics analysis, and gene inactivation experiments (Figure 1.13) (Ito et al., 2009; Kudo et al., 2007). Details of the proposed pathway are described in the following sections.

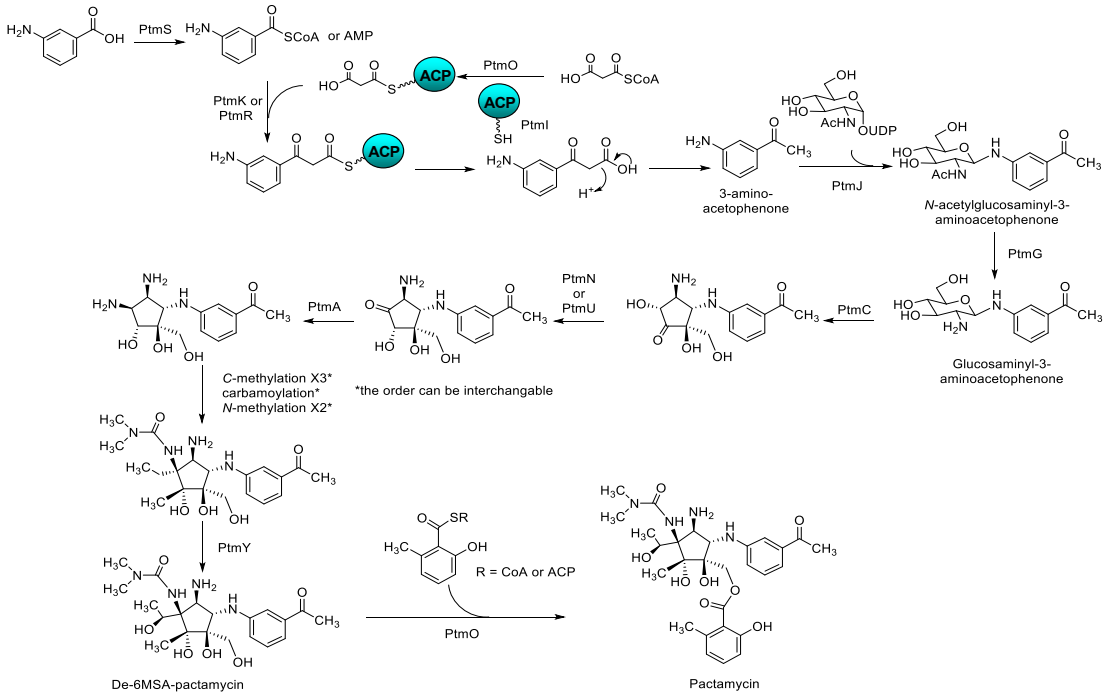

Figure 1.13 Previously proposed biosynthetic pathways to pactamycin.

1.6.4 Formation of 3-aminobenzoic acid and 3-aminoacetophenone

Previous incorporation studies revealed that the 3-aminobenzoyl unit of pactamycin is derived from glucose *via* the shikimate pathway, possibly diverging at the dehydroquinate or dehydroshikimate (Rinehart et al., 1980). The 3ABA, which is derived from dehydroshikimate (Hirayama et al., 2013), is catalyzed by a unique PLP-dependent aminotransferase-aromatase enzyme (PctV/PtmT) (Figure 1.14). Inactivation of the PLP-dependent aminotransferase gene *pctV*/*ptmT* completely abrogated pactamycin production, and chemical complementation with 3ABA and [1-^{13}C]-3ABA in the culture of *S. pactum ΔptmT* could rescue the production of pactamycin, indicating that PtmT is involved in 3ABA formation (Almabruk et al., 2013). Further biochemical studies revealed the mode of formation of 3ABA and its

direct involvement in the biosynthesis of pactamycin (Hirayama et al., 2013) (Figure 1.14).

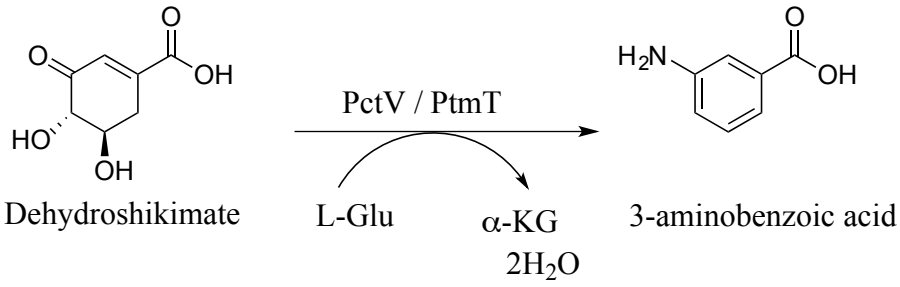

Figure 1.14 Formation of 3ABA from dehydroshikimate by PctV/PtmT catalysis.

Although progress has been made in recent years to understand how pactamycin is synthesized in nature, many aspects of its biosynthetic pathway remain elusive. For instance, it is unclear how 3ABA is converted to 3AAP and when the sugar or cyclopentitol moiety attaches to the aromatic ring. Previously, through *in vitro* experiments using a recombinant protein, (Kudo et al., 2007) reported that the glycosyltransferase PctL/PtmJ catalyzes the glycosylation of 3AAP using Uridine Diphosphate-*N*-acetyl-α-D-glucosamine (UDP-GlcNAc) as sugar donor. The result suggested that 3AAP and *N*-acetylglucosaminyl-3AAP are intermediates in the pactamycin pathway. However, our recent study using the *ptmT/H* mutant strain of *S. pactum* ATCC 27456 revealed that only 3ABA not 3AAP could rescue the production of TM-026 in this mutant, suggesting that 3AAP may not be a free intermediate in pactamycin biosynthesis. Unfortunately, the inactivation of *ptmJ* in *S. pactum* ATCC 27456, while abolishing the production of pactamycin, did not produce any detectable

intermediates, leaving the timing of the glycosylation reaction in pactamycin biosynthesis unclear.

On the basis of the putative functions of genes within the pactamycin cluster, two plausible pathways have been proposed for the formation of the 3AAP moiety. The first one involves the putative adenosine monophosphate-forming acyl-CoA (AMP-forming acyl-CoA) synthetase (PctU/PtmS), which may convert 3ABA to 3ABA-AMP, followed by coupling between 3ABA-AMP and acetyl-CoA to produce β-ketoacyl-CoA ester (Kudo et al., 2007). The second one involves the hydrolysis of the β-ketoacyl-CoA by the putative hydrolase PctQ/PtmO followed by a decarboxylation reaction that would produce 3AAP (Figure 1.15, path A) (Kudo et al., 2007). Our proposed pathway involves discrete polyketide enzymes: PtmI (an ACP), PtmK (a β-ketoacyl-ACP synthase, KAS II), and PtmS (Figure 1.15, path B) (Ito et al., 2009). PtmK is similar to KAS I/II, which is responsible for the elongation steps in fatty acid (FA) biosynthesis (Ahlert et al., 2002; Bibb et al., 1994). In addition, PtmO has been proposed to act as a hydrolase, which cleaves the PKS product from the ACP (PtmI), or as an acyltransferase (AT), which is involved in the loading of malonyl-CoA to the ACP or in the attachment of 6MSA to the core cyclopentitol moiety. However, no experimental evidence is available to determine the mode of formation of the 3AAP moiety and whether PtmO is a hydrolase or an AT.

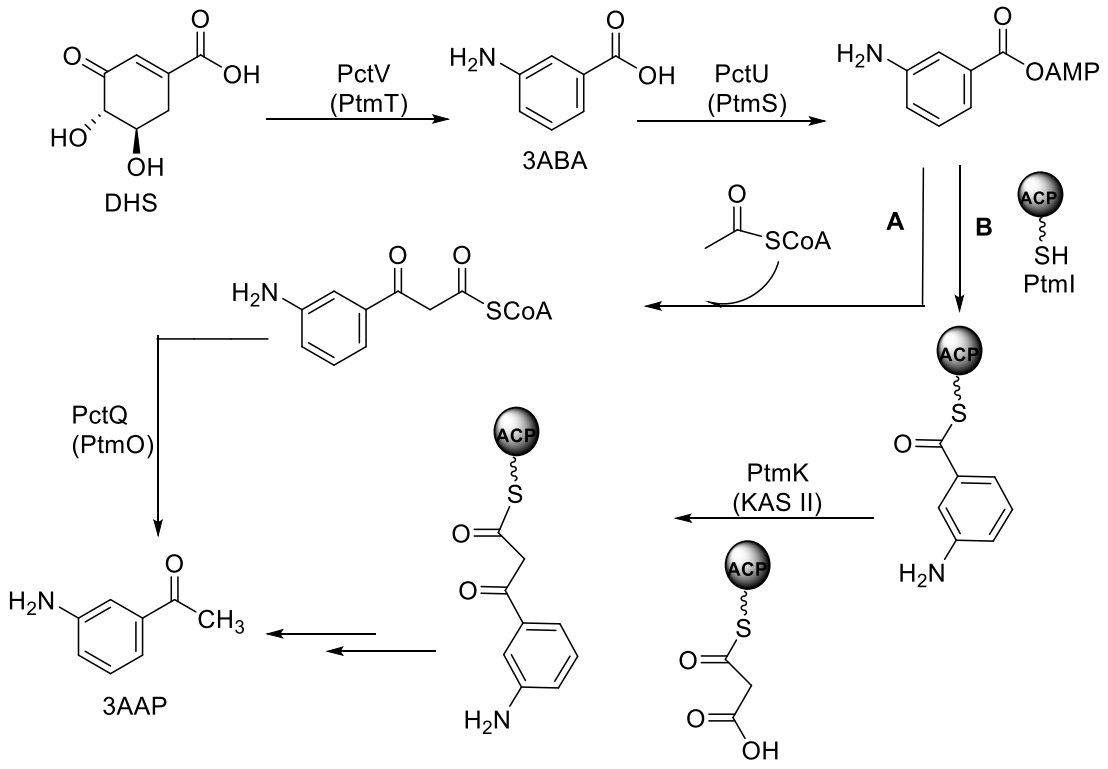

Figure 1.15 Proposed pathways from 3ABA to 3AAP.

1.6.5 Formation of the Aminocyclopentitol Ring

Database searches revealed that PtmC show sequence similarity to radical SAM enzyme MitD in the biosynthetic gene clusters of mitomycin (32% identity at the amino acid level). Kudo and co-workers proposed the formation of the cyclopentitol ring encoded by three essential genes, PtmC (*S*-adenosylmethionine (SAM)-dependent oxidoreductase), PtmJ (glycosyltransferase), and PtmG (deacetylase), and this process may be similar to the formation of the mitosane core structure during mitomycin biosynthesis (Mao et al., 1999). Interestingly, the radical SAM enzyme MitD, the glycosyltransferase MitB, and the putative *N*-deacetylase MitC from the mitomycin biosynthetic gene cluster are close homologs of PtmC, PtmJ, and PtmG in the

pactamycin gene cluster, respectively. During mitomycin biosynthesis, glucosamine (GlcN) is assembled into the mitosane core structure via condensation with an 3-amino-5-hydroxybenzoic acid (AHBA) unit. Although the details of this reaction mechanism have not been elucidated, it was proposed that MitB would mediate the condensation reaction between the two units followed by an unknown mechanism to complete the C-C bond formation (Mao et al., 1999). Results of feeding experiments with isotopically-labeled precursors have shown that the five-member ring aminocyclitol moiety of pactamycin is derived from glucose (Rinehart et al., 1981). Although the majority of cellular glucose uptake is devoted to the pentose phosphate pathway, glycogen synthesis, and glycolysis, a small percentage of glucose is directed to the hexosamine biosynthetic pathway, where it is converted to GlcN and *N*-acetylglucosamine (GlcNAc) (Hart, 2011). The incorporation of ^{13}C-glucose into the cyclopentitol ring addresses the general question of how GlcN and GlcNAc are transformed within the cell to form the cyclopentitol ring. So far, there is no direct enzymatic pathway described to address this question. Free GlcN and GlcNAc are unusual substrates for enzyme reactions. However, in *E. coli* cells, GlcNAc has been shown to be the substrate in which a kinase will convert GlcNAc to GlcNAc-6-phosphate. In addition, it has been illustrated that in *E. coli* cells, UDP-GlcNAc can be regenerated from free GlcNAc through a multistep enzymatic pathway (Hart, 2011). The involvement of such a natural recycling pathway in the selective incorporation of labeled glucose into the cyclopentitol ring of pactamycin could occur.

A number of putative mechanisms have been proposed for the contraction of the GlcN ring to form the cyclopentane ring (Flatt and Mahmud, 2007). Since PtmC is a putative SAM-dependent oxidoreductase, the oxidation may occur on C_4 leading to *endo*-opening and the formation of an oxonium intermediate (Figure 1.16). However, in inositol synthesis, an intramolecular aldol formed as a result of aldehyde intermediate formation (Tian et al., 1999).

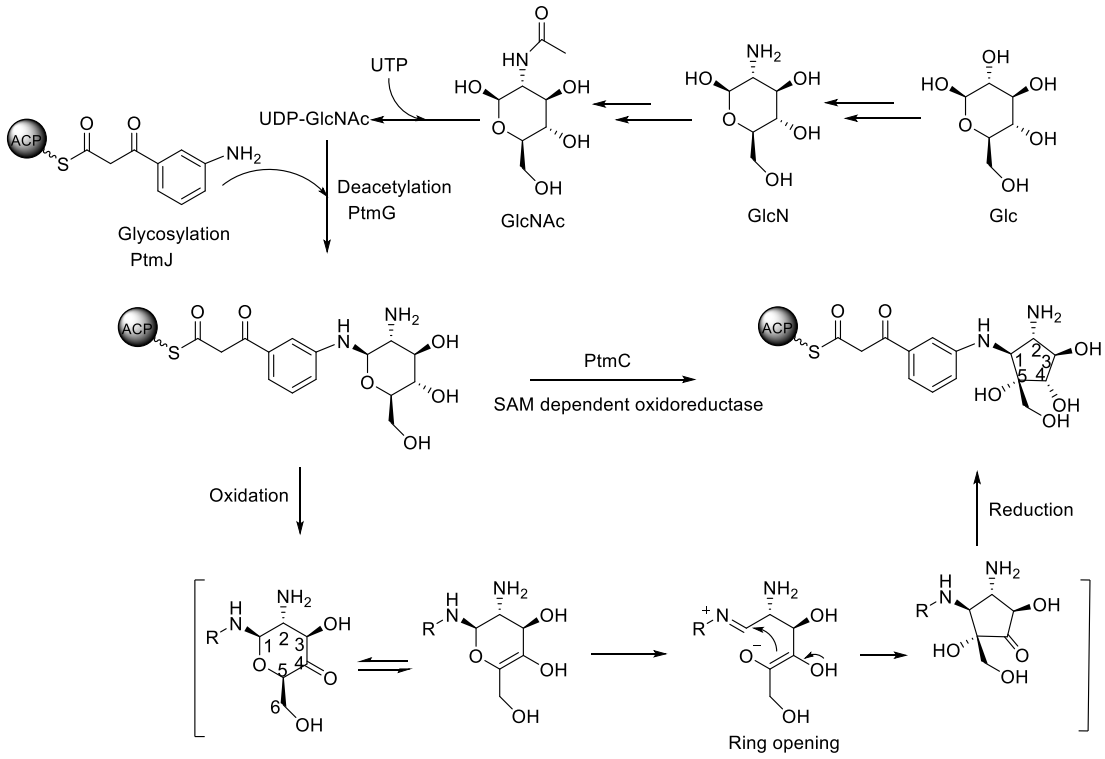

Figure 1.16 A hypothetical biogenetic scheme for the biosynthesis of glycosylated cyclopentitol from glucose.

To confirm the involvement of PtmG, ptmC, and PtmJ in pactamycin biosynthesis, the three genes were inactivated by in-frame deletion in *S. pactum*, and phenotypes were

analyzed (Lu at el., 2010). HPLC and MS analysis of the culture broths revealed that the mutant strains lack the ability to produce pactamycin. In addition, an *in vitro* enzymatic assay using recombinant PtmJ and an *in vivo* feeding experiment with E. *coli* harboring the *ptmJ* gene both demonstrated that the glycosyltransferase PtmJ is capable of coupling UDP-GlcNAc and 3AAP. This result is consistent with that reported by (Kudo et al., 2007).

1.6.6 Biosynthesis of 6-methylsalicylic acid by an Iterative Type I PKS

The 6MSA moiety of pactamycin is assembled from one unit of acetyl-CoA and three units of malonyl-CoA by the 6MSA synthase PtmQ. The enzyme shares high similarity with the iterative type I PKS, ChlB1, and is involved in the biosynthesis of 6MSA in *Streptomyces antibioticus* (Jia et al., 2006). Previously, we heterologously expressed *ptmQ* in *S. lividans* T7, and the resulting transformants were able to produce 6MSA (Ito et al., 2009). To investigate if PtmQ is involved in pactamycin biosynthesis, we genetically inactivated *ptmQ* by in-frame deletion and analyzed the metabolites. ESI-MS analysis of the products revealed the inability of Δ*ptmQ* to produce pactamycin. However, two new pactamycin analogs, de-6MSA-pactamycin and de-6MSA-pactamycate, have been detected (Figure 1.17). The new compounds showed equivalent antibacterial and cytotoxic activities with the corresponding parent molecules, suggesting that the 6MSA moiety is not essential for their antibacterial and cytotoxic activities (Ito et al., 2009).

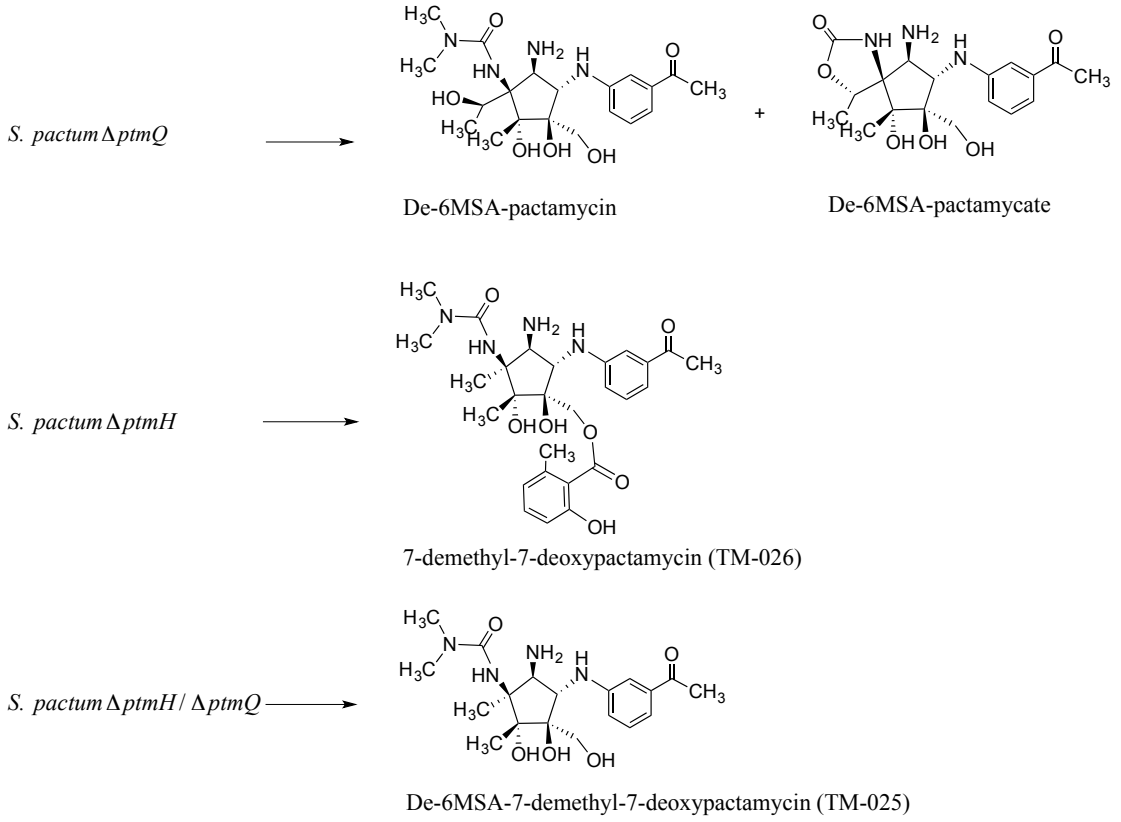

Figure 1.17 Generation of new pactamycin analogs using a genetic engineering approach.

1.6.7 Tailoring Processes

While the order of tailoring reactions that include *C*-methylation, carbamoylation, *N*-methylation, and hydroxylation are currently unclear, putative enzymes that mediate these processes are all accounted for within the *ptm* cluster. PtmB is predicted to catalyze the *N*-carbamoylation of the cyclopentitol core unit. The SAM-dependent *N*-methyltransferase homolog PtmD is then predicted to convert the carbamoyl group into the *N,N*-dimethyl functionality as seen in the final product. The radical SAM homologs, PtmH, PtmL, and PtmM, all contain conserved B12-like binding domains, suggesting that they play a role in the three *C*-methylation reactions involved in

pactamycin biosynthesis. PtmY, which shares a high identity to cytochrome P450 monooxygenases, is proposed to play a role in the hydroxylation reaction (Ito et al., 2009).

1.6.8 Regulation of Pactamycin Biosynthesis

Production of antibiotics in *Streptomyces* is controlled through complex, multi-step pathways. The genes for these pathways are encoded in large biosynthetic gene clusters, which may include regulators, functional and/or resistance genes, and transporters of a particular product (Bibb, 1996; Fernandez-Moreno *et al*., 1992). Generally, these complex molecules are under the control of three recognized levels of regulation:

1. Overarching regulators that have roles in both antibiotic production and morphological differentiation
2. Global regulators (pleiotropic regulators) involved in the production of more than one antibiotic, and
3. Pathway-specific regulators that affect only a single antibiotic (Arias *et al*., 1999).

There are at least fifteen pleiotropic regulators involved in antibiotics biosynthesis in *S. coelicolor*. Predictably, many of these are putative transcription factors and others are less well understood (Van Wezel *et al*., 2009). The literature holds examples of strategies that have either successfully activated novel antibiotic production or increased the titers of antibiotics—both of which are important milestones in antimicrobial research.

In the flanking region of the pactamycin gene cluster, we identified a number of genes that may play role in pactamycin regulation as specific pathway regulators. In addition, we identified and sequenced a number of pleiotropic genes that may play roles in pactamycin regulation.

a) Specific Pathway Regulators within the Pactamycin Gene Cluster

Orf11 shares high homology with the extracytoplasmic function (ECF) subfamily of RNA polymerase sigma factors. The positioning of Orf11 near the biosynthetic enzymes in the pactamycin gene cluster suggests that this factor may be involved with the regulation of pactamycin gene expression. Orf14 and Orf15 are hypothetical proteins that have low identity to the translation initiation factor (IF-2) from *Frankia alni* ACN4a and *Streptomyces avermitilis* MA-4680, respectively. Their function related to pactamycin biosynthesis is unclear but may be involved in regulating the production of biosynthetic enzymes. Orf9, Orf16, and Orf19 are highly related to the family of ATP-dependent (DEAD-box) RNA helicases. These genes may play a role in the translational regulation of pactamycin biosynthetic proteins.

We explored the roles of those enzymes in pactamycin biosynthesis by inactivating the six genes individually. LC-MS analysis of the culture broths of the mutant strains revealed the production of pactamycin in those strains, which directly confirmed that these genes are not involved in the biosynthesis or regulation of pactamycin (unpublished data).

Orf18 and Orf23 share high homology with nourseothricin acetyltransferase from *Streptomyces noursei* and tRNA methyltransferase from *S. avermitilis*, respectively. These genes may be involved in the acetylation and methylation/modification of the cellular tRNA binding site of pactamycin to protect the producer strain from self-toxicity. We cloned Orf18 and Orf23 and overexpressed them in *S. lividans*. No resistance to pactamycin was determined through the Kirby-Bauer antibiotic test indicating that Orf18 and Orf23 do not play a direct role in pactamycin resistance mechanisms.

b) Pleiotropic or Global Regulators

Our aim is to identify the possible pleiotropic genes that may play a role in the regulation of pactamycin. It has been reported that the variety of secondary metabolites produced can be increased by modulating the transcriptional regulators that control their expression (Liu et al., 2013). Moreover, the inactivation of such genes may increase the secondary metabolites titer (Liu et al., 2013). We identified three global regulatory genes, *afsA*, *arpA*, and *phoP*, in the shotgun genome sequence of the *S. pactum* chromosome that could play a role in the expression of the pactamycin biosynthetic gene cluster. These genes play an important role in the production of secondary metabolites in many *Streptomyces* species (Kato et al., 2007; Onaka et al., 1995; Sola-Landa et al., 2003).

1.6.9 Engineering Pactamycin Analogs

Pactamycin was abandoned as a human drug candidate due to its high toxicity. In order to improve its efficacy and reduce its toxicity, structural modification of the

compound is our ultimate goal. Structural modification of pactamycin can be carried out using chemical synthesis; however, due to its structural complexity, this approach is complicated. Therefore, we require alternative approaches such as biosynthetic and genetic modification methods to generate new pactamycin analogs. Recently, the biosynthetic gene cluster of pactamycin was identified by our lab, and the sequence analysis of an 86 kb continuous region of *S. pactum* chromosome revealed the presence of 53 ORFs. According to BLAST analysis, the functional genes *ptmA* to *ptmZ* are predicted to be involved in the biosynthesis of pactamycin (Ito et al., 2009). In order to analyze the function of these genes and generate novel pactamycin analogs, disruption of all functional genes in *S. pactum* were performed using the in-frame deletion strategy.

The putative iterative type-I PKS gene (*ptmQ*) identified within the cluster was heterologously expressed in *Streptomyces lividans* T7, and the resulting transformants were found to produce 6MSA. Inactivation of the *ptmQ* gene in *S. pactum* also impaired the production of pactamycin and pactamycate but led to production of two new pactamycin analogs, de-6MSA-pactamycin and de-6MSA-pactamycate (Figure 1.17). The new compounds showed equivalent antibacterial and cytotoxic activities with the corresponding parent molecules, suggesting that the 6MSA moiety is not essential for their antibacterial and cytotoxic activities (Ito et al., 2009). Inactivation of the *ptmH* gene generated a mutant strain that produced new analog, 7-demethyl-7-deoxypactamycin (TM-026), with an *m/z* of 529. Furthermore, the inactivation of

ptmH and *ptmQ* resulted in a double mutant strain that produced a new compound, de-6MSA-7-demethyl-7-deoxypactamycin (TM-025), with an *m/z* of 395 (Lu et al., 2011). Two *S. pactum* mutant strains have since been constructed (see Chapter 3). The Δ*ptmDH* mutant was constructed by double knock out of *ptmD* and *ptmH*, whereas the Δ*ptmDQ* mutant was constructed by double knock out of *ptmD* and *ptmQ*. The Δ*ptmDH* double mutant produced TM-101, which lacked the two methyl groups on the carbamoyl moiety and a hydroxyl and methyl group on C-7. However, the Δ*ptmDQ* mutant produced TM-102, which also lacked the *N*-methyl groups on the carbamoyl moiety and a hydroxyl group on C-7.

1.7 Research Objectives

A. Determine the function of the putative structural genes within the pactamycin gene cluster by *in vivo* gene inactivation and phenotypic analysis.

1. To identify the genes responsible for the formation of 3AAP and the aminocyclopentitol core unit and to reveal its mode of formation.
2. To investigate the sequence or the timing of the tailoring processes.
3. To identify the gene responsible for the attachment of 6MSA to the aminocyclopentitol unit.

B. Generate pactamycin analogs by combined molecular genetics and mutasynthesis approaches and determine their biological activities.

1. To explore the production of pactamycin analogs by *in vivo* gene inactivation and in *vitro* chemoenzymatic strategies.
2. To isolate, purify, and structurally elucidate the resulting novel analogs.

3. To test the biological activities of novel compounds against bacteria, malarial parasites, and cancer cell lines.

Chapter 2 : Discrete Polyketide Synthase Proteins are Responsible for 3-Aminoacetophenone Formation in Pactamycin Biosynthesis

Mostafa E. Abugrain, Corey J. Brumsted, and Taifo Mahmud

2.1 Abstract

Pactamycin, a potent antitumor antibiotic, inhibits the growth of bacteria, protozoa, and mammalian cells. The unique chemical structure and biological activity of pactamycin have attracted biologists and chemists alike. It has been demonstrated that the 3-aminoacetophenone (3AAP) moiety of pactamycin is derived from 3-aminobenzoic acid (3ABA), whereas the aminocyclopentitol moiety is derived from glucose, possibly via *N*-acetylglucosamine (GlcNAc). However, details of their modes of formation in the producing strain of *Streptomyces pactum* are still elusive. Using gene inactivation, chemical complementation, and biochemical studies, we demonstrated that 3ABA is processed by a set of discrete polyketide synthase (PKS) proteins, i.e., an adenosine monophosphate-forming acyl-coenzyme A (AMP-forming acyl-CoA) synthetase (PtmS), an acyl carrier protein (ACP) (PtmI), and a β-ketoacyl-ACP synthase (PtmK), to produce 3-[3-aminophenyl]3-oxopropionyl-ACP (3AP-3OP-ACP). The hydrolase PtmO is responsible for the cleavage of a β-ketoacyl product from ACP, which then undergoes a spontaneous decarboxylation. This study also revealed that neither free 3AAP nor its glycosylated form are directly involved in pactamycin biosynthesis.

2.2 Introduction

Pactamycin, a microbial-derived natural product, is a potent antitumor antibiotic with antiproliferative activity against bacteria, protozoa, and mammalian cells. Since the discovery of pactamycin in the early 1960's, it has attracted attention from biologists and chemists due to its unique chemical structure and biological activity. Structurally,

it contains a cyclopentitol core unit attached to 3-aminoacetophenone (3AAP), 6-methylsalicylic acid (6MSA), and a dimethylurea (Figure 2.1). The 3AAP moiety is originated from 3-aminobenzoic acid (3ABA), which is derived from dehydroshikimate, and is catalyzed by a unique PLP-dependent aminotransferase-aromatase enzyme (PctV/PtmT) (Almabruk et al., 2013; Hirayama et al., 2013; Rinehart, 1979). Inactivation of *ptmT* gene in the pactamycin producer *Streptomyces pactum* ATCC 27456 abolished pactamycin production, and chemical complementation of the Δ*ptmT* mutant with 3ABA resulted in the recovery of the antibiotic production (Almabruk et al., 2013). Although direct involvement of 3ABA in pactamycin biosynthesis has previously been established, the process underlying its conversion to the 3AAP moiety was unknown.

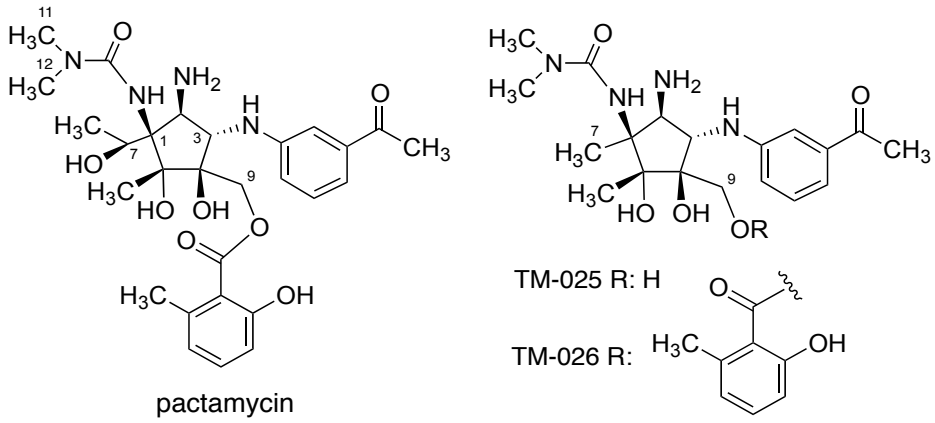

Figure 2.1 Chemical structures of pactamycin, TM-025, and TM-026.

On the basis of the putative functions of genes within the pactamycin cluster, two plausible pathways have been proposed for the formation of the 3AAP moiety. The first one involves the putative adenosine monophosphate-forming acyl-coenzyme A

(AMP-forming acyl-CoA) synthetase (PctU/PtmS), which may convert 3ABA to 3ABA-AMP, followed by coupling between 3ABA-AMP and acetyl-CoA to produce β-ketoacyl CoA ester (Kudo et al., 2007). Hydrolysis of the β-ketoacyl-CoA by the putative hydrolase (PctQ/PtmO) followed by a decarboxylation reaction would produce 3AAP (Figure 2.2, path A) (Kudo, et al., 2007). The other pathway would involve PtmS and discrete polyketide enzymes: PtmI (an acyl carrier protein, ACP) and PtmK (a β-ketoacyl-ACP synthase, KAS) (Figure 2.2, path B) (Ito et al., 2009). PtmK is similar to KAS I/II, which is responsible for the elongation steps in fatty acid (FA) biosynthesis (Bibb et al., 1994; Ahlert et al., 2002) In addition, PtmO has been proposed to act as a hydrolase, which cleaves the PKS product from the ACP (PtmI), or as an acyltransferase, which is involved in the loading of malonyl-CoA to the ACP. However, no experimental evidence is available to determine the mode of formation of the 3AAP moiety.

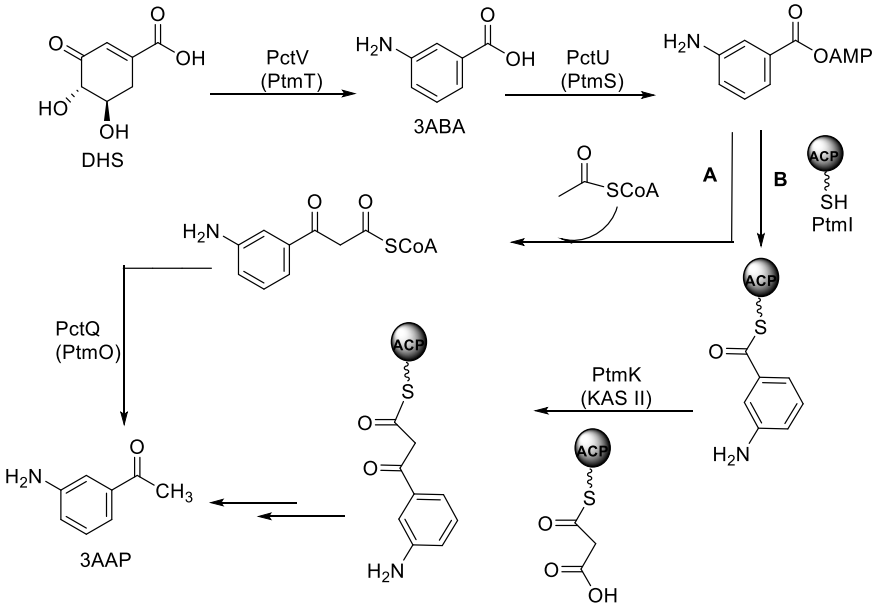

Figure 2.2 Proposed pathways from 3ABA to 3AAP.

2.3 Materials and Methods

2.3.1 General Experimental Procedures

Low-resolution electrospray ionization (ESI) mass spectra were recorded on a ThermoFinnigan Liquid Chromatograph-Ion Trap Mass Spectrometer. High Performance Liquid Chromatography was carried out on a C_{18} column (C_{18} Symmetry 10 x 150 mm, Waters) with a detector set at 355 nm. Thin layer chromatography was performed on aluminum sheets with silica gel 60 F_{254} (EMD chemicals Inc.).

2.3.2 Bacterial Strains and Plasmids Used in this Study

Pactamycin-producing *S. pactum* ATCC 27456 was purchased from American Type Culture Collection (ATCC). *Escherichia coli* DH10B was used as a host strain for the construction of recombinant plasmids. *E. coli* ET12567 (pUZ8002) was used as a donor strain in conjugation experiments. pBlueScript II (SK-) (Stratagene) and pGEM-T Easy (Promega) were used as cloning vectors. pTMN002, a pJTU1278+ derivative containing apramycin-resistance cassette, was used as a vector for gene inactivation (He et al., 2010; Ito et al., 2009). All bacterial strains and plasmids used in this study are listed in Table 2.1 and Table 2.2.

Table 2.1 Bacterial strains used in this study.

Strains	Relevant genotype/comments	Source/Ref
Escherichia coli DH10B	*F⁻ mcrA Δ(mrr-hsdRMS-mcrBC)ϕ80lacZΔM15 ΔlacX74 recA1 endA1 araD139 Δ(ara, leu)7697 galU galK λ⁻ rspL nupG*	GibcoBRL
Escherichia coli BL21*(*DE3*)*pLysS	*F⁻ ompT hsdS$_B$ (r_B^- m_B^-) gal dcm* (DE3) pLysS (CmR)	Promega
E. coli ET12567(pUZ8002)	*dam dcm hsdS,* pUZ8002	(Paget et al., 1999)
Streptomyces pactum ATCC 27456	Wild-type pactamycin producing strain	ATCC

S. pactum Δ*ptmH*	*ptmH* in-frame deletion mutant	(Lu et al., 2011)
S. pactum Δ*ptmI*	*ptmI* in-frame deletion mutant	This study
S. pactum Δ*ptmO*	*ptmO* in-frame deletion mutant	This study
S .pactum ptmK::aac(3)IV	*ptmK* disruption mutant	This study
S. pactum Δ*ptmS*	*ptmO* in-frame deletion mutant	This study
Δ*ptmH/ ptmK::aac(3)IV*	*ptmH/ptmK* disruption mutant	This study
S. pactum Δ*ptmH/* Δ*ptmO*	*ptmH/ptmO* in-frame deletion mutant	This study
S. pactum Δ*ptmH/* Δ*ptmI*	*ptmH/ptmI* in-frame deletion mutant	This study
S. pactum MT-ptmI/TMM082	*ptmI* mutant complementation with pTMM 082	This study

Table 2.2 Plasmids used in this study.

Plasmid	Description	Source/Ref
pBlueScript II SK(-)	ColE1-based phagemid vector with f1 (-) and pUC origins; T3, T7 and lac promoters; *bla*.	Stratagene
pRSET B	N- terminal his-tagged fusion peptide.	Novagen
pTMN002	pJTU1278+ derivative containing a 1 kb *aac(3)IV* apramycin resistance cassette from pOJ446	(Ito et al., 2009)
pTMM007	Two 1 kb PCR fragments upstream and downstream of the *ptmO* gene in pBlueScript II SK(-)	This study
pTMM008	Two 1 kb PCR fragments upstream and downstream of the *ptmO* gene in pTMN002	This study
pTMW050	pTMX12b derivative containing *PermE** promoter from pJTU695 and MCS	(Lu et al., 2011)
pTMM051	Two 1 kb PCR fragments upstream and downstream of the *ptmI* gene in pBlueScript II SK(-)	This study
pTMM052	Two 1 kb PCR fragments upstream and downstream of the *ptmI* gene in pTMN002	This study
pTMM015	Two 1 kb PCR fragments upstream and downstream of the *ptmS* gene in pBlueScript II SK(-)	This study
pTMM016	Two 1 kb PCR fragments upstream and downstream of the *ptmS* gene in pTMN002	This study
pTMM055	0.88 kb PCR fragment of the *ptmK* gene in pTMN002	This study
pTMM080	pRSET B containing complete structural gene of *ptmO*	This study
pTMM081	pRSET B containing complete structural gene of *ptmS*	This study
pTMM082	pSET 152 containing complete structural gene of *ptmI* +100b.p	This study
pTMM083	pTMW050 containing complete structural gene of *ptmO*	This study
pTMM084	pTMW050 containing complete structural gene of *ptmS*	This study

2.3.3 General DNA Manipulations

Genomic DNA of *S. pactum* ATCC 27456 was prepared by standard protocol (Kieser et al., 2000) or using the DNeasy Tissue Kit (QIAGEN). DNA fragments were recovered from an agarose gel by using the QIAquick Gel Extraction Kit (QIAGEN). Restriction endonucleases were purchased from Invitrogen or Promega. Preparation of plasmid DNA was done by using a QIAprep Spin Miniprep Kit (QIAGEN). All other DNA manipulations were performed according to standard protocols (Kieser et al., 2000; Sambrook and Russell, 2001). PCR was performed in 30 or 35 cycles by using a Mastercycler gradient thermocycler (Eppendorf). High-fidelity Platinum *Taq* DNA polymerase (Invitrogen) was used to amplify the upstream and downstream fragments of the target genes. PCR products were ligated into pBluescript SK(-) plasmid at EcoRI/HindIII and EcoRI/Xbal sites and sequenced to confirm that no mutation occurred during PCR amplification. The pTMN002 was used to transfer the target construct into *S. pactum*. *Taq* DNA Polymerase, recombinant (Invitrogen) or AccuTaq LA DNA Polymerase (Sigma), was used for PCR screening for in-frame deletion mutant strains. Oligodeoxyribonucleotides, for PCR primers, were synthesized by Sigma-Genosys. The nucleotide sequence of the gene fragments was determined at the Center for Genome Research and Biocomputing (CGRB) Core Laboratories, Oregon State University. ORFs were analyzed by FramePlot (Ishikawa and Hotta, 1999) analysis and BLAST program (Altschul et al., 1990).

2.3.4 Seed and Production Media Used in this Study

All mutant strains were grown on BTT agar [glucose (1%), yeast extract (0.1%), beef extract (0.1%), casein hydrolysate (0.2%), agar (1.5%), pH 7.4] at 30 °C for 3 days. Single colonies were used to inoculate the BTT seed cultures and incubated at 30 °C for 2 days. Production cultures were prepared in modified Bennett medium (Sakuda et al., 2001) (50 mL) and inoculated with seed cultures [10% (V/V)]. Apramycin (5 μg/mL) was only added to *ptmK* and *ptmKH* mutant strains. The production cultures were incubated at 30 °C for 6 days under vigorous shaking (200 rpm). The mycelia were centrifuged and the supernatants were extracted twice with equal volumes of ethyl acetate and once with equal volume of n-butanol. The organic solvent was evaporated *in vacuo* and the residues were dissolved in 2 mL MeOH and analyzed by MS and reversed-phase HPLC.

2.3.5 Construction of Δ*ptmI*, Δ*ptmI*/Δ*ptmH*, Δ*ptmO*, Δ*ptmO*/Δ*ptmH*, and Δ*ptmS* Mutant Strains

The target genes were inactivated using gene in-frame deletion strategy (Figure 2.3 a) Two ~1 kb PCR fragments upstream (HindIII/EcoRI) and downstream (EcoRI/XbaI), (Table 2.3), of the *ptmI, ptmO,* and *ptmS* genes were fused and cloned into the HindIII/XbaI sites of pBluescript II SK(-) vector. The PCR products of *ptmI, ptmO* and *ptmS* were excised and cloned into the HindIII/XbaI sites of pTMN002 to generate pTMM052, pTMM08, and pTMN016, respectively. All plasmids were then individually introduced into *S. pactum* ATCC 27456 and Δ*ptmH* mutant strain by conjugation using the *E. coli* donor strain ET12567/pUZ8002. Apramycin resistant strains representing single crossover mutants were obtained and subsequently grown

on BTT agar plates containing apramycin (50 µg/mL). Apramycin sensitive colonies were counter-selected by replica plating on BTT agar with and without apramycin (50 µg/mL). The resulting double-crossover candidate strains were confirmed by PCR amplification with F1 and R2 primers flanking the respective targeted gene.

2.3.6 Construction of *ΔptmK* and *ΔptmH/ΔptmK*::apr^R Strains

The *ptmK* gene (1.7 kb) was inactivated using a gene disruption strategy (Figure 2.3 b). The internal fragment (0.88 kb) of *ptmK* was generated by PCR using a forward primer containing a HindIII site and a reverse primer containing a Xbal site, (Table 2.3), and *S*. pactum genomic DNA as a template. The PCR product was cloned into the HindIII/Xbal sites of pTMN002 to generate pTMM055. Plasmid pTMM055 was introduced into *S. pactum* and *ptmH* mutant strain by conjugation, as described by Kieser et al., 2000. The freshly harvested spores and the overnight-grown *E. coli* ET12567/pUZ8002 containing plasmid pTMM055 were mixed and plated onto MS agar plates containing $MgCl_2$ (10 mM). After incubation at 30 °C for 18 h, the plates were overlaid with sterile water (1 mL) containing nalidixic acid (1 mg/mL) and apramycin (1 mg/mL) and incubated at 30°C for 5-7 days. The exconjugant (single-crossover) colonies were purified by plating onto BTT agar plates supplemented with apramycin (50 µg/mL). Disruption of *ptmK* was confirmed by PCR amplification.

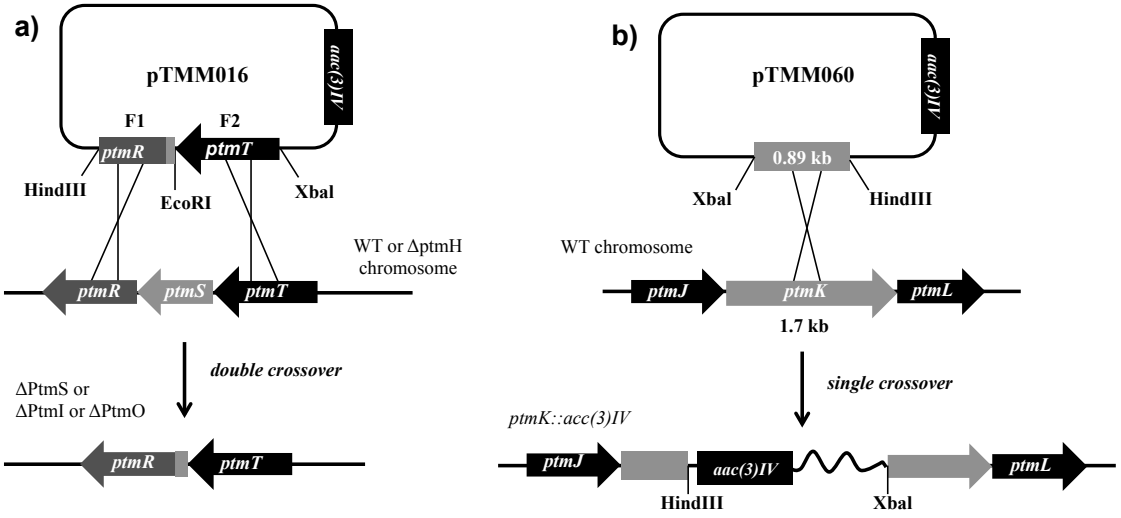

Figure 2.3 a) Construction of Δ*ptmI*, Δ*ptmI*/Δ*ptmH*, Δ*ptmO*, Δ*ptmO*/Δ*ptmH* and Δ*ptmS* mutant strains. **b)** Construction of Δ*ptmK*::aprR and Δ*ptmH*/ Δ*ptmK*::apr^R mutant strains in *S. pactum* and Δ*ptmH* mutant.

Table 2.3 Primers used in this study.

Primer	Sequence*
ptmI-F1	5′-CCC**AAGCTT**GCTGCAGACCATGGACGAAT-3′
ptmI-R1	5′-CCG**GAATTC**GTCCATCGTGTCGTCTCTCC-3′
ptmI-F2	5′-CCG**GAATTC**GTCCATCGTGTCGTCTCTCC-3′
ptmI-R2	5′-GC**TCTAGA**AGGTGGTACGCGACCGTGTCCA-3′
ptmI-BglII	5′- GA**AGATCT**ACATATGTACTTCCGGATGGACCGCTT-3′
ptmI-EcoRI	5′-G**GAATTC**TCACGAAGAGGAGGTGGTTTCGCC-3′
ptmO-BglII	5′-GA**AGATCT**ACATATGGTGCTGCGCGACCGGGA-3′
ptmO-EcoRI	5′-G**GAATTC**TCAGCTCAGGAACCGTACGACCT-3′
ptmS-BglII	5′-GA**AGATCT**ACATATGACCTCCGCCCGCGCGGA-3′
ptmS-EcoRI	5′-G**GAATTC**TCACTGATCGTTCCGCGGCCTGAT-3′
ptmS-F1	5′-CCC**AAGCTT**GTGTGGAGCAGGTCAGGTTC-3′
ptmS-R1	5′-CCG**GAATTC**GGCGGAGGTCATCCGAGTCC-3′
ptmS-F2	5′- CCG**GAATTC**CCGCTTCTGCCGGGAGCGTCT-3′
ptmS-R2	5′-TGC**TCTAGA**GCCAGGTGGTCGAGGTGGATG-3′
ptmO-R1	5′-CCG**GAATTC**GCCGAGGTCGTACGGTTCCT-3′
ptmO-F2	5′-CCG**GAATTC**GCTCCATCTGTTCGACTGG-3′
ptmO-R2	5′-TGC**TCTAGA**ACTGCAGGGTCGCGGGTTGC-3′
ptmK-F1	5′-**CCCAAGCTT**GATGGTGGTCTGCGAGGT-3′
ptmK-F2	5′-TGC**TCTAGA**GTGACCGTGCACGTAGTCC-3′

*nucleotides underlined refer to restriction sites

2.3.7 Synthesis of 3-[3-Aminophenyl]3-Oxopropionyl-SNAC (3AP-3OP-SNAC)

2.3.7.1 Synthesis of Tert-Butyl (3-((2,2-Dimethyl-4,6-Dioxo-1,3-Dioxan-5-Ylidene)(Hydroxy)Methyl) Phenyl) Carbamate (compound 2)

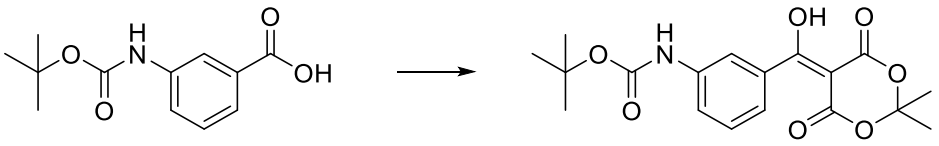

Under an atmosphere of nitrogen, compound **1 (**4.21 mmol, 1 g), was suspended in DCM (21 mL, 0.2 M) and added to *N, N'*-dimethylaminopyridine (DMAP) (5.47 mmol, 669 mg, 1.3 eq) followed by EDCI-HCl (4.84 mmol, 929 mg, 1.15 eq). Meldrum's acid (4.42 mmol, 637 mg, 1.05 eq) was added at room temperature and the reaction was stirred at this temperature for 14 h until the reaction was complete as indicated by TLC (Et_2O-EtOAc = 1: 2, vanillin stain). The reaction was diluted with DCM (20 mL), washed with 0.5 M HCl (3x20 mL), then H_2O (1 x 100 mL), and brine (1 x 50 mL). The organics were dried over Na_2SO_4, filtered and stripped under vacuum to yield compound **2** (1.47 g, 96%) as an orange foam which was used in the next step without further purification (Figure 2.7). ^{1}H NMR (300 MHz, $CDCl_3$) δ 15.39 (s, 1H), 7.68 (s, 1H), 7.58 (d, *J* = 7.7 Hz, 1H), 7.47-7.27 (m, 2H), 6.59 (s, 1H), 1.84 (s, 6H), 1.51 (s, 9H). LRMS (ESI+) found m/z 364.2 $[M+H]^+$; m/z 386.2 $[M+Na]^+$. ^{13}C NMR (75 MHz, $CDCl_3$) δ 189.27, 152.60, 138.57, 133.90, 128.85, 124.04, 123.05, 119.00, 105.13, 91.20, 81.14, 28.44, 26.98; IR data (cm^{-1}): 3333, 2981, 1727, 1673, 1559, 1397, 1289, 1236, 1159, 460.

2.3.7.2 Synthesis of S-(2-Acetamidoethyl)3-(3-Aminophenyl)-3-Oxopropanethioate (compound 4)

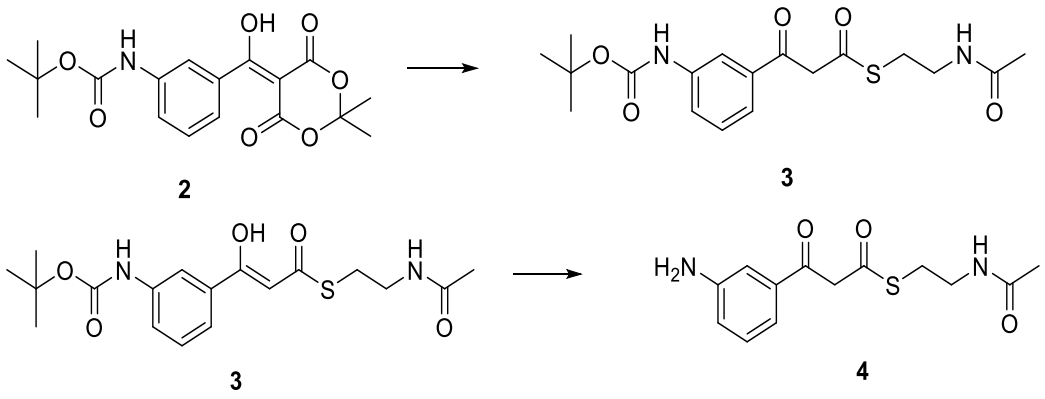

Compound **3 (**0.263 mmol, 100 mg) was dissolved in DCM (200 µL, 1.78 M) under N_2, then cooled in an ice bath. TFA was added dropwise at 0 °C and stirred for 8 h at a temperature range of 0 to 10 °C until the reaction was completed by TLC. The mixture was diluted with DCM (10 mL) and the reaction was quenched at 0 °C by dropwise addition of $NaHCO_3$-phosphate buffer solution (300 mg $NaHCO_3$ in 10 mL, pH 7, phosphate buffer), then extracted with DCM (5x10 mL) and dried over Na_2SO_4, filtered and stripped. After chromatography (Et_2O-MeOH = 100:5 to 50:5), compound **4** was obtained as a yellow oil (59 mg, 80%) (Figure 2.7). ^{1}H NMR (300 MHz, d_6-DMSO) δ 13.34 – 12.70 (m, 1H), 8.03 (m, 2H), 7.28 – 6.93 (m, 6H), δ 6.84 (d, J = 7.8 Hz, 1H), 6.74 (d, J = 7.7 Hz, 1H), 6.26 (s, 1H), 5.36 (s, 1H), 4.33 (s, 2H), 3.42 (m, 4H), 3.04 (t, J = 6.6 Hz, 2H), 2.94 (t, J = 6.8 Hz, 2H), 1.80 (s, 3H), 1.79 (s, 3H). ^{13}C NMR (75 MHz, d_6-DMSO) δ 193.92, 192.94, 192.56, 169.22, 169.12, 149.06, 148.99, 136.63, 132.56, 129.23, 129.17, 119.18, 117.53, 116.39, 113.85, 112.67, 111.27, 96.51, 53.52, 40.35, 40.08, 39.80, 39.52, 39.24, 38.96, 38.69, 38.29, 38.00, 28.49,

27.73, 27.02, 22.45. LRMS ESI(+): found m/z 281 $[M+H]^+$; m/z 303.1 $[M+Na]^+$. IR data (cm^{-1}): 3409, 3005, 2918, 1658, 1435, 1022, 953, 706.

2.3.8 Synthesis of *N*-Acetyl-D-Glucosaminyl-1-Aminoacetophenone (GlcNAc-1-AAP)

N-acetyl-D-glucosamine (GlcNAc) (2.0 mmol, 442 mg) and 3AAP (2.0 mmol, 135 mg) were mixed with 15 mL of methanol and 5.0 mL of acetic acid, and the mixture was stirred at room temperature overnight. After the removal of the solvent, the residue was directly purified by a standard silica-gel chromatography using $CHCl_3/CH_3OH$ (20:1 to 6:3). The glycosylated product was recrystallized from the methanol solution to give a yellow compound (50 mg). ^1H NMR (500 MHz, CD_3OD) δ 7.34 (d, J = 7.6 Hz, 1H), 7.26 (dd, J = 14.3, 6.2 Hz, 2H), 6.93 (dd, J = 8.0, 1.9 Hz, 1H), 4.86 (s, 10H), 4.63 (d, J = 9.3 Hz, 1H), 3.86 (dd, J = 20.2, 10.5 Hz, 2H), 3.71 (d, J = 5.1 Hz, 1H), 3.55 (d, J = 10.2 Hz, 1H), 3.40 (d, J = 6.6 Hz, 2H), 3.33 (d, J = 19.3 Hz, 3H), 2.55 (d, J = 5.7 Hz, 3H), 1.98 (d, J = 4.8 Hz, 3H).

2.3.9 Chemical Complementation of Δ*ptmI*, Δ*ptmI*/Δ*ptmH*, Δ*ptmO*, Δ*ptmO*/ Δ*ptmH*, Δ*ptmS*, Δ*ptmK*, Δ*ptmK*/Δ*ptmH*, and Δ*ptmK*::apr^R Mutant Strains with 3-[3-Aminophenyl]3-Oxopropionyl-SNAC

Δ*ptmI*, Δ*ptmI*/Δ*ptmH*, Δ*ptmO*, Δ*ptmO*/ Δ*ptmH*, Δ*ptmS*, Δ*ptmK*, Δ*ptmK*/Δ*ptmH*, and Δ*ptmK*::apr^R mutant strains were streaked on BTT agar [glucose (1%), yeast extract (0.1%), beef extract (0.1%), casein hydrolysate (0.2%), agar (1.5%), pH 7.4] and incubated at 30 °C for 3 days. Spores of the mutant strains were grown in Erlenmeyer flasks (125 mL) each containing 30 mL seed medium [glucose (1%), yeast extract (0.1%), beef extract (0.1%), casein hydrolysate (0.2%), pH 7.4] for 3 days at 28°C and 200 rpm. The seed cultures of each strain (1 mL each) were used to inoculate 2 x 50

mL Erlenmeyer flasks containing production medium, modified Bennett medium [glucose (1%), yeast extract (0.1%), beef extract (0.1%), soytone (0.2%), pH 7.4] (10 mL in each flask). After incubation for 16 h under the same condition, each mutant strain was fed with 3.0 mM of 3AP-3OP-SNAC and the last flask of each strain was used as a control (No feeding). The feeding was repeated every 12 h for 2 days. After 5 days of incubation, the cultures were centrifuged and the metabolites of each group were extracted twice with equal volume of ethyl acetate and once with 1.5 volume of n-butanol. The organic solvent was evaporated *in vacuo*. The residues were dissolved in methanol and were analyzed by MS and HPLC.

2.3.10 Cloning and Expression of *ptmO and ptmS*

ptmO gene was amplified using the primers *ptmO-BglII* and *ptmO-EcoRI*, and *ptmS* gene was amplified using the primers *ptmS-BglII* and *ptmS-EcoRI*. The PCR products were individually cloned into BamHI and EcoRI sites of the pRSET B to generate the expression vector pTMM080 (pRSET B-*ptmO*) and pTMM081 (pRSET B-*ptmS*) and were introduced into the *E. coli* BL21 (DE3) pLysS (Invitrogen). The empty vector pRSET B was introduced into the *E. coli* BL21 (DE3) pLysS to be used as a control. Additionally, *ptmS* was also cloned into BamHI and EcoRI sites of the pET-28° and was subsequently transformed to *E. coli* BL21 (DE3) pLysS. For protein expression of *ptmS* and *ptmO,* the bacteria were grown in LB medium supplemented with chloramphenicol (50 µg/mL) and ampicillin (100 µg/mL) at 37 °C for 16 h. An aliquot (1 mL) of overnight grown culture was used to inoculate a fresh LB medium (100 mL in 500 mL flask), supplemented with the same antibiotics, at a temperature of 37 °C

under shaking of 230 rpm and was grown until an OD_{600} of 0.6 was reached. Recombinant protein expression was induced with isopropyl β-D-thiogalactopyranoside (IPTG) to a final concentration of 0.1 mM and cultivated further. Fifteen milliliters of culture were harvested from the induced culture by centrifugation at 5000 rpm at 4 °C for 20 min.

2.3.11 The SDS-PAGE of PtmO and PtmS Expressed Proteins

The harvested cells were suspended in 50 mM Tris–HCl (1 mL) and lysed by sonication. The lysed cells were centrifuged at 5000 rpm at 4 °C for 20 min. Cell pellets and supernatant of individual genes were suspended in SDS-PAGE loading buffer (5% 2-mercaptoethanol, 2% SDS, 0.1% bromophenol blue, and 10% glycerol) in 50 mM Tris–HCl buffer (pH 8) and fractioned with 12% separating gel. After electrophoresis, the gels were stained with 0.25% Coomassie brilliant blue dissolved in 50% methanol–10% acetic acid solution and then destained in 30% methanol–10% acetic acid solution.

2.3.12 Enzymatic Assay for PtmO

Enzyme assays (100 μL) were performed at 30 °C for 6 h in 25 mM phosphate buffer (pH 7.5) containing cell-free extract of pRSET B harboring PtmO (50 μL) and cell-free extract of empty vector (50 μL) with 3AP-3OP-SNAC (2 mM). After incubation for 5 h at 30 °C, the reaction was quenched with 100 μL methanol and analyzed by ESI-MS and HPLC.

2.3.13 Enzymatic Assay for PtmS

The cell-free extract of an empty vector was used as a control. The cell-free extract of

pRSET B harboring PtmS (100 µL reaction) was incubated with 50 mM sodium phosphate buffer, 2.0 mM 3ABA, 2.5 mM ATP, 15 mM $MgCl_2$, 1 mM DTT, 1 mM EDTA, and 10% glycerol at 30 °C for 6 h. The enzymatic reaction was quenched by the addition of 100 µL methanol. The protein was precipitated and the supernatant was purified by HPLC using a C_{18} reversed phase column [ODS-A (4.6 mm x 250 mm)] with a detector monitoring at wavelength of 260 nm. A linear gradient between buffer A (25 mM potassium phosphate, pH 5.4) and buffer B (100% acetonitrile) (1 mL/min) was used in the experiment.

2.4 Results and Discussion

2.4.1 *ptmS, ptmI, ptmK, and ptmO* genes, are Critical for the Biosynthesis of Pactamycin.

To investigate the involvement of *ptmS*, *ptmI*, *ptmK*, and *ptmO* in pactamycin biosynthesis, we inactivated the genes individually in *S. pactum* and found that the mutants were not able to produce pactamycin, indicating that these genes are critical in pactamycin biosynthesis. The mutants, *ptmS*, *ptmI*, and *ptmO,* were constructed by an in-frame deletion strategy (Figure 2.3 a), except *ptmK* mutant which was generated using a gene disruption strategy (Figure 2.3 b), as an attempt to obtain an in-frame deletion mutant of *ptmK* was unsuccessful. The resulting double-crossover candidate for *ptmS*, *ptmI*, and *ptmO* strains were confirmed by PCR amplification (Figure 2.4 a, b, and d). The resulting single crossover for *ptmK* was confirmed by PCR amplification (Figure 2.4 c). Additionally, we inactivated the genes in the Δ*ptmH* mutant strain, which produced pactamycin analogs TM-025 and TM-026 (Figure 2.1).

The Δ*ptmH* mutant was used because the products are chemically more stable and are produced in higher quantity than pactamycin.

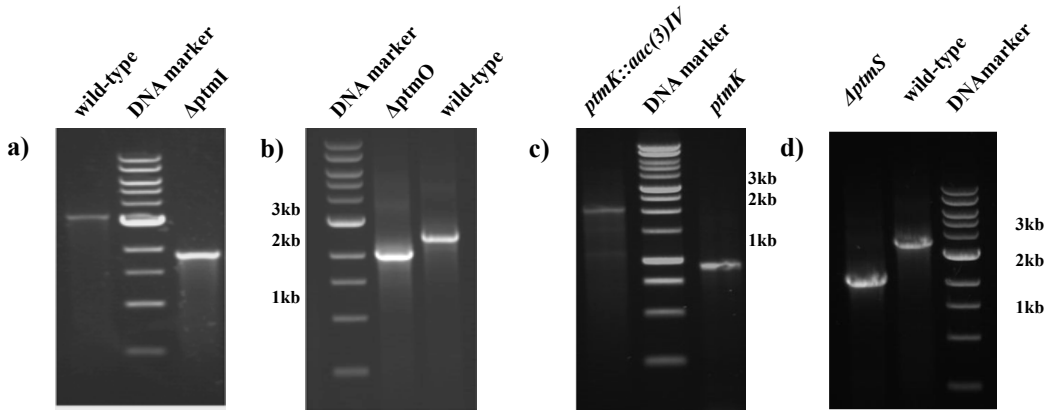

Figure 2.4 Genotypic confirmation of **a)** Δ*ptmI*, **b)** Δ*ptmO*, **c)** Δ*ptmK*::aprR, and **d)** Δ*ptmS* mutant by PCR.

The resulting Δ*ptmH*/Δ*ptmI,* Δ*ptmH*/Δ*ptmK*, and Δ*ptmH*/Δ*ptmO* mutants were cultured and the products were analyzed by ESI-MS. As expected, the results showed that the inactivation of *ptmS, ptmI, ptmK*, and *ptmO* in the Δ*ptmH* mutant entirely diminished the production of TM-025/TM-026 (Figure 2.5 B, E, and H). In addition, the mutants did not give any detectable intermediates, which, based on our observation with other *S. pactum* mutants, indicated that the gene products were involved in the early steps of the pathway (Ito et al., 2009; Lu et al., 2011).

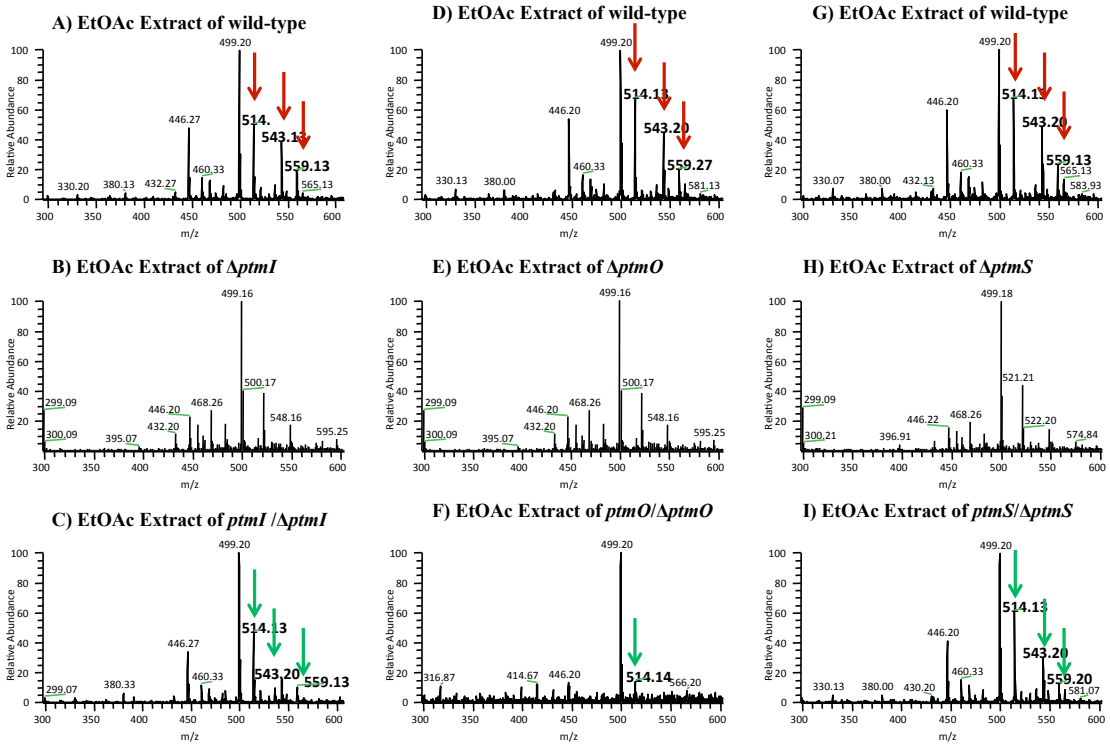

Figure 2.5 ESI-MS analysis of **A)** EtOAc extract of a culture of *S. pactum* wild-type, **B)** EtOAc extract of Δ*ptmI* mutant, **C)** EtOAc extract of Δ*ptmI* complemented with *ptmI*, **D)** EtOAc extract of a culture of *S. pactum* wild-type, **E)** EtOAc extract of Δ*ptmO* mutant, **F)** EtOAc extract of Δ*ptmO* complemented with *ptmO* , **G)** EtOAc extract of a culture of *S. pactum* wild-type, **H)** EtOAc extract of Δ*ptmS* mutant, and **I)** EtOAc extract of Δ*ptmS* complemented with *ptmS*.

Chemical incorporation experiments with either 3ABA or 3AAP using these mutants did not provide any products (data not shown). This is consistent with the notion that discrete PKS enzymes play a role in the conversion of 3ABA to 3AAP moiety. Furthermore, genetic complementation experiments for Δ*ptmI,* Δ*ptmO*, and Δ*ptmS* were performed by re-introducing each of the corresponding genes into the mutant strains. Analysis of the metabolic profile of the complemented strains revealed their

ability to produce pactamycin, confirming that *ptmI, ptmO*, and *ptmS* are directly involved in the biosynthesis of pactamycin (Figure 2.5 C, F, and I).

2.4.2 Characterization of the AMP-Forming Acyl-CoA synthetase Ptms

The putative AMP-forming acyl-CoA synthetase PtmS shares high sequence similarity with the adenylation domains in the loading modules of the rifamycin and ansamitocin PKSs (RifA and AsmA, respectively). The latter proteins convert 3-amino-5-hydroxybenzoic acid (AHBA) to AHBA-AMP, which is then loaded onto an ACP (Admiraal et al., 2003; Yu et al., 2002). However, in contrast to the adenylation domains of RifA and AsmA, which are part of multifunctional multi-modular type I PKSs, PtmS is a discrete protein. To confirm the catalytic function of PtmS, the region encoding PtmS was amplified by PCR from *S. pactum* genomic DNA and cloned into a pRSET B expression vector. The plasmid was transferred into *Escherichia coli* BL21 (DE3) pLysS. The expression of the gene was induced by IPTG to produce the 54 kDa His_6-tagged PtmS (Figure 2.6 A). The expression of PtmS failed to yield a practical amount of soluble protein. We then cloned the gene in the pET-28a vector and attempted to produce soluble Ptms protein by lowering the culture temperature (20 °C) and using LBBS medium. A higher yield of protein was observed; however, a large amount of the protein was expressed as inclusion bodies (Figure 2.6 B). The small amount soluble protein was then subjected to purification using Ni-NTA column; however, this purification was unsuccessful.

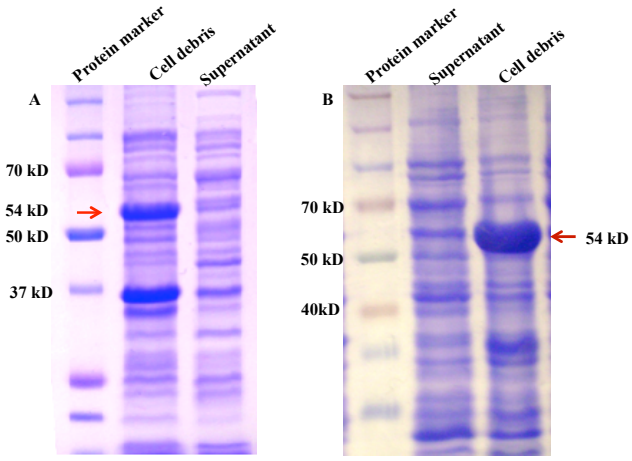

Figure 2.6 SDS PAGE of **A)** Cell extract of *E. coli* harboring the *ptmS* gene in pRSET B grown in LB medium at 20 °C and **B)** Cell extract of *E. coli* harboring the *ptmS* gene in pET-28a grown in LB medium at 20 °C.

Therefore, we used cell-free extract of *E. coli* containing the pRSET B-based recombinant *C*-terminal His_6-tagged PtmS for our enzymatic assays. A cell-free extract of *E. coli* harboring the empty pRSET B vector was used as a negative control. Both were incubated with 3ABA, ATP, coenzyme A, and Mg^{2+} at 28 °C for 3 h, and the product was analyzed by ESI-MS. The results showed no product that is consistent with 3ABA-AMP (m/z 466).

2.4.3 Chemical Complementation of Δ*ptmI*, Δ*ptmI*/Δ*ptmH*, Δ*ptmO*, Δ*ptmO*/Δ*ptmH*, Δ*ptmS*, and Δ*ptmK*::apr^R Mutant Strains with Synthetic 3-[3-aminophenyl]3-oxopropionyl-ACP (3AP-3OP-ACP)

Although we were not able to characterize PtmS biochemically, we hypothesized that 3ABA is activated by PtmS and loaded onto the ACP, PtmI. Claisen condensation between 3ABA-ACP and malonyl-ACP catalyzed by PtmK would yield 3AP-3OP-ACP. To test this hypothesis, we synthesized the acyl-*N*-acetylcysteamine (NAC) thioester of 3-[3-aminophenyl]3-oxopropionate (3AP-3OP), which mimics the β-

ketoacyl-ACP. NAC thioesters have been well-known to resemble the phosphopantetheinyl arm of ACPs and mimic the ACP-bound substrates. 3AP-3OP-SNAC was synthesized from Boc-protected 3ABA **(1)** employing a dehydrative coupling reaction with Meldrum's acid (Figure 2.7). In situ trapping of the β-ketoketene product with NAC followed by a decarboxylation and Boc removal gave 3AP-3OP-SNAC **(4)**.

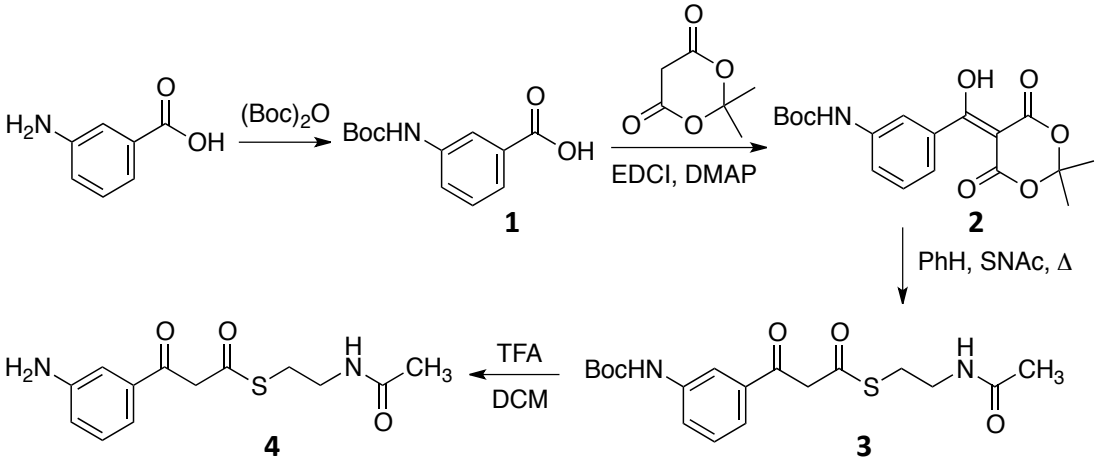

Figure 2.7 Chemical synthesis of 3AP-3OP-SNAC.

3AP-3OP-SNAC was added to the cultures of the Δ*ptmT*/Δ*ptmH* mutant, which is unable to produce 3ABA (Almabruk et al., 2013). The products were analyzed by ESI-MS and MS/MS. The results showed the recovery of TM-025/TM-026 production by the mutant providing strong evidence for the involvement of 3AP-3OP-ACP in the pactamycin pathway (Figure 2.8).

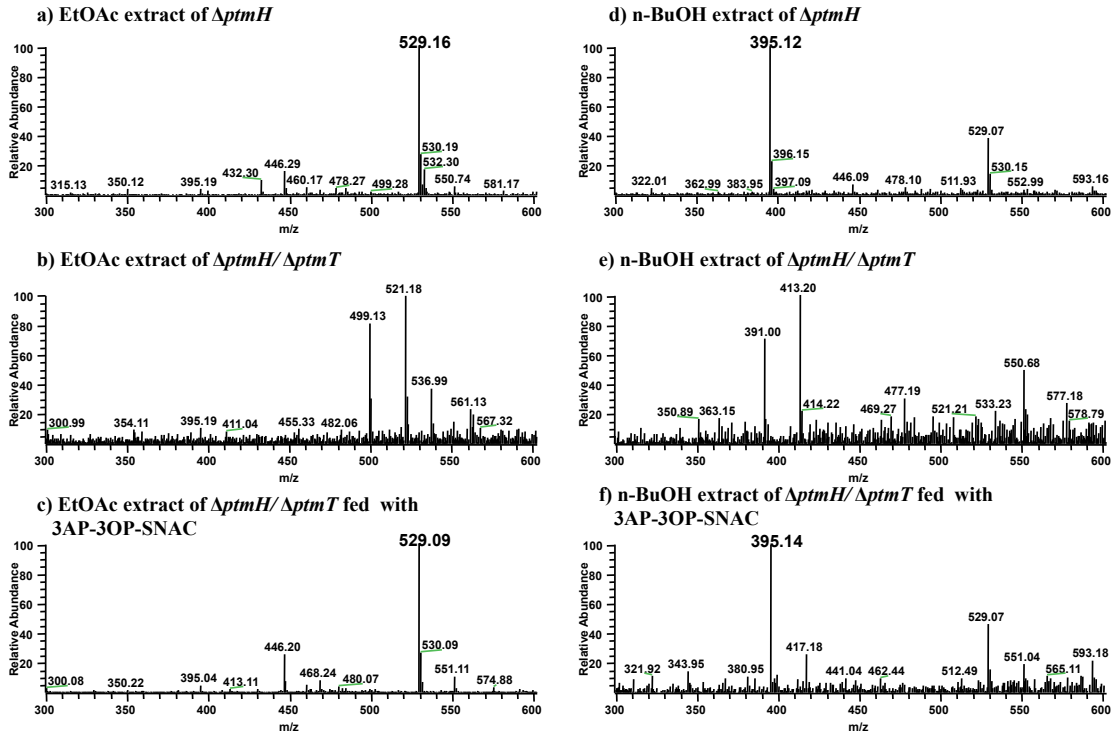

Figure 2.8 ESI-MS analysis of **a)** EtOAc extract of a culture of Δ*ptmH* mutant, **b)** EtOAc extract of Δ*ptmH*/Δ*ptmT* mutant, **c)** EtOAc extract of a culture complemented with Δ*ptmH*/Δ*ptmT* fed with 3AP-3OP-SNAC, **d)** n-BuOH extract of a culture of Δ*ptmH*, **e)** n-BuOH extract of Δ*ptmH*/Δ*ptmT* mutant, and **f)** n-BuOH extract of a culture of Δ*ptmH*/Δ*ptmT* fed with 3AP-3OP-SNAC.

3AP-3OP-SNAC was also added to cultures of Δ*ptmS,* Δ*ptmI,* Δ*ptmK* Δ*ptmO,* Δ*ptmH*/Δ*ptmI,* and Δ*ptmH*/ΔptmK mutants. Interestingly, the compound was unable to rescue the production of pactamycin or TM-025/TM-026 in these mutants. However, as discrete PKSs as well as fatty acid synthases (FASs) usually work in concert, the above result is not entirely unexpected. We proposed that the synthetic β-ketoacyl intermediate has to be initially loaded onto the PtmI, presumably through the ketosynthase PtmK, before being processed by the downstream enzymes (Figure 2.9).

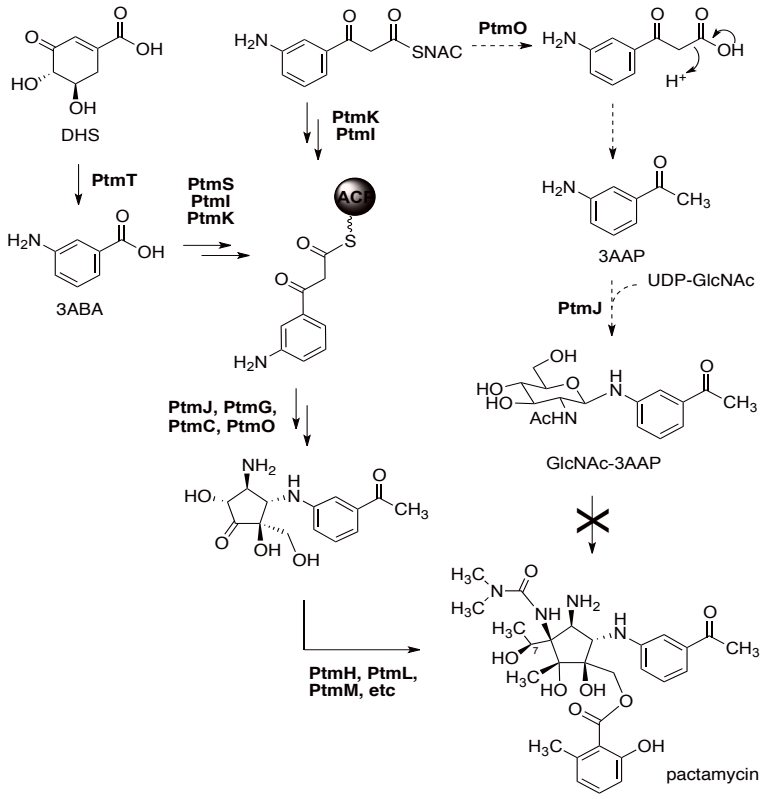

Figure 2.9 Chemical complementation studies with 3AP-3OP-SNAC.

Whereas the Δ*ptmS*, Δ*ptmI*, Δ*ptmK*, Δ*ptmH*/Δ*ptmS*, Δ*ptmH*/Δ*ptmI*, and Δ*ptmH*/Δ*ptmK* mutants fed with 3AP-3OP-SNAC did not produce pactamycin or TM-025/TM-026, they produced a new product with a molecular formula of $C_{16}H_{22}N_2O_6$ (m/z 361.32 $[M+Na]^+$) (Figure 2.10, Figure 2.11, Figure 2.12, and Figure 2.13). We hypothesized that the new product was a result of the glycosylation of AAP. To confirm that, we synthesized authentic GlcNAc-1-AAP compound and confirmed its structure using ^1H NMR (Figure 2.14). HPLC comparison of the product produced by the mutant strains with the synthetically prepared authentic compound confirmed the identity of the product to be GlcNAc-1-AAP. This product may be a result of unspecific hydrolysis of

the NAC thioester by the putative hydrolase PtmO. The resulting β-ketoacid would then undergo non-enzymatic decarboxylation to produce 3AAP, which is subsequently glycosylated by the glycosyltransferase PtmJ to produce GlcNAc-3AAP. The latter compound, however, accumulates in the culture suggesting that it is not an intermediate in pactamycin biosynthesis as previously suggested. Feeding experiments with 3AAP and GlcNAc-3AAP in Δ*ptmT*/Δ*ptmH*, Δ*ptmS*, Δ*ptmI*, and Δ*ptmO* mutants further confirmed that these compounds are not involved in the pactamycin biosynthesis.

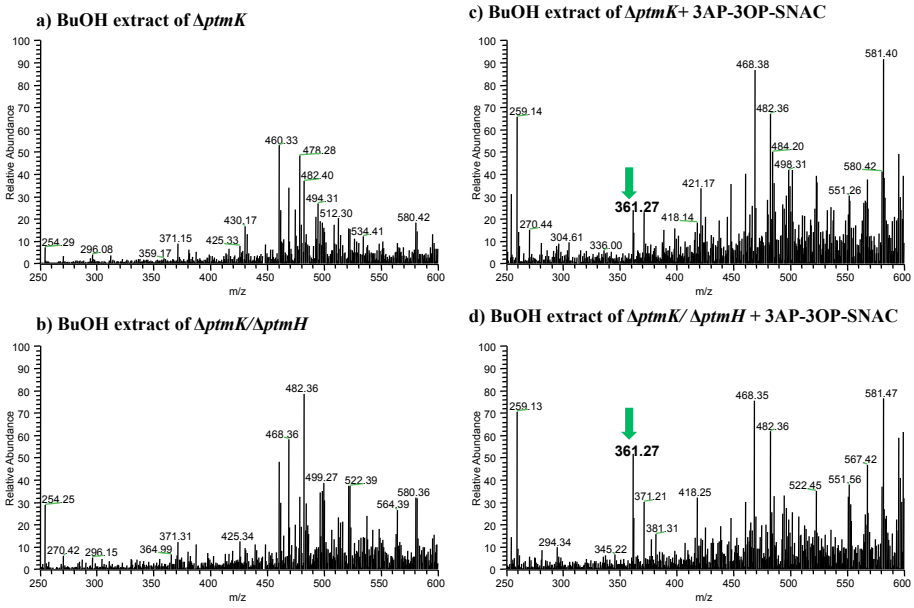

Figure 2.10 ESI-MS analysis of **a)** BuOH extract of a culture of Δ*ptmK*, **b)** BuOH extract of a culture of Δ*ptmK*/Δ*ptmH* mutant, **c)** BuOH extract of a culture of *ΔptmK* fed with 3AP-3OP-SNAC, and **d)** BuOH extract of a culture of Δ*ptmK*/Δ*ptmH* mutant fed with 3-AP-3OP-SNAC. Green arrow indicates m/z 361 for a new product GlcNAc-1-AAP.

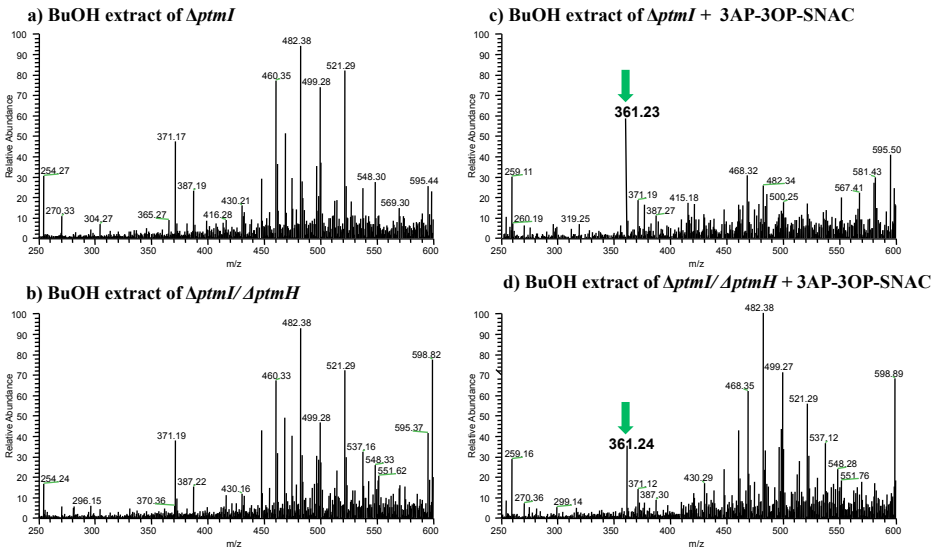

Figure 2.11 ESI-MS analysis of **a)** BuOH extract of a culture of Δ*ptmI*, **b)** BuOH extract of a culture of Δ*ptmI*/Δ*ptmH* mutant, **c)** BuOH extract of a culture of Δ*ptmI* fed with 3AP-3OP-SNAC, and **d)** BuOH extract of a culture of Δ*ptmI*/Δ*ptmH* mutant fed with 3AP-3OP-SNAC. Green arrow indicates m/z 361 for a new product GlcNAc-1-AAP.

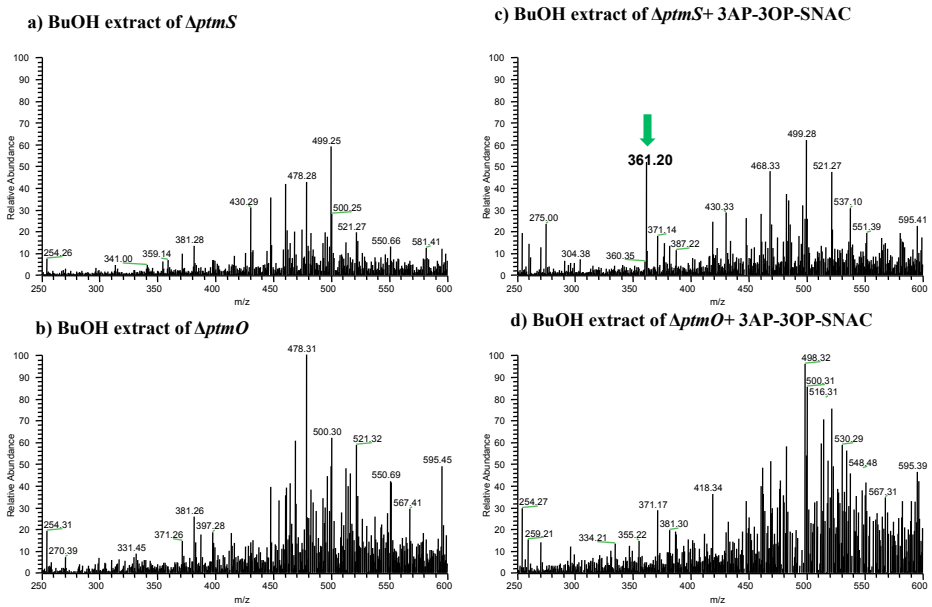

Figure 2.12 ESI-MS analysis of **a)** BuOH extract of a culture of Δ*ptmS*, **b)** BuOH extract of a culture of Δ*ptmO* mutant, **c)** BuOH extract of a culture of Δ*ptmS* fed with 3AP-3OP-SNAC, and **d)** BuOH extract of a culture of Δ*ptmO* mutant fed with 3AP-3OP-SNAC. Green arrow indicates m/z 361.27 for a new product GlcNAc-1-AAP.

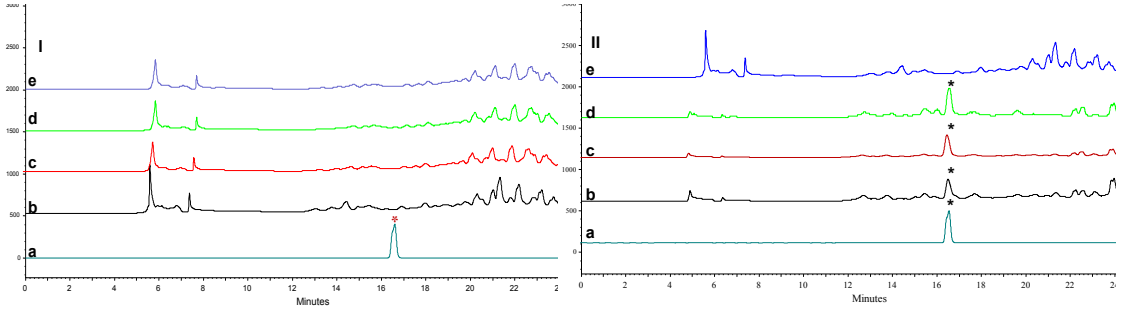

Figure 2.13 HPLC analyses of Δ*ptmK,* Δ*ptmI,* Δ*ptmO*, and Δ*ptmS* mutant strains of *S. pactum*. **I: a)** Authentic GlcNAc-1-AAP, **b)** n-BuOH extract of Δ*ptmK*, **c)** n-BuOH extract of Δ*ptmI*, **d)** n-BuOH extract of Δ*ptmO*, and **e)** n-BuOH extract of Δ*ptmS.* **II: a)** Authentic GlcNAc-1-AAP, **b)** n-BuOH extract of Δ*ptmK* fed with 3AP-3OP-SNAC, **c)** n-BuOH extract of Δ*ptmI* fed with 3AP-3OP-SNAC, **d)** n-BuOH extract of Δ*ptmS* fed with 3AP-3OP-SNAC, and **e)** n-BuOH extract of Δ*ptmO* fed with 3AP-3OP-SNAC.

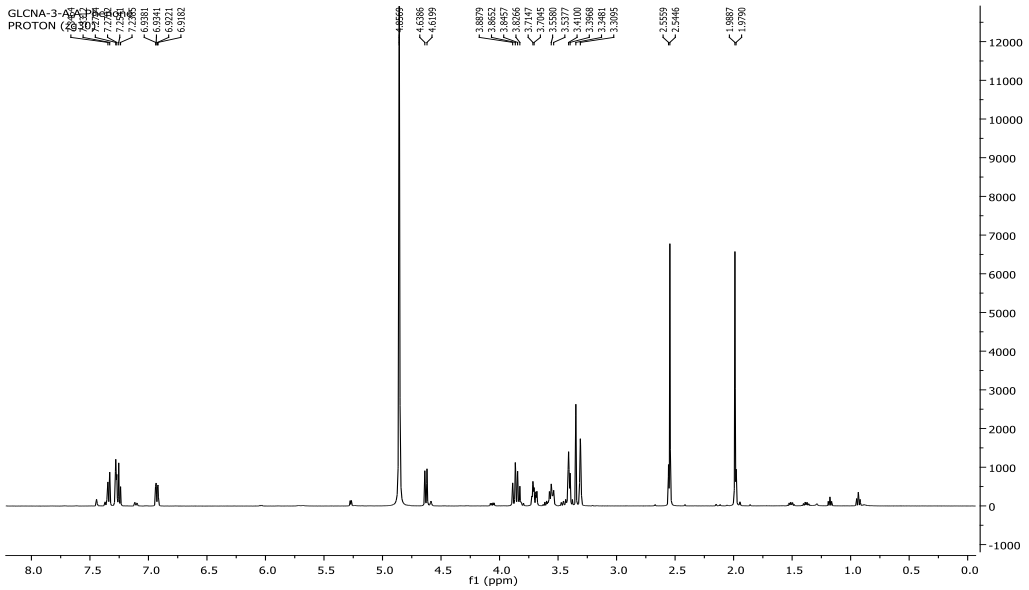

Figure 2.14 ^{1}H NMR spectrum for GlcNAc-1-AAP (500 mHz, CD_3OD).

2.4.4 PtmO Catalyze the Hydrolysis of 3-[3-aminophenyl]3-oxopropionyl-SNAC to Aminoacetophenone

To confirm that PtmO is responsible for the hydrolysis of 3AP-3OP-SNAC, the

compound was added to cultures of Δ*ptmO* mutant. As expected, the mutant neither produced pactamycin nor GlcNAc-3AAP, (Figure 2.12 b and d), suggesting that the hydrolytic functionality of PtmO and its important role in the biosynthesis of pactamycin. To characterize the catalytic function of PtmO *in vitro*, we cloned the gene in the expression vector pRSET B and heterologously expressed it in *E. coli* BL21(DE3)pLysS to give the 32 kDa N-terminal His_6 sequence. The recombinant protein was analyzed by SDS-PAGE (Figure 2.15 A).

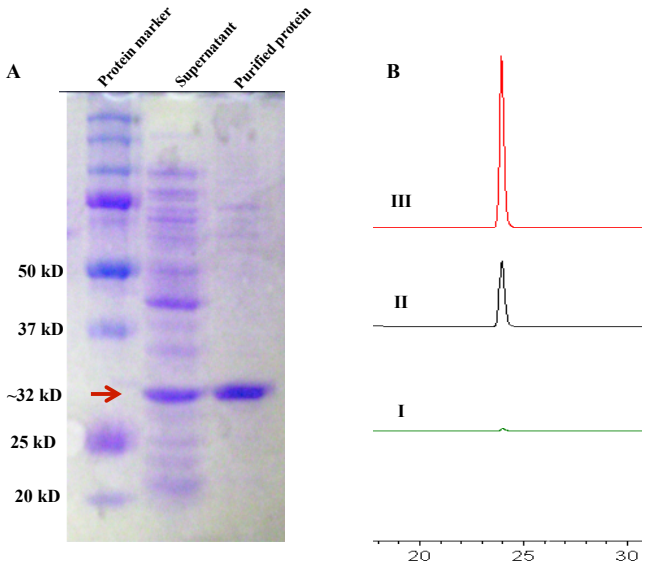

Figure 2.15 A) SDS page of purified PtmO and **B**) HPLC chromatogram of 3AP-3OP-SNAC incubated with cell free extract of **I)** *E. coli* harboring empty vector pRSET B, **II)** *E. coli* harboring pRSET B-PtmO, and **III)** Standard 3AAP.

The HPLC analysis of the reaction product revealed the conversion of 3OP-3AP-SNAC to 3AAP, no product was observed when a cell free extract of empty pRSET B was used (Figure 2.15 B). The results did not only confirm the activity of PtmO as a

hydrolase but also indicated that the β-ketoacetate product can indeed undergo a spontaneous decarboxylation reaction.

In conclusion, this study provided insights into the mode of formation of the 3AAP moiety in pactamycin biosynthesis, involving a set of discrete PKS enzymes. Although 3AAP and GlcNAc-3AAP have previously been proposed to be part of the pactamycin pathway, these compounds appeared to have no direct involvement in pactamycin biosynthesis. Further investigations are necessary to shed light into the fate of the PKS product in this interesting natural product biosynthetic pathway.

Chapter 3 : Interrogating the Tailoring Steps of Pactamycin Biosynthesis and Accessing New Pactamycin Analogues

Mostafa E. Abugrain, Wanli Lu, Yuexin Li, Jeffrey D. Serrill, Adam Alani, Jane X. Kelly, Jane Ishmael, and Taifo Mahmud

In progress

3.1 Abstract

Pactamycin is a bacterial-derived aminocyclitol antibiotic with a wide-range of biological activity. The unique chemical structure and potent biological activity have made pactamycin an interesting lead compound for drug discovery and development. Whereas the biosynthetic origin of pactamycin has been well-studied, the overall biosynthetic scheme of pactamycin remains elusive. Using a combination of genetic and biochemical approaches, we investigated the tailoring processes of pactamycin biosynthesis in *Streptomyces pactum*. The results provide insight into the natural sequence of events during the tailoring steps of pactamycin biosynthesis and explain the unusual production of various pactamycin analogs by *S. pactum* mutants. We also identified two new pactamycin analogs that have better therapeutic index than pactamycin against malarial parasites.

3.2 Introduction

Pactamycin, a member of the aminocyclitol family of natural products, is produced by the soil bacterium *Streptomyces pactum*. Since its discovery over 50 years ago (Bhuyan, 1962), pactamycin has continued to attract significant attention due to its interesting chemical structure and broad-range of biological activities (Figure 3.1). Structurally, it consists of a highly decorated cyclopentitol core unit attached to two aromatic rings, 3-aminoacetophenone (3AAP) and 6-methylsalicylic acid (6MSA), and a 1,1-dimethylurea (Weller and Rinehart, 1978). Pactamycin showed potent antibacterial activities against Gram-(+) and Gram-(-) bacteria (Bhuyan, 1962), as well as antiviral (Taber et al., 1971) and antitumor activities (White, 1962). More recent

studies by our group and others have shown its potent antiprotozoal (antimalarial and antileishmanial) activities (Almabruk et al., 2013; Hanessian et al., 2013; Lu et al., 2011; Otoguro et al., 2010).

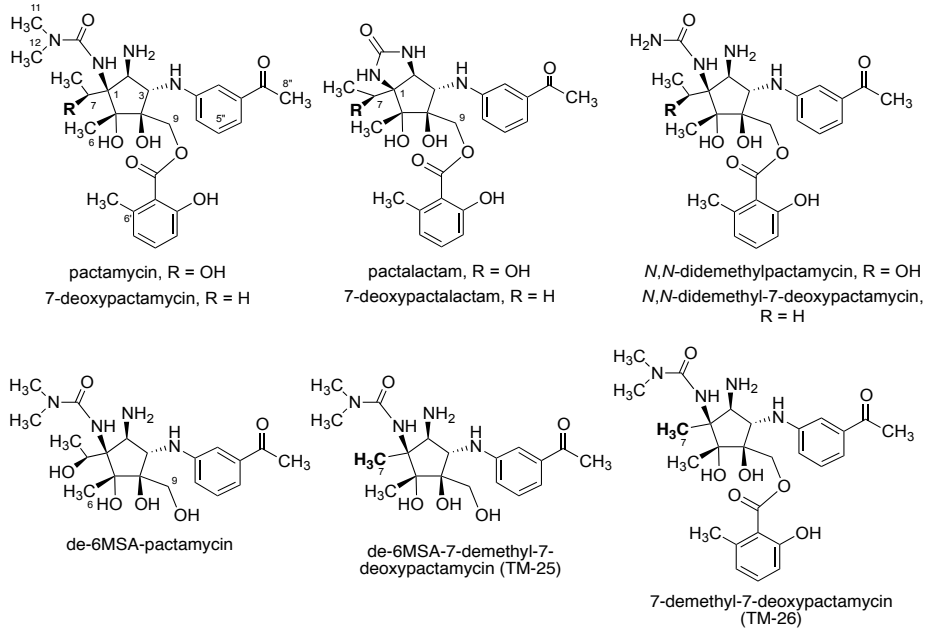

Figure 3.1 Chemical Structures of pactamycin analogs.

Due to its structural complexity, pactamycin has posed significant synthetic challenges. However, a number of sophisticated chemical synthetic strategies to access this densely functionalized natural product have emerged recently, first reported by (Hanessian et al., 2011), involving 32 linear steps from threonine with ~ 3% overall yield, and later by Johnson and co-workers (Malinowski et al., 2013), in 15 steps from acetylacetone with 1.9% overall yield.

In *S. pactum*, pactamycin is derived from three major metabolic pathways: (1) the shikimate pathway which leads to 3-aminobenzoic acid (3ABA) and subsequently

converts to the 3AAP moiety, (2) the amino sugar metabolic pathway which provides the precursor of the aminocyclopentitol moiety, and (3) the acetate pathway which produces 6MSA through catalysis by an iterative type I polyketide synthase (PKS). Although the biosynthetic origin of each component of pactamycin has been well established (Hirayama et al., 2013; Ito et al., 2009; Rinehart et al., 1980), the overall biosynthetic scheme of pactamycin remains elusive. A number of studies involving genetic knockouts in the producing bacterium have been done (Ito et al., 2009; Lu et al., 2011), yet, little is known concerning stepwise reactions involved in pactamycin biosynthesis.

Previously, we reported that inactivation of *ptmD,* an *S*-adenosylmethionine (SAM) dependent *N*-methyltransferase gene, in *S. pactum* resulted in a mutant that produces *N*, *N*-didemethylpactamycin and *N*, *N*-didemethyl-7-deoxypactamycin (Lu et al., 2011). Furthermore, inactivation of *ptmH,* a radical SAM-dependent *C*-methyltransferase gene, resulted in a mutant that produces de-6MSA-7-demethyl-7-deoxypactamycin (TM-025) and 7-demethyl-7-deoxypactamycin (TM-026) (Almabruk et al., 2013; Lu et al., 2011). However, inactivation of *ptmQ,* a PKS gene that is involved in the formation of 6MSA, resulted in a mutant that produces de-6MSA-pactamycin (Ito et al., 2009). Although the results are consistent with the putative function of the genes, the presence of other functionalities intact in those products are rather puzzling. This may be due to the substrate promiscuity of the tailoring enzymes involved in pactamycin biosynthesis, which does not only make it

difficult to determine the sequence or the timing of the tailoring steps but also impedes the production of structurally less-complex analogs of pactamycin.

3.3 Materials and Methods

3.3.1 General Experimental Procedures

Low-resolution electrospray ionization (ESI) mass spectra were recorded on a ThermoFinnigan Liquid Chromatograph-Ion Trap Mass Spectrometer. High Performance Liquid Chromatography was carried out on a C_{18} column (C_{18} Symmetry 10 x 150 mm, Waters) with a detector set at 355 nm. Thin layer chromatography was performed on aluminum sheets with silica gel 60 F_{254} (EMD chemicals Inc.).

3.3.2 Bacterial Strains and Plasmids Used in this Study

Pactamycin producing *S. pactum* ATCC 27456 was purchased from the American Type Culture Collection (ATCC). *Escherichia coli* DH10B was used as a host strain for the construction of recombinant plasmids. *E. coli* ET12567 (pUZ8002) was used as a donor strain in conjugation experiments. pBlueScript II (SK-) (Stratagene) and pGEM-T Easy (Promega) were used as cloning vectors. pTMN002, a pJTU1278+ derivative containing the apramycin-resistance cassette, was used as a vector for gene inactivation (He et al., 2010; Ito et al., 2009). All bacterial strains and plasmids used in this study are listed in Table 3.1.

Table 3.1 Strains and plasmids used in this study.

Strains	Relevant genotype/comments	Source/Ref
Escherichia coli DH10B	*F⁻ mcrA Δ(mrr-hsdRMS-mcrBC)ϕ80lacZΔM15 ΔlacX74 recA1 endA1 araD139 Δ(ara, leu)7697 galU galK λ⁻ rspL nupG*	GibcoBRL
E. coli ET12567(pUZ8002)	*dam dcm hsdS,* pUZ8002	(Paget et al., 1999)
Streptomyces pactum ATCC 27456	Wild-type pactamycin producing strain	ATCC
S. pactum MT-ptmH	*ptmH* disruption mutant	(Lu et al., 2011)
S. pactum MT-ptmD	*ptmD* disruption mutant	(Lu et al., 2011)
S. pactum MT-ptmQ	*ptmQ* disruption mutant	(Ito et al., 2009)
S. pactum MT-ptmH/ptmD	*ptmH/ptmD* disruption mutant	(Lu et al., 2012)
S. pactum MT-ptmD/ptmQ	*ptmD/ptmQ* disruption mutant	(Lu et al., 2012)
Staphylococcus aureus ATCC 12600	Marker strain for antibacterial assay	ATCC
Bacillus subtilis ATCC 6081	Marker strain for antibacterial assay	ATCC
Pseudomonas aeruginosa ATCC 9721	Marker strain for antibacterial assay	ATCC
E. coli ATCC 11775	Marker strain for antibacterial assay	ATCC
Plasmids		
pBlueScript II SK(-)	ColE1-based phagemid vector with f1 (-) and pUC origins; T3, T7 and lac promoters; *bla*.	Stratagene
pGEM-T	High copy number PCR cloning vector containing T7 and SP6 RNA polymerase promoters flanking a multiple cloning region within the alpha-peptide coding region of the enzyme beta-galactosidase; *bla*.	Promega
pOJ446	*E. coli-Streptomyces* shuttle cosmid for conjugal transfer; *aac(3)IV*	(Kieser et al., 2000)
pHZ1358	*tsr*, *bla*, *oriT, ori*(pIJ101)	(Sun et al., 2002)
pJTU1278+	pHZ1358 derivative containing lacZ and MCS	(Ito et al., 2009)
pTMN002	pJTU1278+ derivative containing a 1 kb *aac(3)IV* apramycin resistance cassette from pOJ446	(Ito et al., 2009)
pTMN003	Two 1 kb PCR fragments upstream and downstream of the *ptmD* gene in pTMN002	(Lu et al., 2012)
pTMW026	Two 1 kb PCR fragments upstream and downstream of the *ptmH* gene in pTMN002	(Lu et al.,

		2012)
pTMN101	1 kb *aac(3)IV* apramycin resistance cassette in *ptmQ* gene	(Ito et al., 2009)
pTMN001	*ptmQ-aac(3)IV* fragment from pTMN101 in pHZ1358	(Ito et al., 2009)
pSET152	*lacZ*α, *ori*(pUC19), *oriT*(RP4), *int-attP*(φC31), *aac(3)*IV	(Kieser et al., 2000)
pTMN052	pTMW050 containing complete structural gene of *ptmD*	(Lu et al., 2012)
TIP3	Fosmid clone containing part of the ptm cluster	(Ito et al., 2009)
5A7	Fosmid clone containing part of the ptm cluster	(Ito et al., 2009)

3.3.3 General DNA Manipulations

Genomic DNA of *S. pactum* ATCC 27456 was prepared by standard protocol (Kieser et al., 2000) or using the DNeasy Tissue Kit (QIAGEN). DNA fragments were recovered from an agarose gel by using the QIAquick Gel Extraction Kit (QIAGEN). Restriction endonucleases were purchased from Invitrogen or Promega. Preparation of plasmid DNA was done by using a QIAprep Spin Miniprep Kit (QIAGEN). All other DNA manipulations were performed according to standard protocols (Kieser et al., 2000; Sambrook and Russell, 2001). PCR was performed in 30 or 35 cycles by using a Mastercycler gradient thermocycler (Eppendorf). High-fidelity Platinum *Taq* DNA polymerase (Invitrogen) was used to amplify the upstream and downstream fragments of the target genes. PCR products were ligated into pBluescript SK(-) plasmid at EcoRI/HindIII and EcoRI/Xbal sites and sequenced to confirm that no mutation occurred during PCR amplification. The pTMN002 was used to transfer the target construct into *S. pactum*. *Taq* DNA Polymerase, recombinant (Invitrogen) or AccuTaq LA DNA Polymerase (Sigma), was used for PCR screening for in-frame deletion

mutant strains. Oligodeoxyribonucleotides, for PCR primers, were synthesized by Sigma-Genosys. The nucleotide sequence of the gene fragments was determined at the Center for Genome Research and Biocomputing (CGRB) Core Laboratories, Oregon State University. ORFs were analyzed by FramePlot (Ishikawa and Hotta, 1999) analysis and BLAST program (Altschul et al., 1990).

3.3.4 Seed and Production Media Used in this Study

All mutant strains were grown on BTT agar [glucose (1%), yeast extract (0.1%), beef extract (0.1%), casein hydrolysate (0.2%), agar (1.5%), pH 7.4] at 30 °C for 3 days. Single colonies were used to inoculate the BTT seed cultures and incubated at 30 °C for 2 days. Production cultures were prepared in modified Bennett medium (Sakuda et al., 2001) (50 mL) and inoculated with seed cultures [10% (V/V)]. The production cultures were incubated at 30 °C for 6 days under vigorous shaking (200 rpm). The mycelia were centrifuged and the supernatants were extracted twice with equal volumes of ethyl acetate and once with equal volume of n-butanol. The organic solvent was evaporated *in vacuo* and the residues were dissolved in 2 mL MeOH and analyzed by MS and reverse-phase HPLC.

3.3.5 Generation of *ΔptmD/ΔptmQ* and *ΔptmH/ΔptmD* Mutant Strains

For the construction of *ptmQ* in-frame deletion knock-out plasmid, two ~1.2 kb PCR fragments upstream and downstream of the *ptmQ* gene were generated with primers, *ptmQ*-F1/*ptmQ*-R1 and *ptmQ*-F2/*ptmQ*-R2, respectively, and separately cloned into pBlueScript II SK(-) cloning vector for DNA sequencing. HindIII and EcoRI were used to digest the upstream DNA fragment, EcoRI and XbaI to digest the downstream

DNA fragment, and HindIII and XbaI to digest pTMN002, which was ligated to create pTMW077. The *ptmQ* gene in-frame deletion was performed as described previously (Ito et al., 2009; Lu et al., 2011). Briefly, pTMW077 was introduced into *S. pactum ΔptmD* mutant strain by conjugation with the *E. coli* donor strain ET12567 (pUZ8002). Apramycin resistant strains representing single crossover mutants were obtained and subsequently grown on nonselective mannitol-soy flour agar containing $MgCl_2$ (10 mM, MS-Mg) to allow the formation of double crossover recombinants. Apramycin sensitive colonies were counter-selected by replica plating onto MS-Mg agar with and without apramycin (50 μg/mL). The resulting double-crossover candidate strains were screened by PCR amplification with external primers *ptmQ*-P1 and *ptmQ*-P2 (Table 3.2) flanking the targeted *ptmQ* gene. The resulting PCR fragment from putative double crossover mutants was subcloned into pGEM-T Easy vector and sequenced to confirm that part of *ptmQ* has been removed from the genomic DNA. Similarly, pTMN003 (two 1 kb PCR fragments upstream and downstream of the *ptmD* gene in pTMN002) was introduced into *S. pactum ΔptmH* strain (Lu et al., 2011). Putative *S. pactum ΔptmH-ptmD* mutant strains were screened by PCR amplification with primers *ptmD*-P1 and *ptmD*-P2 and confirmed by DNA sequencing.

Table 3.2 Primers used in this study.

Primer	Sequence*
ptmD-F1	5'- CCCAAGCTTGCTGAAGGGCTCCACCGA -3'
ptmD-R1	5'- CCG**GAATTC**GGCCGAAATCCCGTCCAC-3'
ptmD-F2	5'- CCG**GAATTC**GTCGGCCGGTTCAGCTGA -3'
ptmD-R2	5'- TGC**TCTAGA**CAGGAGCTGAAGGAGATC -3'
ptmD-P1	5'- GCGACGGACAGAACCGCCTCAA -3'

ptmD-P2	5'- ACGCCCTGCTGGTCTCCTTCCA -3'
ptmD-C1	5'- CG**CATATG**ATATCCGTGGACGGGATTTCGGC -3'
ptmD-C2	5'- TA**GAATTC**TCAGCTGAACCGGCCGACG -3'
ptmH-F1	5'- CCC**AAGCTT**GCTCGGCGTAGTAGGGGTCC -3'
ptmH-R1	5'- CCG**GAATTC**TCCCCAGACGCCTTGCTGTA -3'
ptmH-F2	5'- CCG**GAATTC**CCCAACACCGAGTACCACGA -3'
ptmH-R2	5'- TGC**TCTAGA**CGTCGCTTCCATCTTCGTCA -3'
ptmH-P1	5'- TGAAGCCCAGCAGCTCCACC -3'
ptmH-P2	5'- CGACCAGGATGACCTCGAACC -3'
ptmH-C1	5'- AT**CATATG**GCCCCATTGCGTGGGAGAT -3'
ptmH-C2	5'- ATGGATC**CAATTG**TCAAACGCGCGTGAACTGGTG -3'
ptmQ-P1	5'- AGGTCGCCTCCTGCCTGGTG-3'
ptmQ-P2	5'- CGGCCTCTTCGTCGCCAAGG-3'

*nucleotides underlined refer to restriction sites

3.3.6 Isolation, Purification, and Characterization of TM-101 and TM-102

The mutant strains of *ΔptmD/ΔptmQ* and *ΔptmD/ΔptmH* were grown on BTT agar [glucose (1%), yeast extract (0.1%), beef extract (0.1%), casein hydrolysate (0.2%), agar (1.5%), pH 7.4] at 30 °C for 3 days. Single colonies were used to inoculate the BTT seed cultures (400 mL) and incubated at 30 °C for 3 days. Production cultures were prepared in modified Bennett medium (4 L) and inoculated with seed cultures [10% (V/V)]. The production cultures were incubated at 30 °C for 5 days under vigorous shaking (200 rpm). The mycelia were centrifuged and the supernatants were extracted twice with equal volume of ethyl acetate and once with 1.5 volume of n-butanol. The organic layer was evaporated to dryness *in vacuo*. The n-butanol extract (4 g) was applied to flash column chromatography. The extraction strategy for the isolation of TM-101 and TM-102 is illustrated in Figure 3.2. Fractions eluted with chloroform: methanol (95:5 and 90:10) contained TM-101 and TM-102.

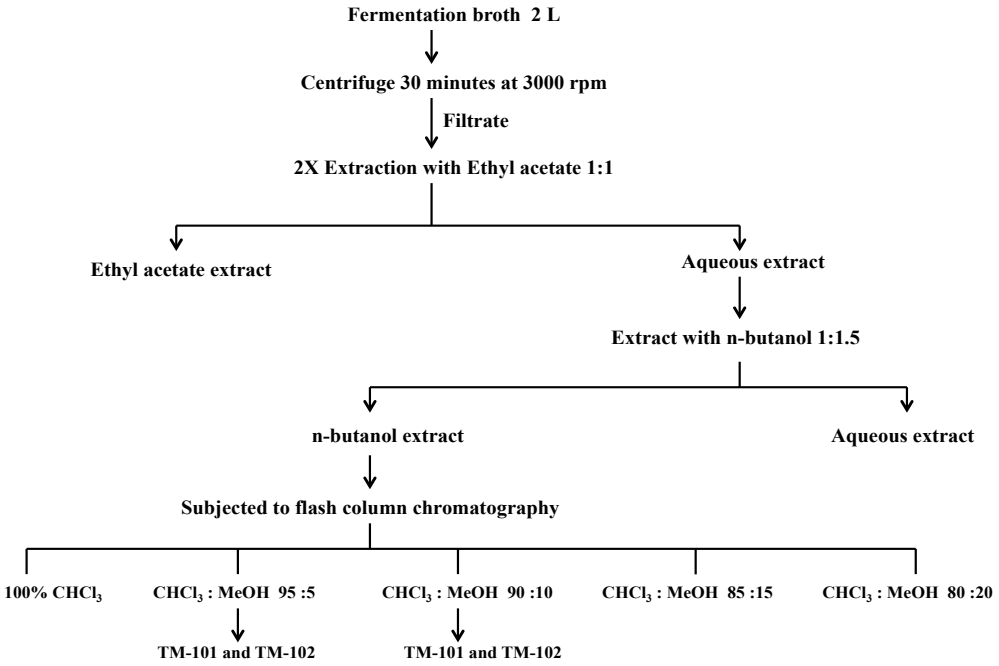

Figure 3.2 Extraction strategy for the isolation of TM-101 and TM-102**.**

The sample containing target compound was loaded onto a silica gel column, which was eluted with chloroform: methanol-5% NH_4OH (9:1) to give fractions that contained TM-101 (~14 mg) or TM-102 (11 mg). TM-101: Yellowish powder ^1H NMR (700 MHz, MeOD) (+)-ESIMS: *m/z* = 367 $[M+H]^+$. HR-ESIMS *m/z* 367.1970 $[M+H]^+$, calcd. for $C_{17}H_{27}N_4O_5$ *m/z* 367.1981. TM-102: Yellowish powder, ^1H NMR (700 MHz, MeOD) (+)-ESIMS: *m/z* = 381 $[M+H]^+$. HR-ESIMS *m/z* 381.2132 $[M+H]^+$, calcd. for $C_{18}H_{29}N_4O_5$ *m/z* 381.2138.

3.3.7 Antimalarial Activity Assay

Antimalarial activity assays were performed at the Oregon Translational Research and Drug Development Institute (OTRADI). *Plasmodium falciparum* strains (chloroquine-sensitive clone D6 and chloroquine-resistant and MDR clone Dd2) were obtained from

the Malaria Research and Reference Reagent Resource Center (MR4) (Manassas, VA). A minor modification to the method of Trager and Jensen, 1976 was used to culture the parasite strains. The cultures were maintained in human erythrocytes, (Lampire Biological Laboratories, Pipersville, PA), and were suspended at 2% hematocrit in RPMI 1640 (Sigma) containing 45 μg/L hypoxanthine (Lancaster), 50 μg/L gentamicin (Invitrogen), and 0.5% Albumax (Invitrogen). The cultures were incubated at 37 °C with a gaseous phase of 5% O_2, 5% CO_2, and 90% N_2, according to standard protocol. *In vitro* antimalarial activity was determined by a SYBR Green I fluorescence-based method described previously (Smilkstein et al., 2004). Frozen stock solutions of each test drug (1 mM in DMSO) were thawed, heated to a temperature of 37 °C, and mixed thoroughly before startup. Drug solutions were serially diluted with culture medium, and then distributed to asynchronous parasite cultures on 96-well plates in quadruplicate in a total volume of 100 μL to reach 0.2% parasitemia with 2% hematocrit in a total volume of 100 μL. Automated pipeting and dilution was carried using programmable Precision XS (Bio-Tek, Winooski, VT) and Sciclone ALH3000 (Caliper, Hopkinton, MA) robotic stations. Then, the plates were incubated for 72 h at temperature and gas condition as described previously. To each plate, 100 μL of lysis buffer with SYBR Green I (Smilkstein et al., 2004; Winter et al., 2006) was added. The plates were then incubated at room temperature for 1 h and placed in a 96-well fluorescence plate reader (Synergy4, BioTek, Winooski, VT) with excitation and emission wavelength at 485 nm and 528 nm, respectively. The half

maximal inhibitory concentration (IC_{50}) was determined by non-linear regression analysis of logistic dose-response curves (GraphPad Prism software).

3.3.8 Antibacterial Activity Assay

Agar diffusion and micro-dilution assays were used to determine the antibacterial activity of pactamycin and pactamycin analogs. The biological markers, *E. coli, P. aeruginosa, B. subtilis, and S. aureus*, were streaked on nutrient agar (Difco) and grown overnight at 37 °C. Colonies were transferred to liquid broth media and were further incubated at 37 °C for 24 h. The inoculum density was measured using density BioRad, SmartSpec 3000 until an OD_{600} was reached. Plates were prepared by mixing an inoculum (500 μL) with thoroughly mixed warm nutrient agar (50 mL) and the mixture was poured into 25 mL plates. The agar plates were allowed to solidify and dry for 30 min prior to performing the assay. 20 μL of various concentrations of pactamycin and its analogs were impregnated on sterile bland paper disks (Becton-Dickinson), and the paper disks were kept dried at room temperature. The disks were then placed onto inoculated agar plates and incubated at 37 °C for 24 h. 0.25% 3-(4,5-Dimethylthiazol-2-yl)-2,5-Diphenyltetrazolium Bromide (MTT) developing dye (1 mL) was added to plates to produce a contrast background of the inhibition zone. Micro-dilution assays were performed in a 96-well plate. The compounds were serially diluted and added to the bacterial suspension at final concentrations of 1 mM- 10 nM. After incubation at 37 °C for 24 h, 0.25% MTT developing dye (50 μL) was added. Each assay was done in triplicate.

3.3.9 Cell Viability by the WST-8 Assay

10,000 HCT116 cells per well were seeded onto a 96-well plate. Cells were treated for 48 h with either TM-101 (5, 50, 500 or 5000 nM), TM-102 (5, 50, 500 or 5000 nM), or pactamycin (5, 25, 50, 100 nM) in triplicate. Cells were treated for 24 or 48 h with either TM-101 (0.5, 1, 2 or 4 μM TM-101), TM-102 (1, 2, 3 or 5 μM), or pactamycin (0.5, 2, 5 or 12.5, 25, 50, 100 nM) in triplicate for the narrow range concentration assays. WST-8 [2-(2-methoxy-4-nitrophenyl)-3-(4-nitrophenyl)-5-(2,4-disulfophenyl)-2H-tetrazolium, monosodium salt] (Dojindo, Rockville, Maryland) was added to each well to produce an orange colored formazan product (soluble in tissue culture medium). Absorbance was measured at 450 nm and the percent cell viability was calculated relative to the no treatment and solvent only wells.

3.4 Results and Discussion

3.4.1 Double Knockout of *ptmD* and *ptmH*

To investigate the tailoring steps of pactamycin biosynthesis and to obtain less-complex analogs of pactamycin, we constructed *S. pactum* Δ*ptmD*/Δ*ptmH* double mutant. The mutant was generated by directed in-frame deletion of *ptmD* in a Δ*ptmH* strain. Analysis of the fermentation broths of this double mutant by ESI-MS revealed that the mutant produced a new pactamycin analog having *m/z* 367 $[M+H]^+$ and was identified as TM-101 (Figure 3.3 D, E, and F).

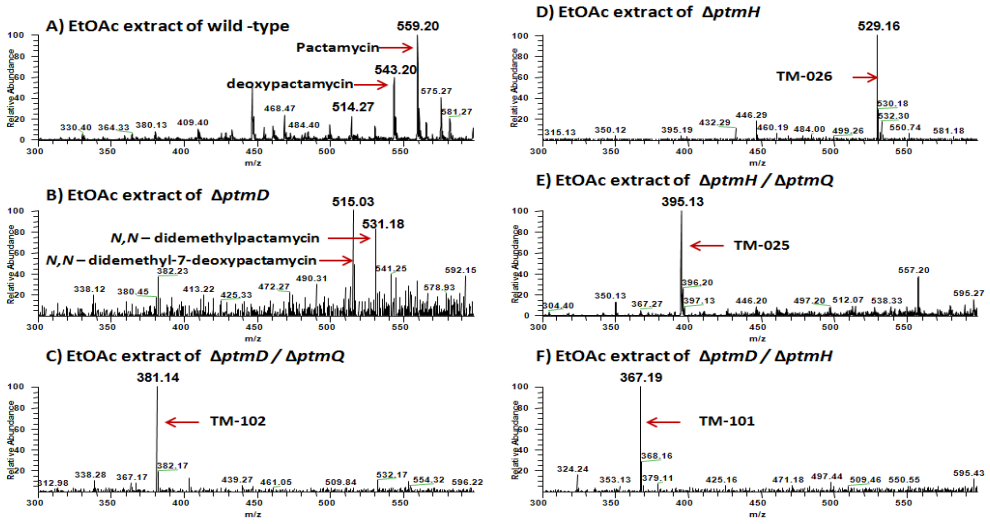

Figure 3.3 Mass spectra for the ethyl acetate extracts obtained from the culture broths of the wild-type and the mutant strains of *S. pactum*. **A)** wild-type, **B)** Δ*ptmD*, **C)** Δ*ptmD*/Δ*ptmQ*, **D)** Δ*ptmH*, **E)** Δ*ptmH*/Δ*ptmQ*,and **F)** Δ*ptmD*/Δ*ptmH*. Arrows indicate the masses of pactamycin and pactamycin analogs.

3.4.2 Structural Characterization of TM-101

To fully characterize the chemical structure of TM-101, we cultured the Δ*ptmD*/Δ*ptmH* mutant (4 L) and isolated the product by solvent partitioning, silica gel column chromatography, and HPLC. The pure compound was analyzed using HR-ESI-MS as well as 1D and 2D NMR. HR-ESI-MS data revealed a molecular formula of $C_{17}H_{26}O_5N_4$ for TM-101. The ^{1}H and ^{13}C NMR spectral data for TM-101 are listed in Table 3.3. The ^{1}H NMR spectrum for TM-101 showed three methyl proton singlets corresponding to 6-CH_3, 7-CH_3, and 8'-CH_3 groups, whereas signals for *N,N*-$(CH_3)_2$, 8-CH_3, and 6′-CH_3 of pactamycin were missing in this spectrum. In the aromatic region, there are a singlet, two doublets, and a triplet, which are consistent with the protons of 3AAP, but not with those of 6MSA, suggesting that the latter moiety in TM-101 is lacking.

Table 3.3 ^{1}H and ^{13}C NMR spectral data of TM-101 in CD_3OD (700 mHz).

Position	σ_C	σ_H (int, mult,J in Hz)	Position	σ_C	σ_H (int, mult,J in Hz)
1	64.60		1’	137.82	
2	62.94	3.70 (1H, d, 10.8)	2’	111.85	7.43 (1H,s,)
3	64.65	4.15 (1H, d, 10.8)	3’	148.56	
4	81.62		4’	118.07	7.06 (1H, dd, 1.9,7.7)
5	81.43		5’	128.92	7.26 (1H, t, 7.84)
6	13.66	1.43 (3H, s)	6’	117.27	7.30(1H, d, 7.7)
7	15.26	1.63 (3H, s)	7’	200.04	
8	62.51	3.47 (1H,d,11.48) 4.08 (1H,d,11.48)	8’	25.41	2.55 (3H, s)
9	161.40				

Similar observation was also made in the ^{13}C NMR spectrum for TM-101, in which only 17 carbon signals were present, including a carbonyl carbon signal (δc 200.0 ppm), which belongs to 3AAP. Together these data suggested that TM-101 lacks the *N*, *N*-$(CH_3)_2$, 8-CH_3, 7-OH groups, and 6MSA moiety as shown in Figure 3.4. Further analysis using ^{1}H NMR, ^{13}C NMR, HSQC, HMBC, and COSY (Figure 3.5, Figure 3.6, Figure 3.7, Figure 3.8, and Figure 3.9), unambiguously confirmed the chemical structure of TM-101 as de-6MSA-*N*,*N*-didemethyl-7-demethyl-7-deoxypactamycin.

The production of TM-101 by the Δ*ptmD/*Δ*ptmH* strain suggests that the *N,N*-dimethylation of the urea group may occur after, rather than prior to , *C*-methylation at C-7, because the inactivation of *ptmD* alone resulted in the production of *N*,*N*-didemethyl-7-deoxypactamycin and *N*, *N*-didemethylpactamycin, which contain a C-8 methyl group. Also, the production of TM-025 and TM-026 by the Δ*ptmH* strain suggests that PtmD as well as 6MSA transferase PtmR have relaxed substrate specificity.

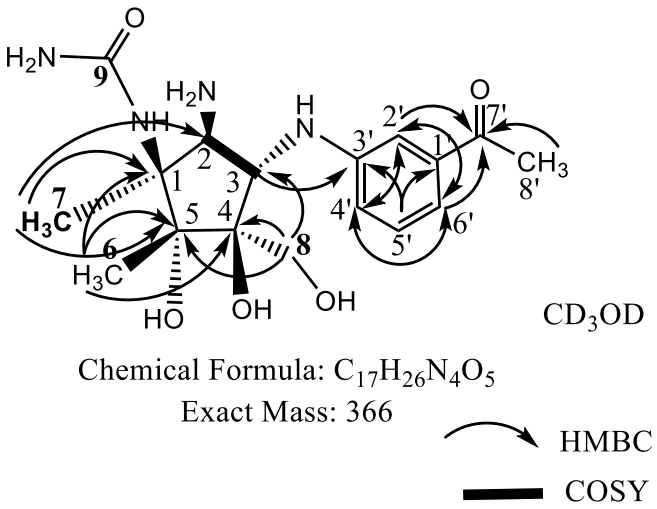

Figure 3.4 COSY and HMBC correlations of TM-101.

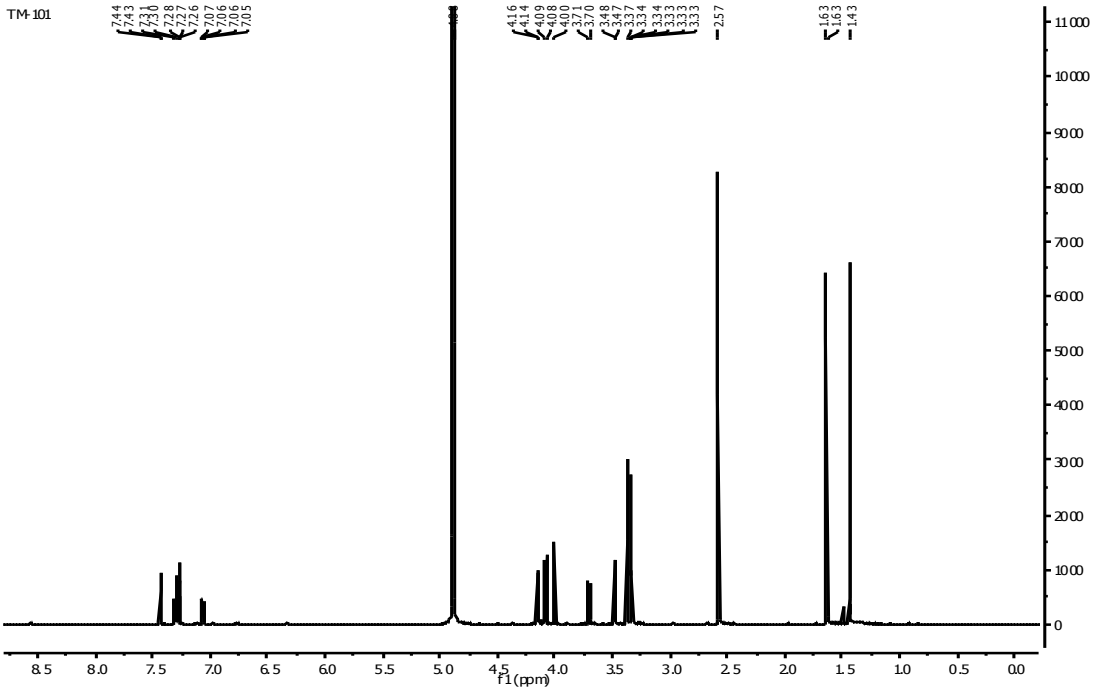

Figure 3.5 ^{1}H-NMR spectrum of TM-101 (700 mHz, CD_3OD).

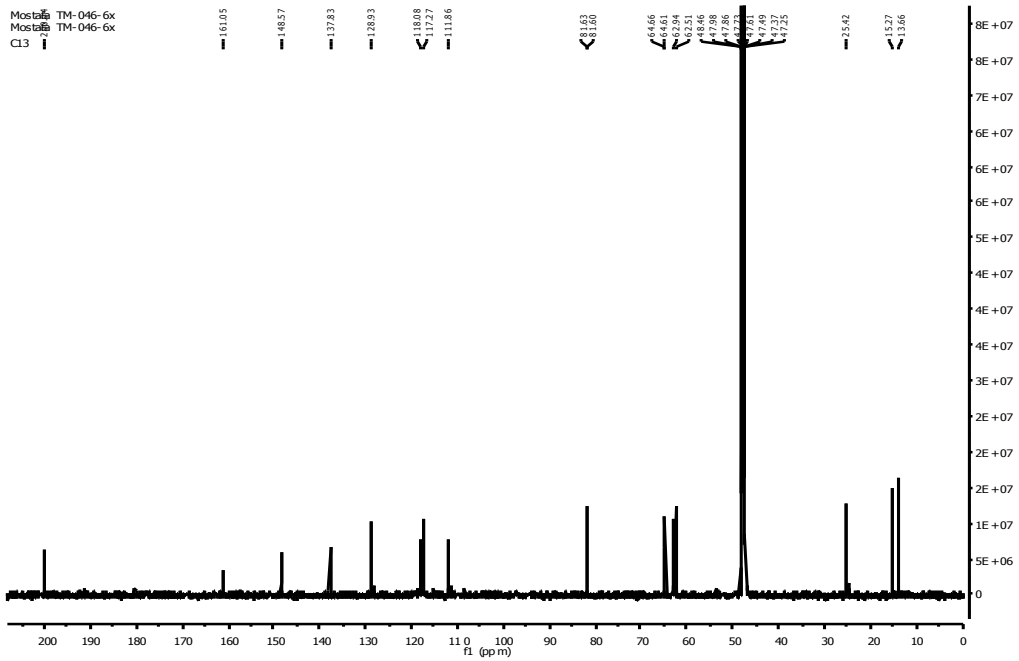

Figure 3.6 ^{13}C-NMR spectrum of TM-101 (700 mHz, CD_3OD).

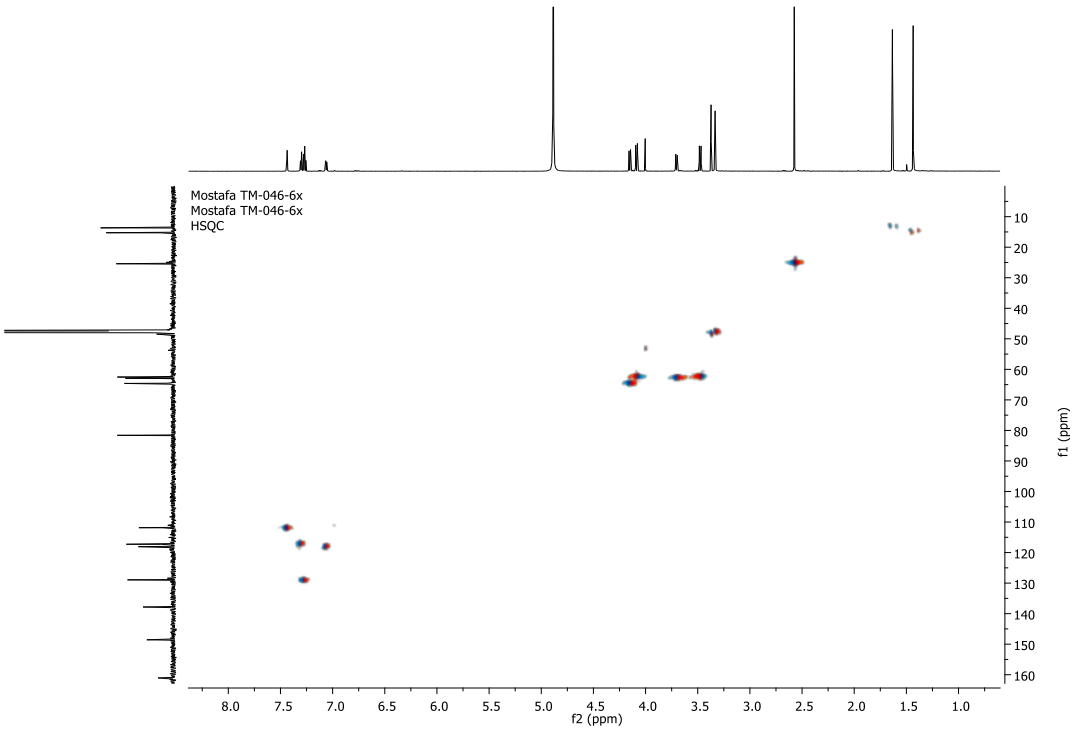

Figure 3.7 HSQC spectrum of TM-101.

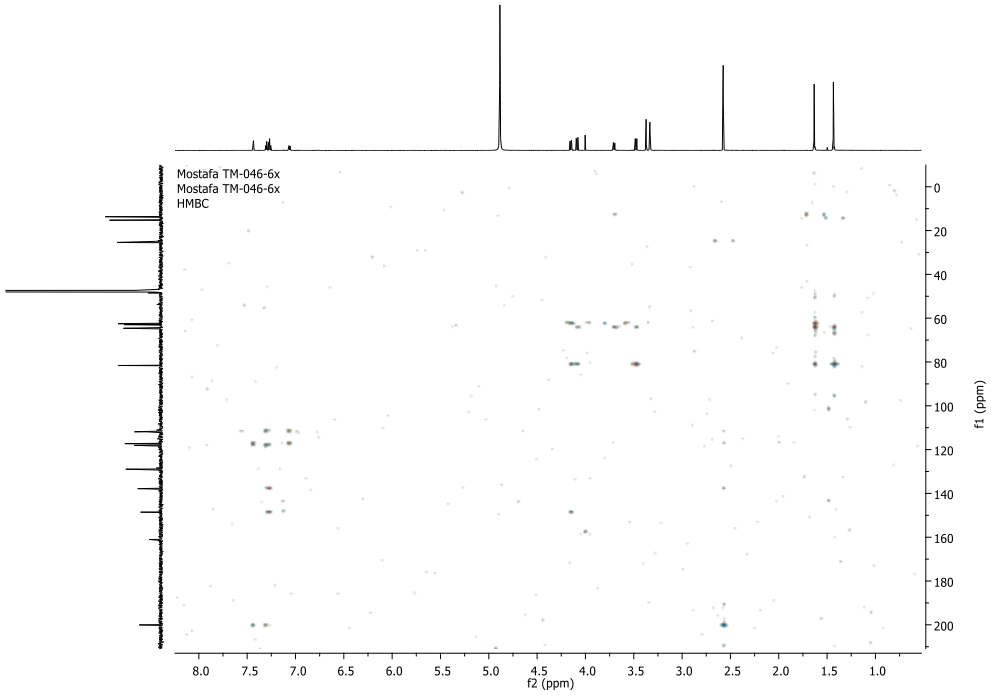

Figure 3.8 HMBC spectrum of TM-101.

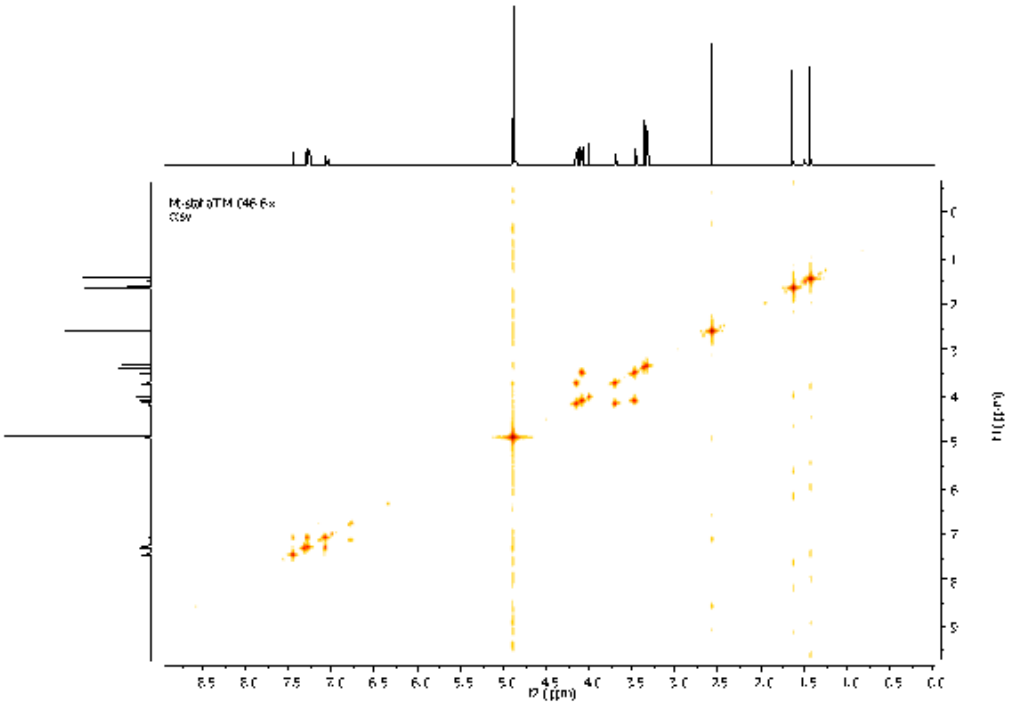

Figure 3.9 COSY spectrum of TM-101.

3.4.3 Double knockout of *ptmD* and *ptmQ*

To confirm that dimethylation takes place after *C*-7 methylation, we constructed a Δ*ptmD/*Δ*ptmQ* double mutant strain of *S. pactum.* Inactivation of *ptmQ* has previously been demonstrated to halt the synthesis of 6MSA in *S. pactum*, thus, it eliminates the possibility of 6MSA modification of the product. The construction of Δ*ptmD/*Δ*ptmQ* mutant was carried out by directed in-frame deletion of *ptmQ* in Δ*ptmD* mutant. The mutant was then cultivated in Bennett medium and the product was analyzed by ESI-MS. The results showed that Δ*ptmD/*Δ*ptmQ* mutant produces a new pactamycin analogue with *m/z* 381 $[M+H]^+$ (Figure 3.3 C), identified as TM-102. HR-ESI-MS data for TM-102 indicated a molecular formula of $C_{18}H_{28}O_5N_4$.

3.4.4 Structural Characterization of TM-102

The ^1H and ^{13}C NMR spectroscopicdata for TM-102 are listed in Table 3.4. The ^1H NMR spectrum for TM-102 showed two singlets (δ 1.51 and 2.55 ppm, 6H) and a triplet (δ 1.04 ppm, 3H) for methyl protons. In addition, two doublets of quartets were observed at δ 2.10 and 2.42 ppm indicating the presence of an isolated methylene adjacent to a methyl group or diastereotopic protons in an isolated methylene adjacent to a methyl. ^{13}C NMR and HSQC spectra for TM-102 revealed the presence of a methylene carbon (δC 20.9 ppm) and an additional methyl carbon (δC 7.9 ppm) in this compound (Figure 3.10).

Table 3.4 ^{1}H and ^{13}C NMR spectral data of TM-102 in CD_3OD (700 mHz).

Position	σ_C	σ_H (int, mult,J in Hz)	Position	σ_C	σ_H (int, mult,J in Hz)
1	67.24		10	161.37	-------
2	62.44	3.62 (1H, d, 10.2)	1’	137.8	-------
3	64.39	4.14 (1H, d, 10.2)	2’	111.9	7.41 (1H,t1.89)
4	82.30		3’	148.5	------
5	81.43		4’	118.1	7.04(1H,ddd, 0.88, 2.42, 7.98)
6	17.73	1.51 (3H, s)	5’	128.9	7.24(1H, t, 7.84)
7	20.90	2.10 (1H, dq, 14.56, 7.28) 2.42 (1H, dq, 14.87 7.47)	6’	117.3	7.28(1H, dd,1.3, 6.4)
8	7.90	1.01 (3H, t 7.49))	7’	200.0	------
9	62.41	3.48 (1H, d,11.41) 4.00 (1H, d, 11.48)	8’	25.42	2.55 (3H, s)

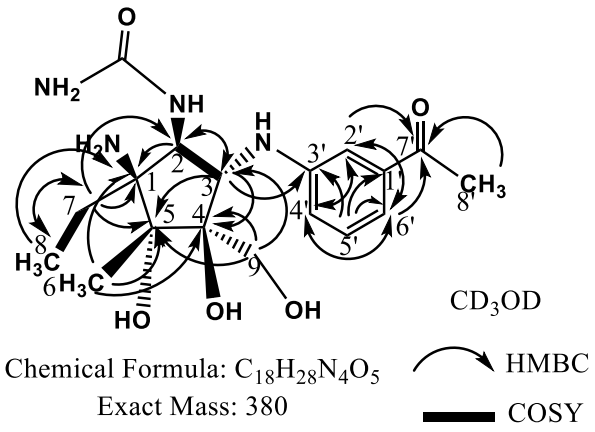

Figure 3.10 COSY and HMBC correlations of TM-102.

These observations, together with the ESI-MS data, suggest that the 7-CH_3 of TM-101 has been further methylated to form an ethyl side chain in TM-102. As in TM-101, TM-102 does not contain *N*, *N*-$(CH_3)_2$ and 6′-CH_3 groups indicating the presence of free urea and the lack of 6MSA moiety in this compound. Further analysis using ^{1}H NMR, ^{13}C NMR, HSQC, HMBC, and COSY (Figure 3.11, Figure 3.12, Figure 3.13,

Figure 3.14, and Figure 3.15) confirmed the chemical structure of TM-102 as de-6MSA-*N*,*N*-didemethyl-7-deoxypactamycin.

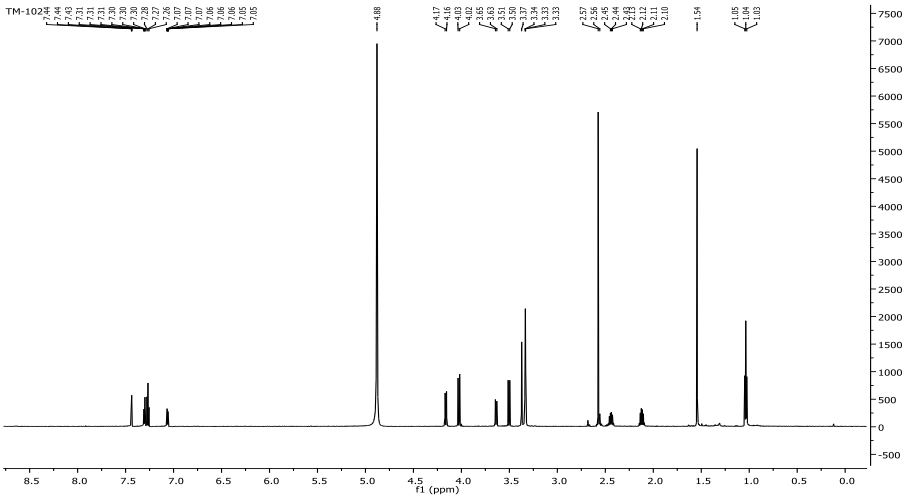

Figure 3.11 ^{1}H-NMR spectrum of TM-102.

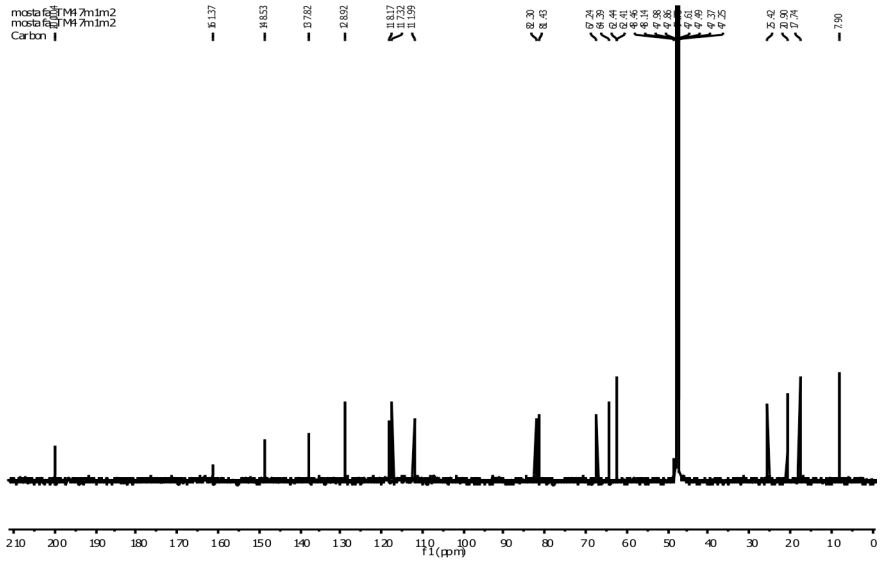

Figure 3.12 ^{13}C-NMR spectrum of TM-102.

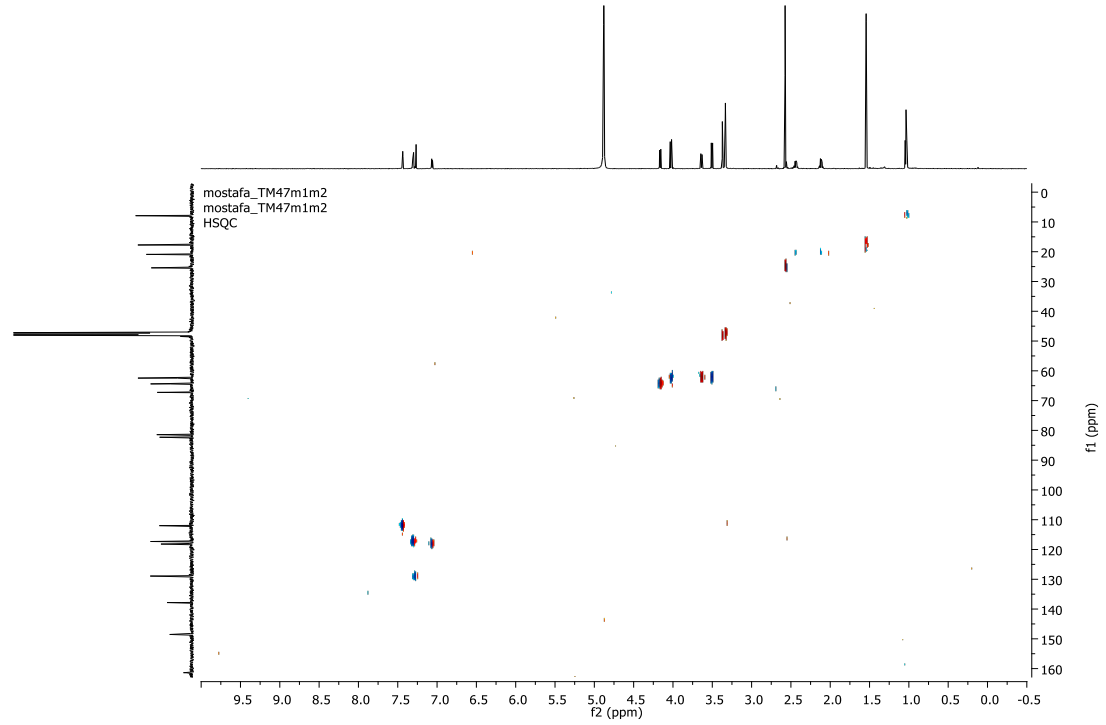

Figure 3.13 HSQC spectrum of TM-102.

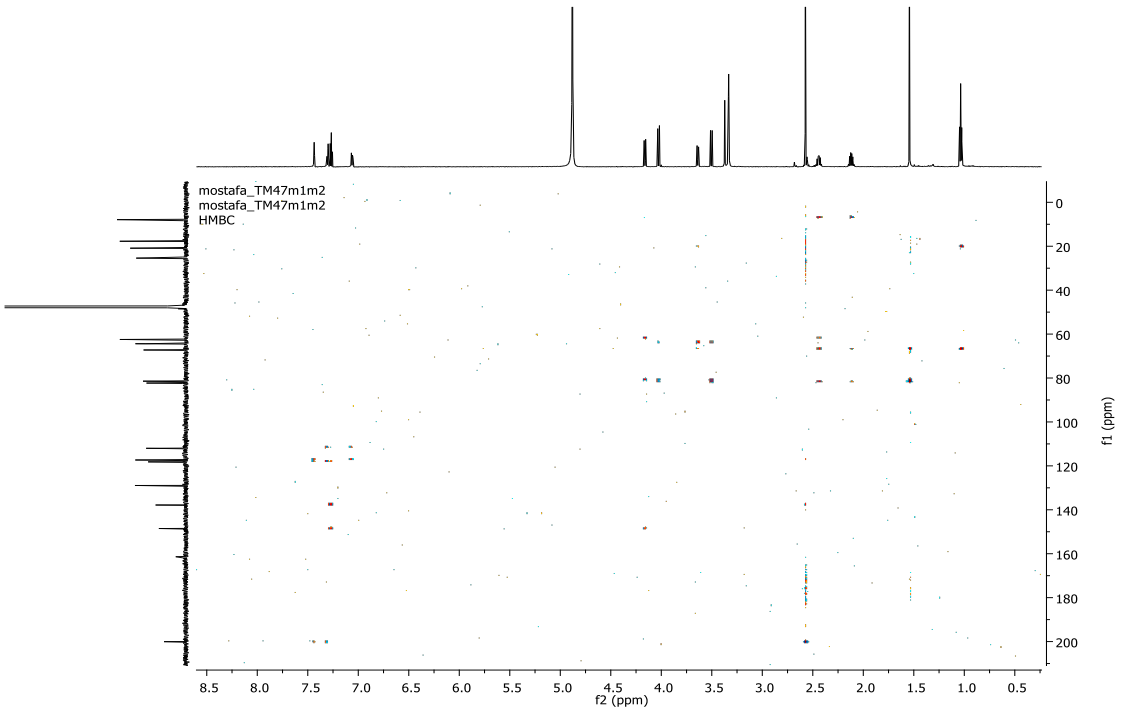

Figure 3.14 HMBC spectrum of TM-102.

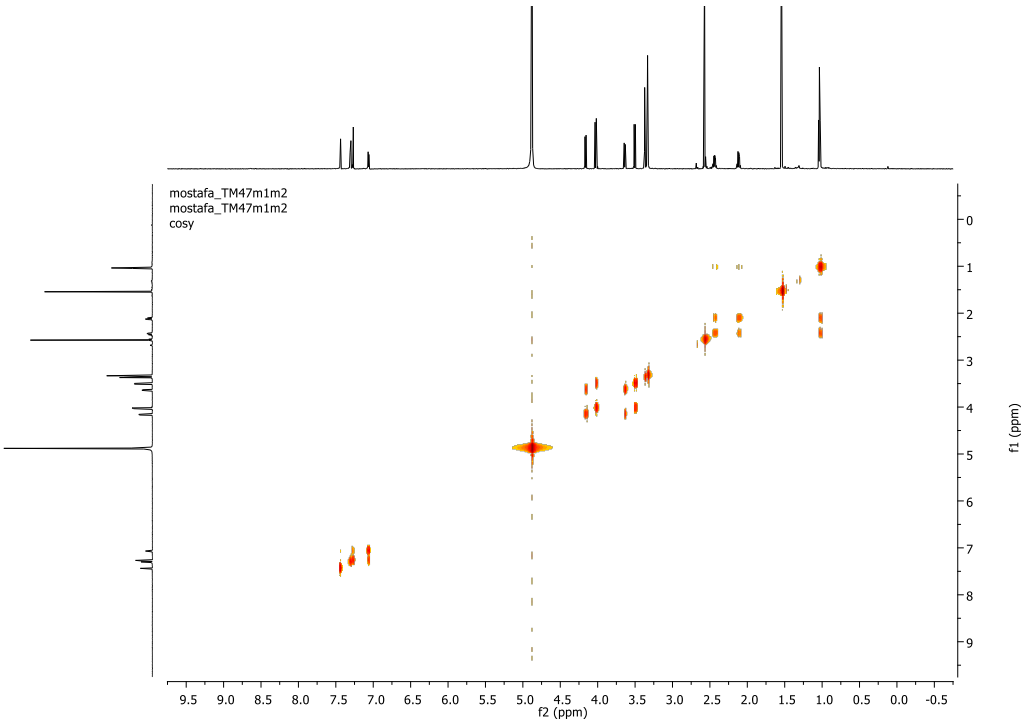

Figure 3.15 COSY spectrum of TM-102.

3.4.5 Spontaneous Transamidation of TM-101 and TM-102

TM-101 and TM-102 appear to be easily converted to their transamidation isomers, in which the urea group is transferred from the tertiary amine to the neighboring secondary amine. This phenomenon appears to occur more easily in methanol (within several days in the NMR tube) (Figure 3.16). In deuterium oxide, the compounds appear to be very stable (only a single compound and no change observed up to 7 days). However, it is not clear if the compound may have spontaneously undergone a complete conversion in deuterium oxide (Figure 3.17).

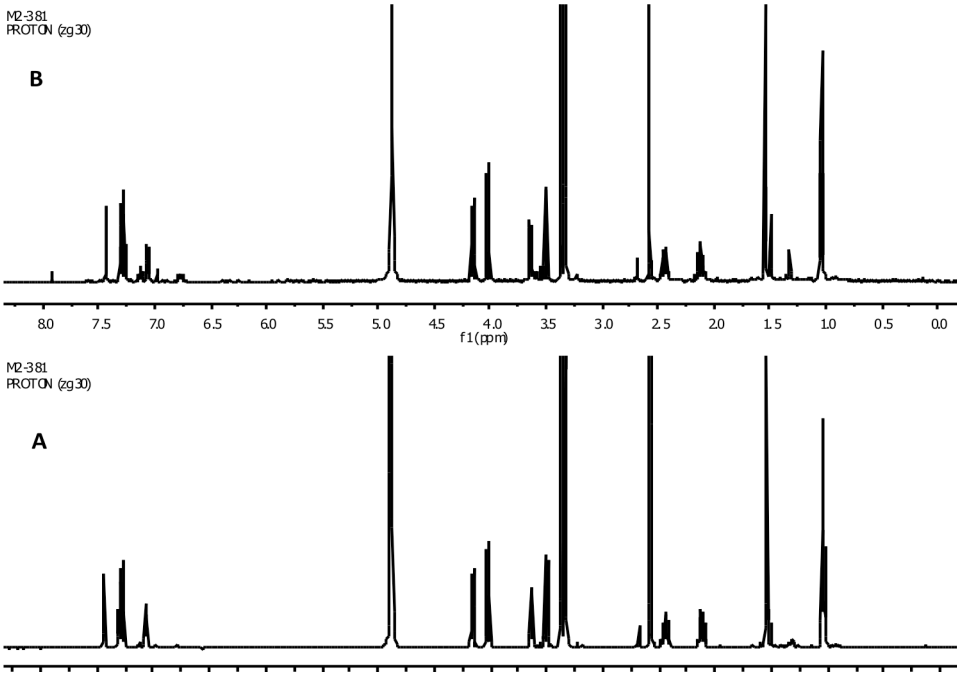

Figure 3.16 ^{1}HNMR of TM-102 in CD_3OD. **A)** overnight and **B)** after 2 days in NMR tube.

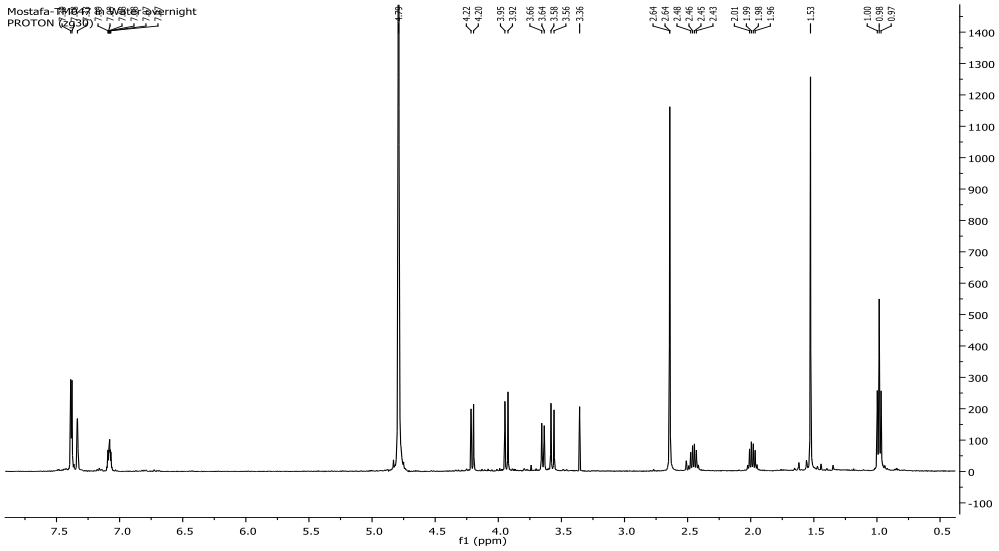

Figure 3.17 ^{1}H-NMR spectrum of TM-102 in D_2O.

3.4.6 Antimalarial Activity of TM-101 and TM-102

During our search for new antimalarial natural products, we generated de-6MSA-pactamycin from the *ptmQ* mutant. Like pactamycin, de-6MSA-pactamycin showed a significant antimicrobial activity and high cytotoxicity against mammalian cells (Ito et al., 2009). The high activity of pactamycin and 7-deoxypactamycin against both the drug-resistant K1 and drug-susceptible FCR3 strains of *P. falciparum* have been reported (Otoguro et al., 2010). Moreover, TM-025 and TM-026 showed pronounced antimalarial activity with IC_{50} values between 25 – 30 nM against both strains (Lu et al., 2011). The new pactamycin analogs, TM-101 and TM-102, were subjected to testing against *P. falciparum* D6 (chloroquine-sensitive) and Dd2 (chloroquine-resistant) strains. TM-102 showed acceptable antimalarial activity with IC_{50} values between 63 – 67 nM against both strains, whereas TM-101 showed antimalarial activity with IC_{50} values between 218-270 nM, which is significantly lower than TM-102 (Figures 2.18 B, C, and E). However, as a comparison, the less active analog, pactamycate, showed IC_{50} at around 300 nM.

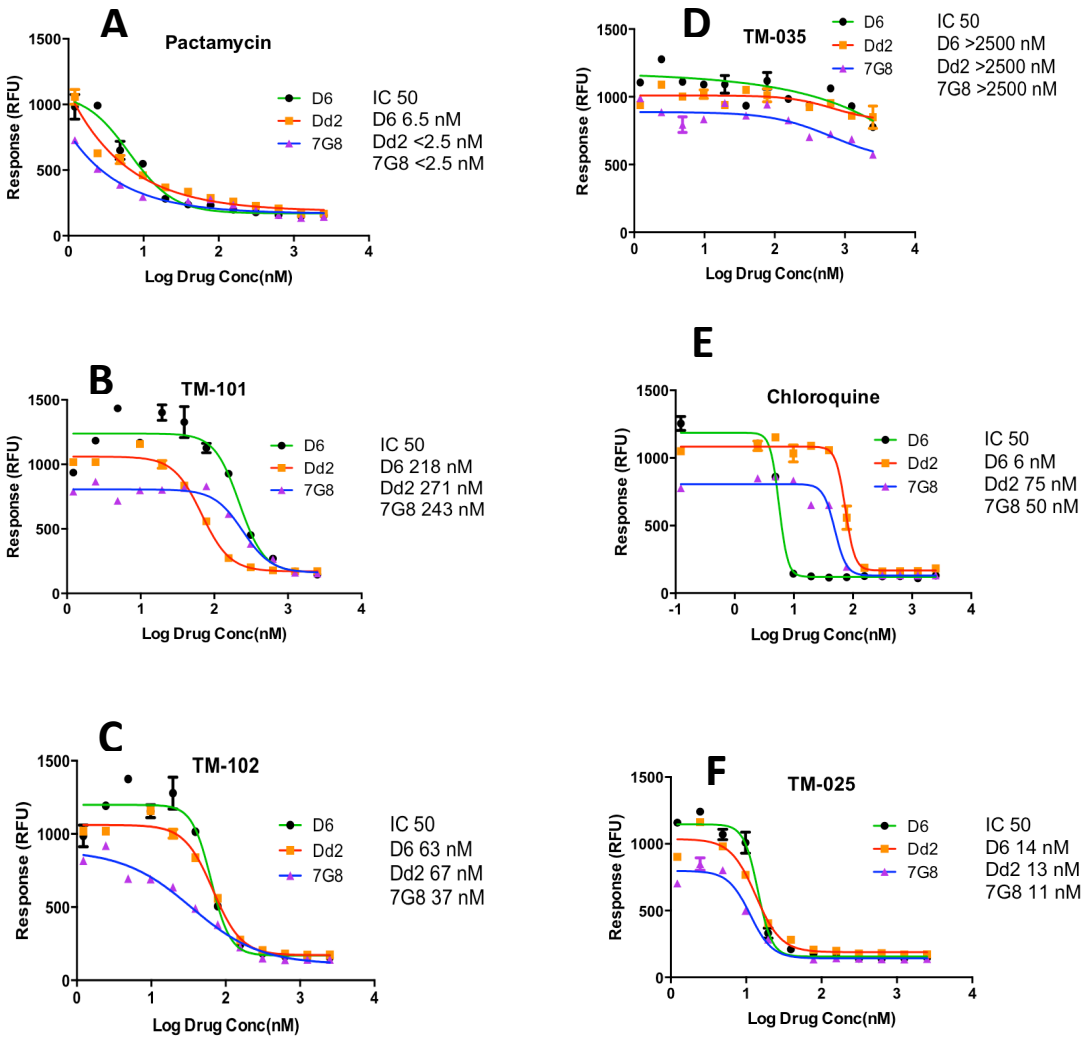

Figure 3.18 Antimalarial activity assay of pactamycin analogs against the chloroquine-sensitive (D6) and chloroquine-resistant (Dd2) strains of *P. falciparum*. **A)** pactamycin, **B)** TM-101, **C)** TM-102, **D)** TM-035, **E)** chloroquine, and **F)** TM-025.

3.4.7 Antibacterial Activity of TM-101 and TM-102

Pactamycin and de-6MSA-pactamycin showed a strong antibacterial activity against both Gram-positive and Gram-negative bacteria, e.g., *Staphylococcus aureus*, *Bacillus subtilis*, *Pseudomonas aeruginosa*, and *Escherichia coli*. Therefore, TM-101 and TM-102 were also subjected to antibacterial activity with both agar diffusion and micro-

dilution assays. Surprisingly, TM-101 and TM-102 showed very little activitiy against both Gram-positive and Gram-negative bacteria (Figures 3.19 A-H). The results suggest that the new analogs have less affinity to the bacterial ribosomes or interact with it in a less damaging fashion than pactamycin. This might also contribute to the relatively high production yield of TM-101 in *S. pactum* Δ*ptmD* /Δ*ptmH*.

3.4.8 Cytotoxic Activity of TM-101 and TM-102

The *in vitro* cytotoxic activity of pactamycin, TM-101, and TM-102 was evaluated at different concentrations (0, 25, 50, 75, and 100 μM) against HCT116 human colorectal cancer cells and HEPG2 human liver carcinoma. The IC_{50} values for all tested compounds in the above cell lines are shown in Table 3.5. TM101 and TM-102 showed cytotoxicity activity (IC_{50} < 10 μM) against both HCT116 colorectal cancer cell line and HEPG2 liver cancer. The results revealed that the new analogs are significantly less toxic than pactamycin with estimated IC_{50} values between 5,000 and 10,000 nM, or about 50-100 times higher than that of pactamycin (IC_{50} ~100 nM). The results support the notion that the new analogs have less affinity towards the ribosome of mammalian cells, or their antimalarial activity is due to a different mechanism of action. The selectivity of new analogs toward the malarial parasites might be due to the lack of methyl and hydroxyl groups at the C-7 position and *N*,*N*-dimethyl group on carbamoyl moiety. Previously, we reported that de-6MSA-pactamycin showed no substantial differences from pactamycin in its antibacterial and cytotoxicity profiles (Ito et al., 2009). Further work currently underway to determine the structure-activity relationship of this untapped class of natural products and to unveil their mechanism(s)

of action against plasmodium parasites. The new pactamycin analogs TM-101 and TM-102 have therapeutic indices of 26 and 150, respectively, and are considered to be safer drug candidates (2-fold and 17-fold, respectively) than their parent compound, pactamycin (Table 3.6).

Table 3.5 IC_{50} of pactamycin and its analogues against HCT116 and HEPG2 cells.

Cell line	Pactamycin	TM-101	TM-102	TM-025	TM-026	TM-035
HCT116	93 nM	5.6 μM	~9.5 μM	1.6 μM	2.9 μM	ND*
HEPG2	86 nM	≥5.6 μM	≥9.5 μM	NT*	NT	NT

*ND, not defined; NT, not tested

Table 3.6 Estimated Therapeutic Index.

	Pactamycin	TM-101	TM-102	TM-025	TM-026	TM-035
Cytotoxicity	93 nM	5.6 μM	~9.5 μM	1.6 μM	2.9 μM	ND
Antimalarial	6.5 nM	218 nM	63 nM	14 nM	17 nM	>2500 nM
Ther. Index	14	26	150	114	170	-

Due to the promiscuity of some of the tailoring enzymes in the biosynthesis of pactamycin, the sequence or the timing of the tailoring processes were unclear. However, results from the present study shed some light on the tailoring steps in pactamycin biosynthesis in *S. pactum* (Figure 3.20). Inactivation of both *ptmD* and *ptmH* resulted in a mutant that produced TM-101, which suggested that *C*-methylation at C-1 and C-5, as well as urea formation, take place early in the pathway. TM-101 is then converted to TM-102 by the radical SAM-dependent enzyme PtmH. However, the inactivation of this enzyme alone did not produce TM-101. Due to the promiscuity of the *N*-methyltransferase PtmD and the 6MSA-transferase enzyme PtmR, TM-101 was modified further to TM-025 and TM-026. Inactivation of the 6MSA synthase PtmQ, however, halted the modification by 6MSA.

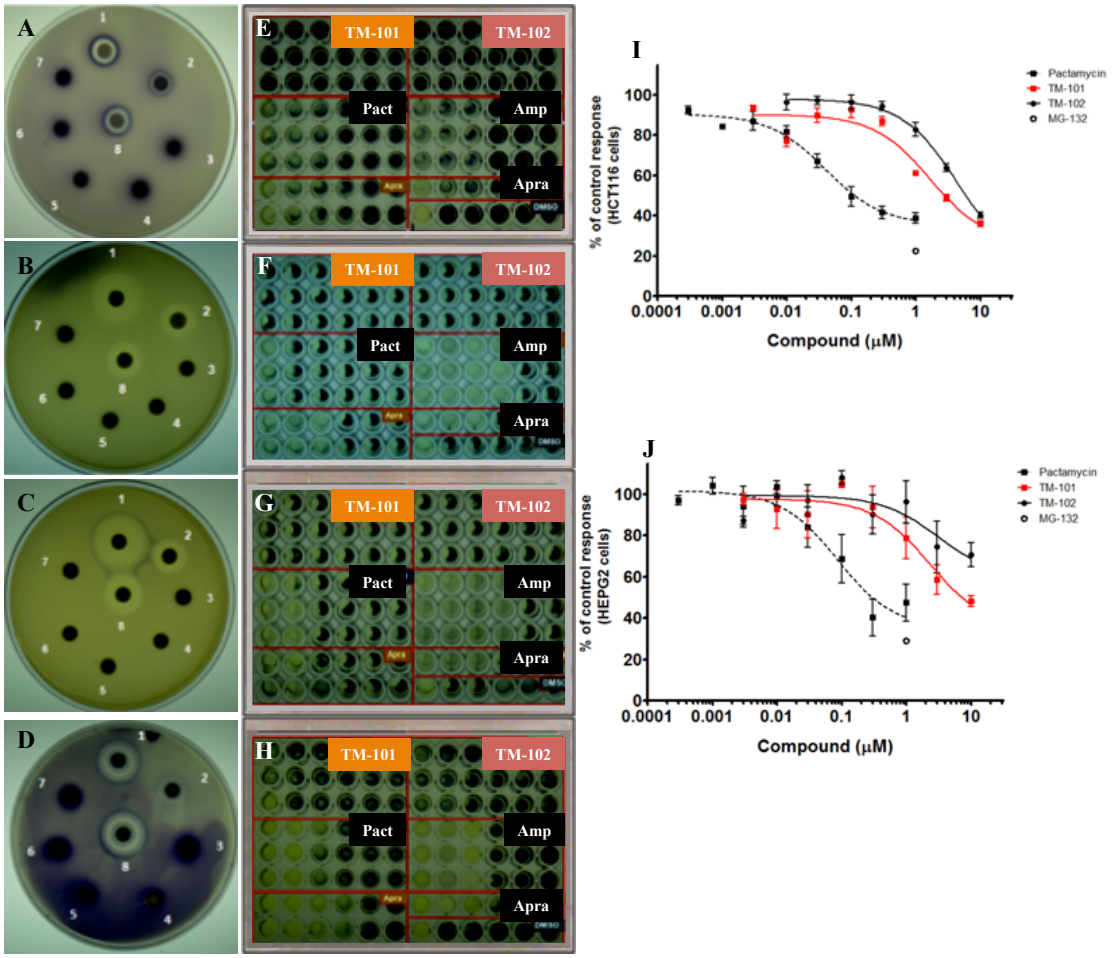

Figure 3.19 Antibacterial and cytotoxicity assays of pactamycin analogs. **(A-D)** Agar-diffusion assay of pactamycin analogs against *S. aureus* **(A)**, *B. subtilis* **(B)**, *P. aeruginosa* **(C)**, and *E. coli* **(D)**. 1, 20 μL 10 mM pactamycin; 2, 20 μL 1 mM pactamycin; 3, 20 μL 10 mM TM-101; 4, 20 μL 1 mM TM-101; 5, 20 μL 10 mM TM-102; 6, 20 μL 1 mM TM-102; 7, 20 μL 10 mM DMSO; 8. 5 μL 1 mg/mL ampicillin; **(E-H)** Micro-dilution assay of pactamycin analogs against *S. aureus* **(E)**, *B. subtilis* **(F)**, *P. aeruginosa* **(G)**, and *E. coli* **(H)**. TM-101: 1 mM – 10 nM; TM-102: 1 mM – 10 nM; Pct (pactamycin): 0.5 mM – 10 nM; Amp (ampicillin): 10 mg/mL – 0.1 μg/mL; Apra (apramycin): 5 mg/mL – 50 ng/mL. 10mM DMSO.; **(I-J)** Cytotoxicity assay of pactamycin analogs against HCT116 human colorectal cancer cells using broad-range concentrations at 48 h **(I)** and cytotoxicity assay of pactamycin analogs against HEPG2 human liver cancer cells using broad-range concentrations at 48 h **(J)**. Black squares represent pactamycin, red squares represent TM-101 and black circle represent TM-102.

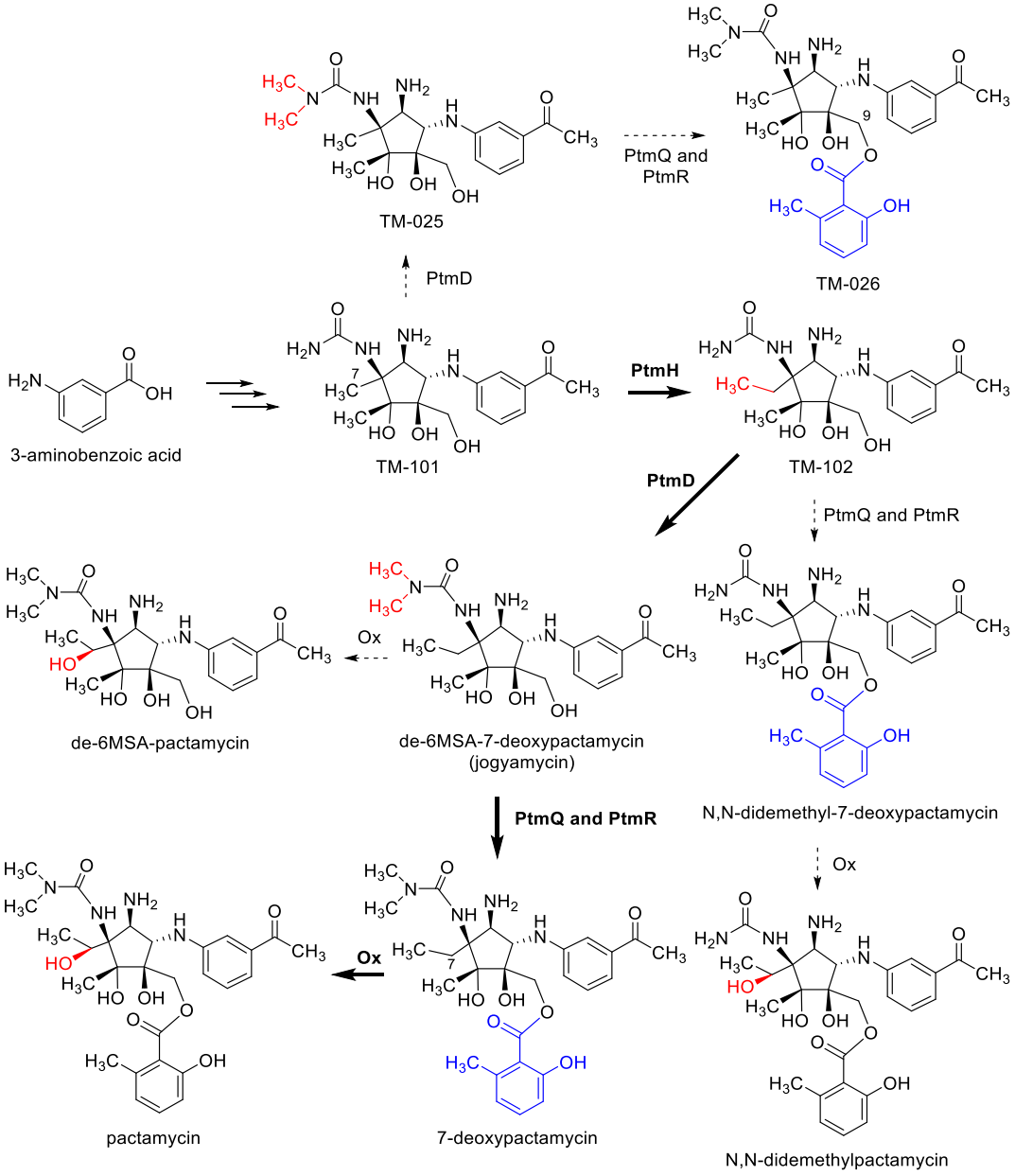

Figure 3.20 Tailoring steps in pactamycin biosynthesis in *S. pactum.*

TM-102 is believed to be the natural substrate for PtmD, as the inactivation of both *ptmD* and *ptmQ* gave TM-102 as the main product. However, the inactivation of PtmD

alone did not give TM-102 as the later compound can be shunted to *N*,*N*-didemethyl-7-deoxypactamycin and *N*,*N*-didemethylpactamycin by the 6MSA-transferase and a hydroxylase enzyme. PtmY, a cytochrome P450 monooxygenase, is proposed to play a role in the C-7 hydroxylation reaction. However, the inactivation of *ptmY* in *S. pactum* did not completely block the hydroxylation reaction; thus, there might be other enzymes in the cells that can complement PtmY function.

Dimethylation of TM-102 is expected to yield de-6MSA-7-deoxypactamycin (jogyamycin). This compound is present in the wild-type strain of *S. pactum*, indicating that it is a natural intermediate in the biosynthesis pathway of pactamycin. Previously, we reported that the inactivation of PtmQ resulted in the production of de-6MSA-pactamycin and its cyclic product de-6MSA-pactamycate. However, upon investigation of the polar (n-BuOH) fractions of the extract, we found that de-6MSA-7-deoxypactamycin is also produced by the Δ*ptmQ* mutant. Therefore, the originally reported de-6MSA-pactamycin appears to be a shunt product resulting from the hydroxylation reaction.

In conclusion, using single and double gene knock out experiments and characterization of their products, we are now able to elucidate some of the tailoring processes in pactamycin biosynthesis in *S. pactum.*

Chapter 4 : Acyl Transfer Reactions Catalyzed by a Highly Promiscuous β-Ketoacyl-Acyl Carrier Protein Synthase (KAS) III-like Protein.

Mostafa E. Abugrain, Corey J. Brumsted, Andrew R. Osborn, and Taifo Mahmud

4.1 Abstract

β-Ketoacyl-acyl carrier protein (β-Ketoacyl-ACP) synthase (KAS) III catalyzes the first step in fatty acid biosynthesis, involving a Claisen condensation of the acetyl-CoA starter unit with the first extender unit, malonyl-ACP, to form acetoacetyl-ACP. KAS III-like proteins have also been reported to catalyze acyltransferase reactions using coenzyme A esters or discrete ACP-bound substrates. Here, we report the *in vivo* and *in vitro* characterizations of a KAS III-like protein (PtmR), which directly transfers the 6-methylsalicylyl (6MSA) moiety from an iterative type I polyketide synthase (PKS) to an aminocyclopentitol unit in pactamycin biosynthesis. PtmR is highly promiscuous, recognizing a wide array of acyl-*N*-acetylcysteamines as substrates to produce a suite of pactamycin derivatives with diverse alkyl and aromatic features. The results suggest that KAS III-like proteins may be used as versatile tools for acylation of complex natural products.

4.2 Introduction

Acyl transfer reactions are ubiquitous in nature and they play critical roles in various aspects of biological systems, such as in gene expression, neurotransmission, and antibiotic resistance (Norris et al., 20009; Ramirez and Tolmasky, 2010). They are also widely involved in primary and secondary metabolism, most notably in the biosynthesis of fatty acids, polyketides, non-ribosomal peptide, and other natural products. In fatty acid and polyketide biosyntheses, both the starter and extender units are recruited from their respective coenzyme A (CoA) esters to the acyl carrier proteins by the function of acyltransferase (AT) proteins or domains (Dunn et al.,

2014). CoA esters serve as a universal acyl source for the acylation of most natural compounds, including sugars, fatty acids, and peptides. However, adenosine monophosphate (AMP) esters are sometimes used; for example, in amino acyl transfer catalyzed by the non-ribosomal peptide synthetase (Gulick, 2009). Moreover, in fatty acid and polyketide biosyntheses, the growing fatty acyl or polyketide chain is transferred from an acyl carrier protein (ACP) to a β-Ketoacyl-acyl carrier protein (β-Ketoacyl-ACP) synthase (KAS) (Jenner et al., 2015).

KAS enzymes play a central role in type I (modular) and type II (dissociable) fatty acid synthases (FASs) and polyketide synthases (PKSs), as well as in chalcone synthases (Dawe et al., 2013). In the type II dissociable FASs, three types of KAS enzymes are known, KAS I (FabB) and KAS II (FabF) are responsible for the elongation steps, whereas KAS III (FabH) catalyzes the initiation step involving a Claisen condensation of the acetyl-CoA starter unit with the first extender unit, malonyl-ACP, to form acetoacetyl-ACP (Figure 4.1 a). In *Streptomyces*, KAS III can also recruit alternative starter units, such as isobutyryl-CoA and methylbutyryl-CoA, to form branched chain fatty acids. Less efficiently, it can also catalyze acyl-CoA:ACP transacylase (ACAT) reactions (Han et al., 1998).

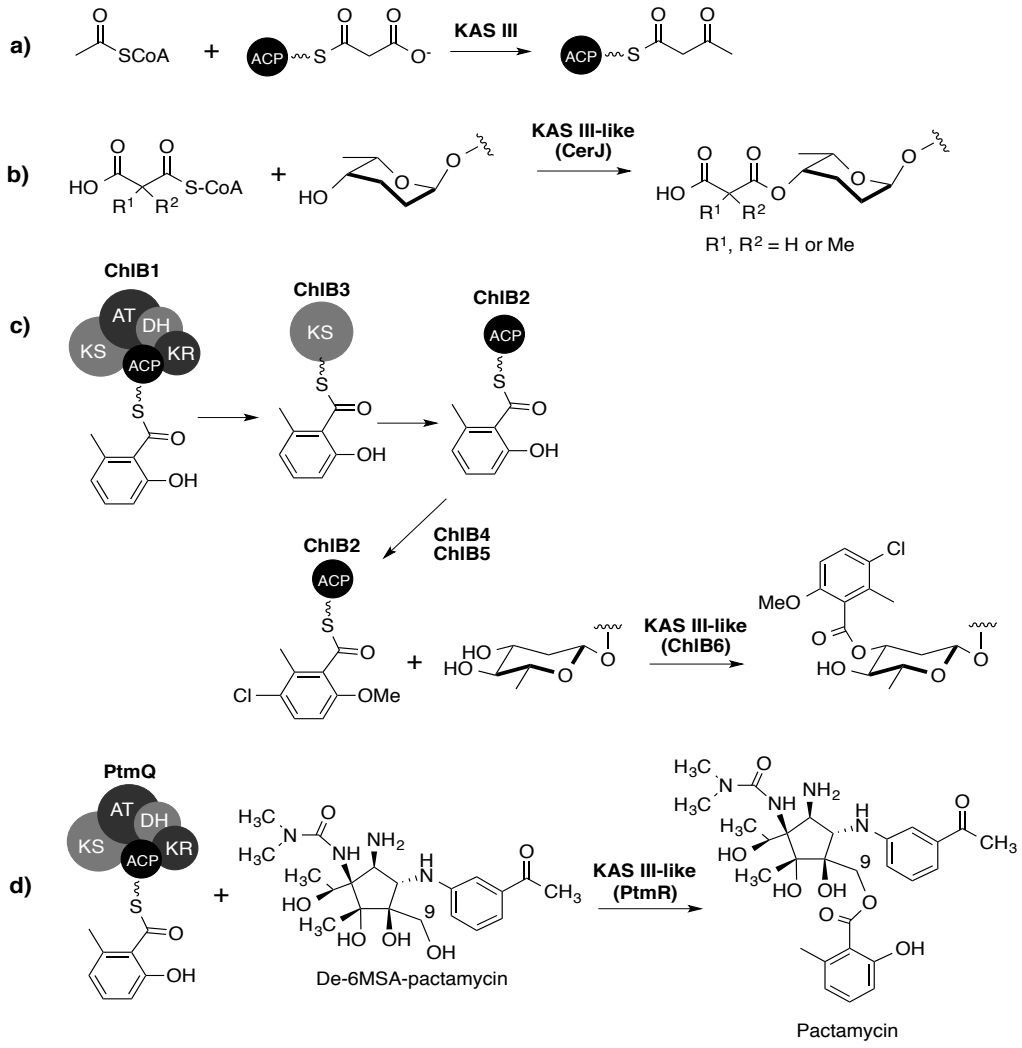

Figure 4.1 Distinct catalytic activities of KAS III and KAS III-like proteins. **a)** KAS III catalyses a Claisen condensation of acetyl-CoA and malonyl-ACP. **b)** CerJ uses malonyl units to form esters in cervimycin biosynthesis. **c)** ChlB6 catalyzes the transfer of the 3-chloro-6-methoxy-2-methylbenzoyl moiety from the discrete acyl carrier protein ChlB2 to a sugar moiety of chlorothricin. **d)** PtmR catalyzes an acyl transfer reaction from a PKS to an aminocyclopentitol unit. Only partial structures of the cervimycins and chlorothricin are shown.

Over the past decade, a number of KAS III-like enzymes have also been reported to have unusual catalytic functions. The *cloN2* gene of the clorobiocin cluster in *Streptomyces roseochromogenes* var. *oscitans* DS 12.976 has been found through a

gene inactivation study to be responsible for the transfer of the pyrrolylcarbonyl unit to the sugar moiety of clorobiocin (Xu et al., 2003). The KAS III-like protein CerJ uses malonyl-CoA analogs to form sugar esters in cervimycin biosynthesis (Figure 4.1 b) (Bretschneider et al., 2012), whereas ChlB6 from the chlorothricin pathway transfers a 3-chloro-6-methoxy-2-methylbenzoyl moiety from a discrete acyl carrier protein, ChlB2, to a sugar moiety of chlorothricin (Figure 4.1 c) (He et al., 2009). The 3-chloro-6-methoxy-2-methylbenzoyl unit is derived from 6-methylsalicylyl (6MSA) unit, a product of an iterative type I PKS (ChlB1). Incorporation of this PKS product to the sugar moiety of chlorothricin requires multiple intermediary acyl transfer reactions involving two discrete KAS III-like proteins (ChlB3 and ChlB6) and a discrete ACP (ChlB2) (Figure 4.1 c) (He et al., 2009).

Genes encoding proteins homologous to ChlB6 have been found in a number of natural product biosynthetic gene clusters such as *aviN* of the avilamycin A cluster in *Streptomyces viridochromogenes* Tü57 (Weitnauer et al., 2001), *evrI* of the evernimicin cluster in *Micromonospora carbonacea* var. *africana* ATCC 39149 (Hosted et al., 2001), *calO4* of the calicheamicin cluster in *Micromonospora echinospora* subsp. *Calichensis,* (Ahlert et al., 2002), *pokM2* of the polyketomycin cluster in *Streptomyces diastatochromogenes* Tü6028, (Duum et al., 2009), *tiaf* of the tiacumicin cluster in *Dactylosporangium aurantiacum* subsp. hamdenensis NRRL 18085, (Xiao et al., 2011), and *esmD1* of esmeraldin pathway in *Streptomyces antibiotics* Tü2706 (Rui et al., 2012). Except esmeraldin, all of these natural products.

contain one or more sugar moieties decorated with 6MSA or orsellinic acid derivatives. However, in contrast to the chlorthricin pathway, they lack the genes that code for the second KAS III and the discrete ACP in their clusters.

A gene encoding a protein homologous to KAS III was also found in the pactamycin cluster in *S. pactum* (Ito et al., 2009). This gene (*ptmR*) may be involved in the attachment of 6MSA, which is synthesized by the iterative type I PKS PtmQ, to the aminocyclopentitol core unit in pactamycin biosynthesis. Also present in the cluster are genes that code for a KAS I protein (PtmK), a discrete ACP (PtmI), and a putative hydrolase/acyltransferase (PtmO). The roles of these genes in pactamycin biosynthesis are currently unknown, but their possible involvement in the attachment of 6MSA cannot be ruled out. In addition, a putative acyltransferase gene (*orfX2*) is located outside of the cluster but adjacent to the pactamycin resistance gene. The resistance gene encodes a *S*-adenosylmethionine (SAM)-dependent methyltransferase, which transfers a methyl group to the 16S rRNA, resulting in inhibition of pactamycin binding (Calcutt and Cundliffe, 1990b). Therefore, OrfX2 may also take part in 6MSA attachment.

4.3 Materials and Methods

4.3.1 Bacterial Strains and Plasmids

Pactamycin producing *S. pactum* ATCC 27456 was purchased from American Type Culture Collection (ATCC). *Escherichia coli* DH10B was used as a host strain for the construction of recombinant plasmids. *E. coli* ET12567 was used as a donor strain in

conjugation experiments. pBlueScript II (SK-) (Stratagene) ware used as cloning vectors. pET2b(+), pET28a(+), and pRSET B were used as heterologous expression vectors. pTMW050 was used for construction of integrative shuttle plasmids for complementation experiments (Kieser et al., 2000). pHZ1358 is a pIJ101 derivative containing an OriT transfer element required for conjugation (Sun et al., 2002). Other bacterial strains and plasmids used in this study are listed in Table 4.1 and Table 4.2.

Table 4.1 Bacterial strains used in this study.

Strains	Relevant genotype/comments	Source/Ref
Escherichia coli DH10B	*F⁻ mcrA Δ(mrr-hsdRMS-mcrBC)ϕ80lacZΔM15 ΔlacX74 recA1 endA1 araD139 Δ(ara, leu)7697 galU galK λ⁻ rspL nupG*	GibcoBRL
Escherichia coli BL21*(*DE3*)*pLysS	*F⁻ ompT hsdS$_B$ (r_B^- m_B^-) gal dcm* (DE3) pLysS (CmR)	Promega
E. coli ET12567(pUZ8002)	*dam dcm hsdS,* pUZ8002	(Paget et al., 1999)
S. pactum ATCC 27456	Wild-type pactamycin producing strain	ATCC
S. pactum ΔptmH	*ptmH* in-frame deletion mutant	(Lu et al., 2011)
S. pactum ΔptmR	*ptmR* in-frame deletion mutant	This study
S. pactum ΔptmH/ΔptmR	in-frame deletion of *ptmR* in ΔptmH	This study
ΔptmH/ΔptmR/TMM058	ΔptmH/ΔptmR mutant complemented with pTMM058	This study
S. pactum ΔptmI	*ptmI* in-frame deletion mutant	This study
S. pactum orfX2::aac(3)IV	*orfX2* disruption mutant	This study
S. pactum ΔptmO	*ptmO* in-frame deletion mutant	This study
S. pactum ptmK::aac(3)IV	*ptmK* disruption mutant	This study
S. pactum ΔptmS	*ptmS* disruption mutant	This study

Table 4.2 Plasmids used in this study.

Plasmid	Description	Source/Ref
pBlueScript II SK(-)	ColE1-based phagemid vector with f1 (-) and pUC origins; T3, T7 and lac promoters; *bla*.	Stratagene
pET-20b(+)	f1 (-) and pBR322 origins; *pelB*; T7 promoter; *bla*; C-terminal histag.	Novagen
pTMN002	pJTU1278+ derivative containing a 1 kb *aac(3)IV*	(Ito et al., 2009)

	apramycin resistance cassette from pOJ446	
pTMM007	Two 1 kb PCR fragments upstream and downstream of the *ptmO* gene in pBlueScript II SK(-)	This study
pTMW008	Two 1 kb PCR fragments upstream and downstream of the *ptmO* gene in pTMN002	This study
pTMW050	pTMX12b derivative containing *PermE** promoter from pJTU695 and MCS	(Lu et al., 2011)
pTMM051	Two 1 kb PCR fragments upstream and downstream of the *ptmI* gene in pBlueScript II SK(-)	This study
pTMM052	Two 1 kb PCR fragments upstream and downstream of the *ptmI* gene in pTMN002	This study
pTMM015	Two 1 kb PCR fragments upstream and downstream of the *ptmS* gene in pBlueScript II SK(-)	This study
pTMM016	Two 1 kb PCR fragments upstream and downstream of the *ptmS* gene in pTMN002	This study
pTMM055	0.88 kb PCR fragment of the *ptmK* gene in pTMN002	This study
pTMM056	Two 1 kb PCR fragments upstream and downstream of the *ptmR* gene in pBlueScript II SK(-)	This study
pTMW057	Two 1 kb PCR fragments upstream and downstream of the *ptmR* gene in pTMN002	This study
pTMM058	pTMW050 containing complete structural gene of *ptmR*	This study
pTMN059	pBlueScrip II SK- containing complete structural gene of *ptmR*	This study
pTMN060	pET-20b(+) containing complete structural gene of *ptmR*	This study

4.3.2 General DNA Manipulations

Genomic DNA of *S. pactum* ATCC 27456 was prepared by standard protocol (Kieser et al., 2000) or using the DNeasy Tissue Kit (QIAGEN). DNA fragments were recovered from an agarose gel by using the QIAquick Gel Extraction Kit (QIAGEN). Restriction endonucleases were purchased from Invitrogen or Promega. Preparation of plasmid DNA was done by using a QIAprep Spin Miniprep Kit (Promega). All other DNA manipulations were performed according to standard protocols (Kieser et al., 2000; Sambrook and Russell, 2001). PCR was performed in 30 cycles by using a Mastercycler gradient thermocycler (Eppendorf) and Platinum *Taq* high-fidelity DNA polymerase (Invitrogen). Oligodeoxyribonucleotides for PCR primers were

synthesized by Sigma-Genosys. The nucleotide sequences of the gene fragments were determined at the Center for Genome Research and Biocomputing (CGRB) Core Laboratories, Oregon State University. ORFs were analyzed by FramePlot (Ishikawa and Hotta, 1999) analysis and BLAST program (Altschul et al., 1990).

4.3.3 Construction of *ΔptmR and ΔptmH/ΔptmR* Mutant Strains

The target genes were inactivated using a gene in-frame deletion strategy (Figure 4.2 a). Two ~1 kb PCR fragments, upstream (HindIII/EcoRI) and downstream (EcoRI/XbaI) of the *ptmR* gene, were fused and cloned into the HindIII/XbaI sites of pBluescript II SK(-) vector to generate pTMM056 (Table 4.2). The fused PCR fragment was excised and cloned into the HindIII/XbaI site of pTMN002 to generate pTMM057. The plasmid was then introduced into the wild-type and the *ΔptmH* mutant strains of *S. pactum* ATCC 27456 by conjugation using *E. coli* ET12567/pUZ8002 as a donor strain. Apramycin resistant strains representing single crossover mutants were obtained and grown on BTT [glucose (1%), yeast extract (0.1%), beef extract (0.1%), casein hydrolysate (0.2%), agar (1.5%), pH 7.4] agar plates containing apramycin (50 µg/mL). Subsequently, apramycin sensitive colonies were counter-selected by replica plating on BTT agar with and without apramycin (50 µg/mL). The resulting double-crossover candidate strains were confirmed by PCR amplification with *ptmR*-F1 and *ptmR*-R2 primers (Table 4.3) flanking the respective targeted gene.

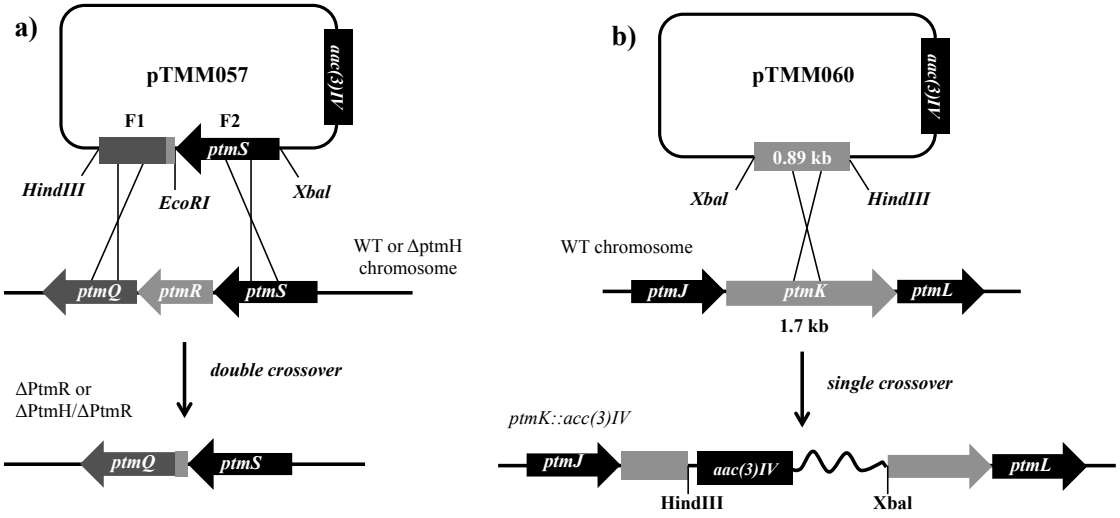

Figure 4.2 Cloning strategies for in-frame and gene disruption mutations of *S. pactum*. **a)** Double crossover recombination strategy for the in-frame deletion of *ptmR* in *S. pactum* wild-type or in *ΔptmH* mutant. Construction of *ΔptmI, ΔptmO, and ΔptmS* adopted the same strategy. **b)** Single crossover recombination strategy for the disruption of *ptmK* in *S. pactum*. Construction of *orfX2::aac(3)IV* adopted the same strategy.

Table 4.3 Primers used in this study.

Primer	Sequence*
ptmI-F1	5′-CCC**AAGCTT**GCTGCAGACCATGGACGAAT-3′
ptmI-R1	5′-CCG**GAATTC**GTCCATCGTGTCGTCTCTCC-3′
ptmI-F2	5′-CCG**GAATTC**GTCCATCGTGTCGTCTCTCC-3′
ptmI-R2	5′-GC**TCTAGA**AGGTGGTACGCGACCGTGTCCA-3′
ptmR-F1	5′-CCC**AAGCTT**ACGCCTACGGGTTCGGGCTGT-3′
ptmR-R1	5′-CCG**GAATTC**TGTTCTCACTCTTCCGATGT-3′
ptmR-F2	5′-CCG**GAATTC**TGGTGAGCGCGGCCAAGGAC-3′
ptmR-R2	5′-TGC**TCTAGA**TCGGTACGGCCGTCCTGGCT-3′
ptmR-pET-F	5′-GAA**GATCTACATATG**GTGAGAACACCGGGCATTTTCCT-3′
ptmR-pET-R	5′-CGCG**GAATTC**CCACGCGCCGCTC-3′
ptmR-C-R	5′-G**GAATTC**TCCGACCGGTGCCCGTCCTT-3′
ptmS-F1	5′-CCC**AAGCTT**GTGTGGAGCAGGTCAGGTTC-3′
ptmS-R1	5′-CCG**GAATTC**GGCGGAGGTCATCCGAGTCC-3′
ptmS-F2	5′- CCG**GAATTC**CCGCTTCTGCCGGGAGCGTCT-3′
ptmS-R2	5′-TGC**TCTAGA**GCCAGGTGGTCGAGGTGGATG-3′

orfX2-F	5′-CCC**AAGCTT**GACAACACCCTGTGGGACG-3′
orfX2-R	5′-TGC**TCTAGAA**TCAGCCAGCGCAGGAAC-3′
ptmO-F1	5′- CCC**AAGCTT**GAGCTGCTGGCGGTGAACAT-3′
ptmO-R1	5′-CCG**GAATTC**GCCGAGGTCGTACGGTTCCT-3′
ptmO-F2	5′-CCG**GAATTC**GCTCCATCTGTTCGACTGG-3′
ptmO-R2	5′-TGC**TCTAGA**ACTGCAGGGTCGCGGGTTGC-3′
ptmK-F1	5′-**CCCAAGCTT**GATGGTGGTCTGCGAGGT-3′
ptmK-F2	5′-TGC**TCTAGA**GTGACCGTGCACGTAGTCC-3′

*nucleotides underlined refer to restriction sites

4.3.4 Complementation of *ΔptmH/ΔptmR* Mutant

For complementation of the *ΔptmH/ΔptmR* mutant, the *ptmR* gene was amplified by PCR using the primers *ptmR*-pET-F and *ptmR*-C-R (Table 4.3). The PCR products were digested with BglII and EcoRI and ligated into the BamH/EcoRI sites of the cloning vector pBluescript II SK(-) to generate pTMM058. DNA sequencing confirmed the correct sequence of the construct. The resulting plasmid was digested with Ndel/EcoRI and the DNA fragment was ligated into the integration vector pTMW50, predigested with the same restriction enzymes, to generate pTMM059. The pTMM059 plasmid was then transferred into *E. coli* ET12567/pUZ8002, which was subsequently used to transform *ΔptmH* strain by conjugation (Kieser et al., 2000). Selection of the exconjugants (*ΔptmH/ΔptmR* mutants) was performed on BTT agar containing apramycin (50 μg/mL) and ampicillin (100 μg/mL).

4.3.5 Analysis of *ΔptmR*, Δ*ptmH/ΔptmR*, and *ΔptmH/ΔptmR*+pTMM059 Metabolic Profiles

The *ΔptmR, ΔptmH/ΔptmR*, and *Δ*ptmH/Δ*ptmR*+pTMM059 strains were grown on BTT agar at 30 °C for 3 days. Single colonies were used to inoculate the BTT seed cultures [medium for *ΔptmH/ΔptmR*+pTMM059 was supplemented with apramycin

(10 μg/mL) and ampicillin (20 μg/mL)] and incubated at 30 °C for 2 days. Production cultures were prepared in modified Bennett's medium (50 mL) (Ito et al., 2009) and inoculated with seed cultures [10% (V/V)]. The production cultures were incubated at 30 °C for 5 days under vigorous shaking (200 rpm). The mycelia were centrifuged and the supernatants were extracted twice with equal volumes of EtOAc followed by extraction with n-BuOH. The organic solvent from each extraction was evaporated *in vacuo* and the residues were dissolved in MeOH and were analyzed by reversed-phase HPLC and/or ESI-MS. Analysis of the metabolites of the mutants and those complemented with *ptmR* were carried out by reversed-phase HPLC with a C_{18} column (Supelcosil LC-18-DB 15 cm x 4.6 cm, 5 μm) using H_2O (95%) and CH_3CN (5%) containing 0.1% TFA as mobile phase at 1 mL/min flow rate.

4.3.6 Construction of *ptmK::aac(3)IV* and *orfX2::aac(3)IV* Mutants

The *ptmK* gene (1.7 kb) and AT gene (*orfX2*) were inactivated using a gene disruption strategy (Figure 4.2 b). The internal fragment (0.89 kb) of *ptmK* was generated by PCR using a forward primer containing a HindIII site and a reverse primer containing a Xbal site, and *S. pactum* genomic DNA was used as template. The PCR product was cloned into the HindIII/Xbal sites of pTMN002 to generate pTMM055. The internal fragment of (1.7 kb) *orfX2* was generated by PCR using a forward primer containing a HindIII site and a reverse primer containing a Xbal site, and *S. pactum* genomic DNA was used as template. The PCR product was inserted into the HindIII/Xbal sites of pTMN002 to generate pTMMA04. Plasmids pTMM055 and pTMMA04 were introduced to *S. pactum* strain by conjugation as described in our previous publication

(Lu et al., 2011). Briefly, the freshly harvested spores and the overnight-grown *E. coli* ET12567/pUZ8002 containing plasmids pTMM055 and pTMMA04 individually were mixed and plated onto MS agar plates containing 10 mM $MgCl_2$. After incubation at 30 °C for 18 h, the plates were overlaid with sterile water (1 mL) containing nalidixic acid (1 mg/mL) and apramycin (1 mg/mL) and incubated at 30°C for 5-7 days. The exconjugant (single crossover) colonies were purified by plating on BTT agar plates supplemented with apramycin (50 μg/mL). The disruption of *ptmK* and *orfX2* were confirmed by PCR amplification.

4.3.7 Construction of Δ*ptmI*, Δ*ptmO* and Δ*ptmS* Mutant Strains

The target genes were inactivated using a gene in-frame deletion strategy (Figure 4.2 a). Two ~1 kb PCR fragments upstream (HindIII/EcoRI) and downstream (EcoRI/XbaI) of the *ptmI, ptmO,* and *ptmS* genes were fused and cloned into the HindIII/XbaI sites of pBluescript II SK(-) vector to generate pTMM051, pTMM007, and pTMM015, respectively. The PCR products of *ptmI, ptmO,* and *ptmS* were excised and cloned into the HindIII/XbaI sites of pTMN002 to generate pTMM052, pTMM08, and pTMM016, respectively. All plasmids were then individually introduced into *S. pactum* ATCC 27456 strain by conjugation using *E. coli* ET12567/pUZ8002 as a donor strain. Apramycin resistant strains representing single crossover mutants were obtained and subsequently grown on BTT agar plates containing apramycin (50 μg/mL). Apramycin sensitive colonies were counter-selected by replica plating on BTT agar with and without apramycin (50 μg/mL). The resulting double-crossover

candidate strains were confirmed by PCR amplification with HindIII/Xbal primers flanking the respective targeted gene.

4.3.8 Cloning and Overexpression of PtmR

The *ptmR* gene was amplified using primer pairs *ptmR*-pET-F and *ptmR*-pET-R (Table 4.3). *Taq* high-fidelity DNA polymerase (Invitrogen) was used for PCR, and the resulting 1 kb PCR product was cloned into the pET-20b(+) vector (Novagen) to generate the expression vector pTMM060, which was introduced into *E. coli* BL21(DE3) pLysS (Invitrogen). For protein production, the bacteria were grown in LB medium supplemented with ampicillin (100 μg/mL) and chloramphenicol (25 μg/mL) at 30 °C with shaking at 250 rpm until an OD_{600} of 0.8-1 was reached. Protein expression was induced by the addition of IPTG (0.5 mM) with further cultivation for 8 h. The cells were harvested by centrifugation and resuspended in sodium phosphate buffer (50 mM, pH 7.5) containing NaCl (500 mM) and imidazole (10 mM) and then disrupted by sonication. After centrifugation of the sample, the supernatant was directly loaded onto a Ni-NTA spin column (QIAGEN). The recombinant PtmR was eluted using sodium phosphate buffer (50 mM, pH 7.5) containing NaCl (500 mM) and imidazole (50 mM). The PtmR-containing fractions were dialyzed (3 times, 4 h each) in 1 L solution containing sodium phosphate buffer (50 mM, pH 7.5), $MgCl_2$ (10 mM), glycerol (10%), and dithiothreitol (0.5 mM).

4.3.9 Feeding Experiments of Δ*ptmQ* and Δ*ptmH*/Δ*ptmQ* with 6MSA

The Δ*ptmQ* and Δ*ptmH*/Δ*ptmQ* mutants were streaked on BTT agar [glucose (1%), yeast extract (0.1%), beef extract (0.1%), casein hydrolysate (0.2%), agar (1.5%), pH

7.3] and incubated at 30 °C for 3 days. Spores of the Δ*ptmQ* and Δ*ptmH/*Δ*ptmQ* mutants were individually grown in two Erlenmeyer flasks (125 mL) containing 50 ml seed medium [glucose (1%), yeast extract (0.1%), beef extract (0.1%), casein hydrolysate (0.2%), pH 7.3] for 3 days at 30°C and 200 rpm. Each of these seed cultures (10 mL each) was used to inoculate 4 Erlenmeyer flasks (250 mL) containing modified Bennett medium (100 mL). After incubation for 18 h under the same condition, the cultures were grouped into two groups; the first group was fed with 6MSA (5 mM, 250 μL) and the second group was used as a control. The feeding was repeated every 12 h for 2 days. After 5 days of incubation, the cultures were centrifuged. The metabolites of each group were extracted with ethyl acetate (2x 100 mL). The organic solvent was evaporated using a rotary evaporator and the products were analyzed by MS.

4.3.10 Co-cultures of Δ*ptmJ*:Δ*ptmH/*Δ*ptmQ*, Δ*ptmS*:Δ*ptmH/*Δ*ptmQ*, and Δ*ptmI*:Δ*ptmH/*Δ*ptmQ*

The Δ*ptmJ*, Δ*ptmI*, Δ*ptmS* and Δ*ptmH/*Δ*ptmQ* mutants were streaked on BTT agar [glucose (1%), yeast extract (0.1%), beef extract (0.1%), casein hydrolysate (0.2%), agar (1.5%), pH 7.3] and incubated at 30 °C for 3 days. Spores of the Δ*ptmJ*, Δ*ptmI*, Δ*ptmS* and Δ*ptmHQ* mutants were individually grown in 4 Erlenmeyer flasks (125 mL) containing 50 mL seed medium [glucose (1%), yeast extract (0.1%), beef extract (0.1%), casein hydrolysate (0.2%), pH 7.3] for 3 days at 30°C and 200 rpm. Each of these seed cultures (5 mL each) was used to inoculate 4 Erlenmeyer flasks (150 mL) containing modified Bennett medium (5 mL) as a control. The Δ*ptmH/*Δ*ptmQ* mutant seed medium (5 mL) was co-culture in 9 Erlenmeyer flasks (3 flasks for each co-

cultured mutant strains) with 5 mL seed medium of Δ*ptmJ*, Δ*ptmS*, and Δ*ptmI* mutant individually. After five days of incubation, the cultures were centrifuged. The metabolites of each control and co-cultures were extracted with ethyl acetate (2x 50 mL). The organic solvent was evaporated using a rotary evaporator and the products were analyzed by MS.

4.3.11 Acyltransferase Assay

The acyltransferase reaction was typically carried out in 50 μL mixtures containing TM-25 or de-6MSA-pactamycin (1 mM), NAC thioester (2 mM), a cell- free extract containing PtmR (47 μL), and $MgCl_2$ (10 mM) in sodium phosphate buffer (50 mM, pH 7.5). The reaction was incubated at 37 °C. After 5 h, the reaction was quenched by the addition of one volume MeOH, and the products were analyzed by reversed-phase HPLC and/or ESI-MS.

4.3.12 Representative Synthesis of NAC Thioesters

S-(2-acetamidoethyl) 2-hydroxy-6-methylbenzothioate (6MSA-SNAC): To 2-hydroxy-6-methylbenzoic acid in dichloromethane (10 mL) was added to HOBT (1.05 eq, 0.69 mmol, 92 mg), EDCI (1.05 eq, 0.69 mmol, 131 mg), HSNAc (1.4 eq, 0.92 mmol, 110 mg), then triethylamine (2 eq, 1.32 mmol, 133 mg) at 0 °C and stirred for 18 h gradually until reached room temperature. The reaction was diluted with dichloromethane (20 mL) and washed successively with saturated $NaHCO_3$ solution (5 mL), water (10 mL), 1 M HCl (15 mL), and brine (5 mL). The organic fraction was then dried over Na_2SO_4, filtered and the solvent was removed *in vacuo*. The product was purified by flash column chromatography (hexane – EtOAc = 6:1, 4:1) to produce

pure 6MSA-SNAC (40 mg, 25%). ^{1}H NMR (700 MHz, $CDCl_3$): δ 9.84 (s, 1H), 7.20 (td, *J* = 8.0, 1.8 Hz, 1H), 6.81 (d, *J* = 8.3 Hz, 1H), 6.72 (d, *J* = 7.5 Hz, 1H), 6.17 (d, *J* = 13.4 Hz, 1H), 3.56 (q, *J* = 6.2 Hz, 2H), 3.23 (t, *J* = 6.3 Hz, 2H), 2.51 (d, *J* = 3.9 Hz, 3H), 1.98 (s, 3H). ^{13}C NMR (176 MHz, $CDCl_3$): δ 197.7, 171.3, 157.2, 157.1, 137.6, 137.5, 132.9, 132.9, 124.3, 124.2, 122.9, 115.4, 115.4, 77.3, 77.2, 76.9, 39.5, 29.7, 23.3, 22.2, 22.2. HR ESI-MS: calcd for $C_{12}H_{15}NO_3SNa$ *m/z* 276.0665 $[M+Na]^+$, found *m/z* 276.0667.

4.4 Results and Discussion

4.4.1 Inactivation of *orfX2* and *ptmO*

To investigate if any of the putative acyltransferase genes is involved in pactamycin biosynthesis, we genetically inactivated *orfX2* and *ptmO* by gene disruption with the apramycin resistance gene (*aac(3)IV*) and in-frame deletion, respectively (Figure 4.2 and Figure 4.3 b and d), and analysed their metabolites. ESI-MS analysis of the products revealed the ability of *ΔorfX2::aac(3)IV* to produce pactamycin, indicating that *orfX2* does not play a direct role in pactamycin biosynthesis (Figure 4.4 e). On the other hand, inactivation of *ptmO* complete abrogated the production of pactamycin and its analogs, (Ito et al., 2009) (Figure 4.4 c), suggesting that PtmO is most likely involved in the early steps of the pathway, not in the attachment of 6MSA, which has been demonstrated to occur later in the pathway (Ito et al., 2009).

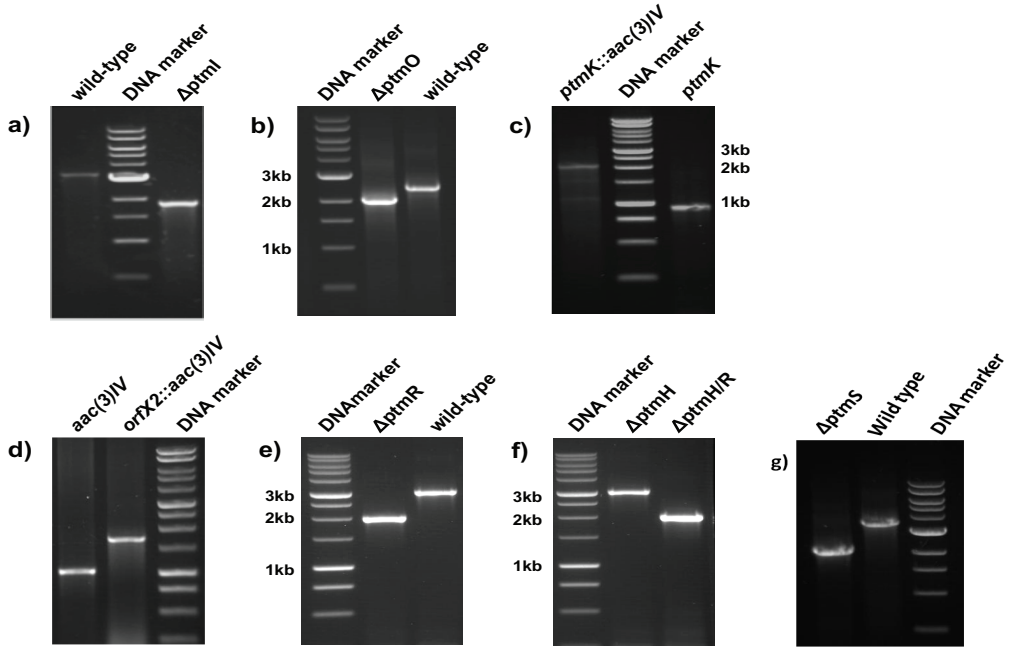

Figure 4.3 Genotypic confirmation of *ΔptmI, ΔptmO, ΔptmR, ΔptmH/ΔptmR, ptmK::aac(3)IV, and orfX2::aac(3)IV* mutants by PCR. **a)** DNA gel electrophoresis of PCR product of ΔPtmI, **b)** DNA gel electrophoresis of PCR product of ΔPtmO **c)** DNA gel electrophoresis of PCR product of *ptmK::aac(3)IV* mutant, **d)** DNA gel electrophoresis of PCR product of *orfX2::aac(3)IV* mutant, **e)** DNA gel electrophoresis of PCR product of ΔPtmR, f) DNA gel electrophoresis of PCR product of ΔPtmH/ΔPtmR, and g) DNA gel electrophoresis of PCR product of ΔPtmS.

4.4.2 Inactivation of *ptmI*, *ptmK*, and *ptmR*

Next, we investigated the involvement of *ptmI*, *ptmK*, and *ptmR* in the transfer of the 6MSA moiety. We generated *ptmI*, *ptmK*, and *ptmR* mutant strains of *S. pactum* by either in-frame deletion or gene disruption with *acc(3)IV* (Figure 4.2 and Figure 4.3 a, c, and e) and characterized their products by ESI-MS and HPLC. A gene disruption method was pursued for *ptmK* because an in-frame deletion approach was not successful. Similar to *ΔptmO*, the *ΔptmI* and *ptmK::acc(3)IV* mutants did not produce pactamycin or its analogs (Figure 4.4 b and d); again, suggesting their involvement in

the early steps of the pathway. On the other hand, the Δ*ptmR* mutant produced de-6MSA-pactamycin and its degradation product, de-6MSA-pactamycate (Figure 4.5 and Figure 4.6 a), which are identical with those of Δ*ptmQ* (the 6MSA synthase knockout mutant), (Ito et al., 2009) and consistent with the absence of acyltransferase activity in this mutant.

Furthermore, we inactivated *ptmR* in the mutant *(ΔptmH*) strain of *S. pactum* which produced 7-deoxy-7-demethylpactamycin (TM-026) (Lu et al., 2011). The double gene knockout mutant, *ΔptmH/ΔptmR*, produces de-6MSA-7-deoxy-7-demethylpactamycin (TM-025) (Figures 4.6 g and Figure 4.7), confirming the function of PtmR as an acyltransferase. These results were further corroborated by a successful gene complementation experiment, in which an integrative plasmid harbouring the intact *ptmR* gene was introduced into the *ΔptmH/ΔptmR* mutants. As expected, the resulting conjugants were able to produce TM-026 (Figure 4.6 f)

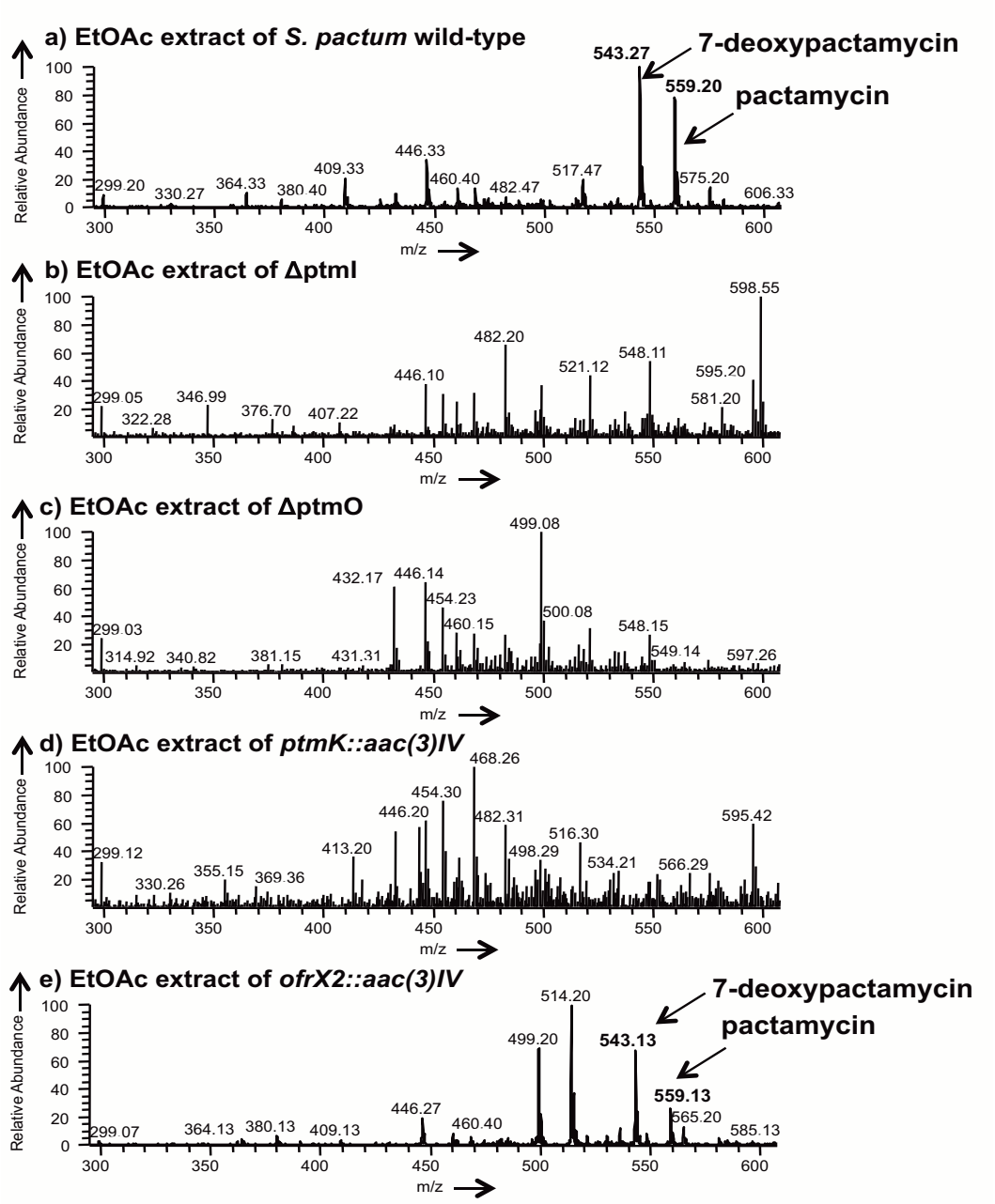

Figure 4.4 ESI-MS analysis of **a)** EtOAc extract of a culture of *S. pactum* wild-type, **b)** EtOAc extract of a culture of *ΔptmI,* **c)** EtOAc extract of a culture of *ΔptmO*, **d)** EtOAc extract of a culture of *ptmK::aac(3)IV*, and **e)** EtOAc extract of a culture of *orfX2::aac(3)IV*.

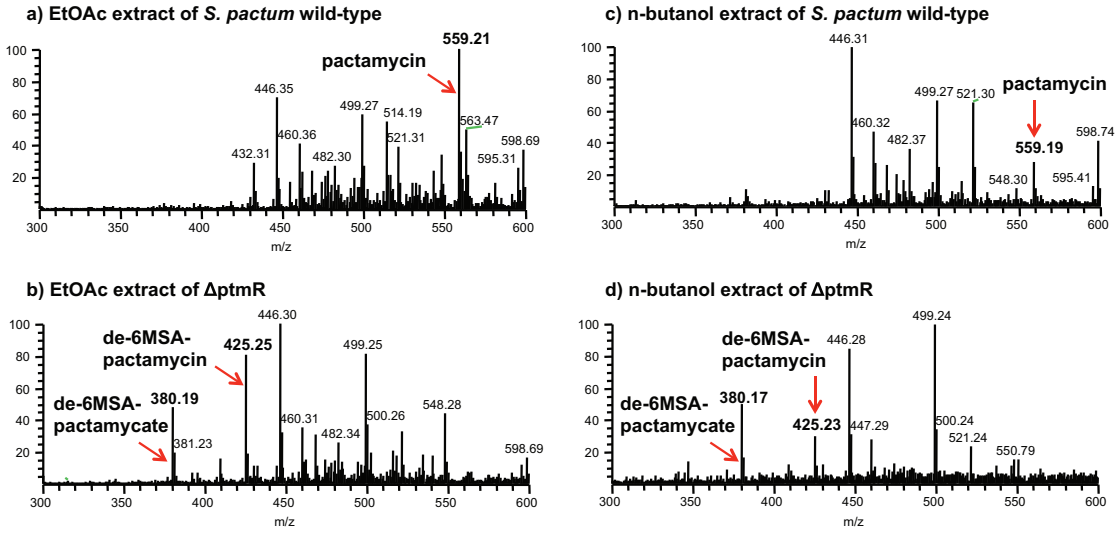

Figure 4.5. ESI-MS analysis of *ΔptmR* mutant. **a)** EtOAc extract of a culture of *S. pactum* wild type. **b)** EtOAc extract of a culture of *ΔptmR* mutant. **c)** Butanol extract of a culture of *S. pactum* wild type. **d)** Butanol extract of a culture of *ΔptmR* mutant.

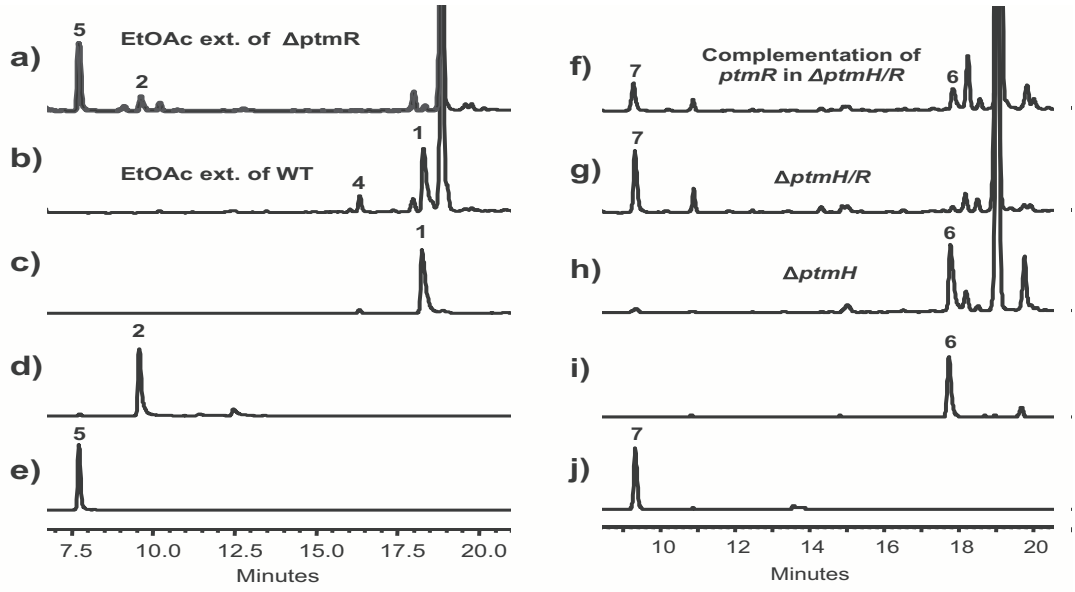

Figure 4.6 HPLC analyses of *ΔptmR* and *ΔptmH/ΔptmR* mutant strains of *S. pactum*. **a)** EtOAc extract *of ΔptmR*. **b)** EtOAc extract of wild type. **c)** Pactamycin standard. **d)** De-6MSA-pactamycin standard. eg., de-6MSA-pactamycate standard. **f)** EtOAc extract of ΔptmH/ΔptmR mutant complemented with the intact *ptmR* gene. **g)** EtOAc extract of *ΔptmH/ΔptmR* mutant. **h)** EtOAc extract of *ΔptmH mutant*. **i)** TM-026 standard. **j)** TM-025 standard.

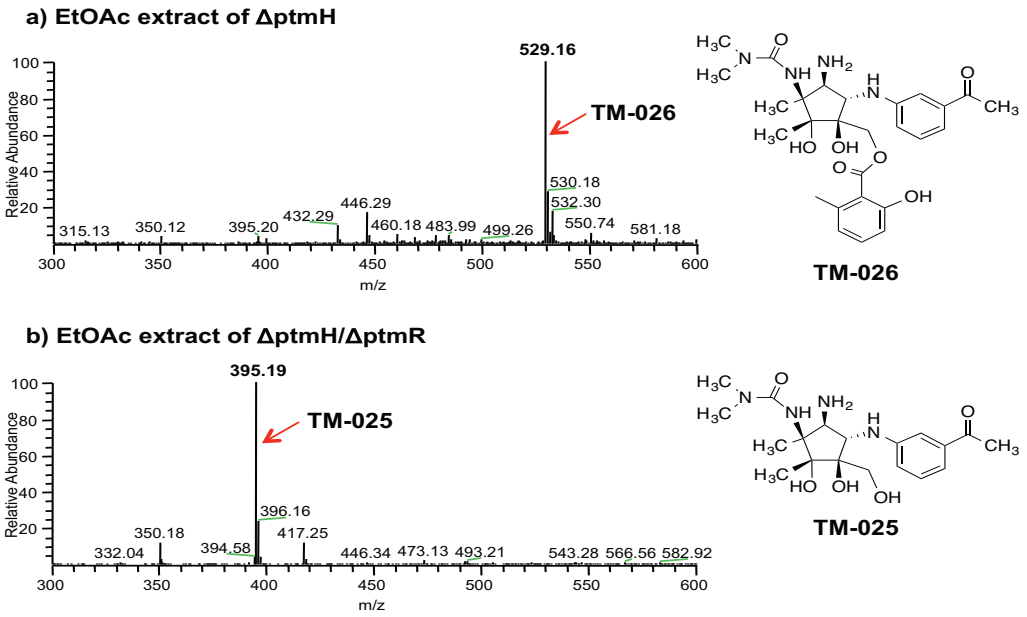

Figure 4.7. ESI-MS analysis of ΔptmH/ΔptmR mutant. **a)** EtOAc extract of a culture of *ΔptmH* mutant, which produces TM-026 (*m/z* 529). **b)** EtOAc extract of a culture of *ΔptmH/ΔptmR* double mutant.

4.4.3 Characterization of PtmR *in vivo*

To characterize the catalytic function of PtmR *in vitro*, we cloned the gene in the expression vector pET-20b(+) and heterologously expressed it in *E. coli* BL21(DE3)pLysS to give a 42 kDa C-terminal His_6-tagged protein. However, this recombinant protein only binds weakly to the Ni-NTA columns (Figure 4.8 a). Attempts to express the gene using a pRSET B vector, which contains an N-terminal His_6 sequence, and a pET-28a vector, which contains both N-terminal and C-terminal His_6 sequences, in *E. coli* under several growth conditions did not give the desired soluble proteins. Therefore, we decided to employ cell-free extracts of *E. coli* containing the pET-20b(+)- based recombinant C-terminal His_6-tagged PtmR for our enzymatic assays. A cell-free extract of *E. coli* harboring the empty pET20b(+) vector

was used as a negative control. Initial enzymatic experiments were carried out with EtOAc extracts of the ΔptmR mutant containing de-6MSA-pactamycin and de-6MSA-7-deoxypactamycin. The synthetically prepared *N*-acetylcysteamine (NAC) thioester of 6MSA was used as a model substrate. NAC thioesters have been known to resemble the phosphopantetheinyl arm of ACPs and have been widely used as mimics of ACP-bound substrates. ESI-MS and HPLC analyses of the reaction products revealed the conversion of the de-6MSA analog to their corresponding 6MSA esters (Figure 4.8 b).

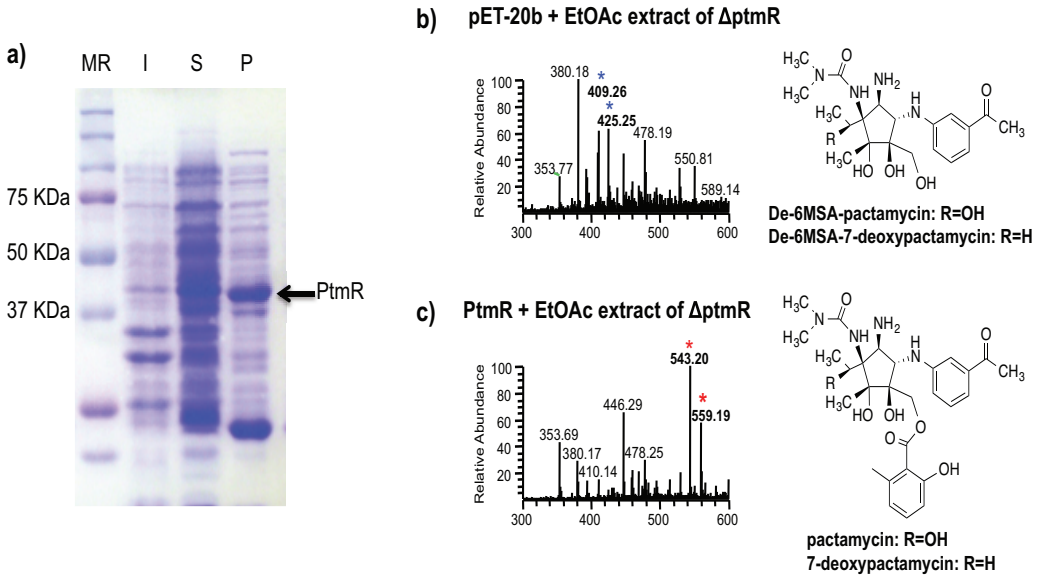

Figure 4.8 Production of recombinant PtmR and characterization of its AT activity. **a)** SDS PAGE of partially purified PtmR. The protein only binds weakly to the Ni-NTA resin and was eluted using sodium phosphate buffer (50 mM, pH 7.5) containing NaCl (500 mM) and imidazole (50 mM). MR, protein marker; I, insoluble proteins; S, soluble proteins (cell free extract); P, partially purified PtmR. **b)** ESI-MS spectrum of EtOAc extract of a culture of *ΔptmR* strain incubated with cell free extract of *E. coli* harboring empty vector pET-20b. **c)** ESI-MS spectrum of EtOAc extract of a culture of *ΔptmR* strain.

Similar experiments using pure de-6MSA-pactamycin, de-6MSA-pactamycate, and TM-025 as substrates gave pactamycin, pactamycate, and TM-026, respectively, which unambiguously confirmed the acyltransferase activity of PtmR (Figures 4.9, Figure 4.10, and Figure 4.11).

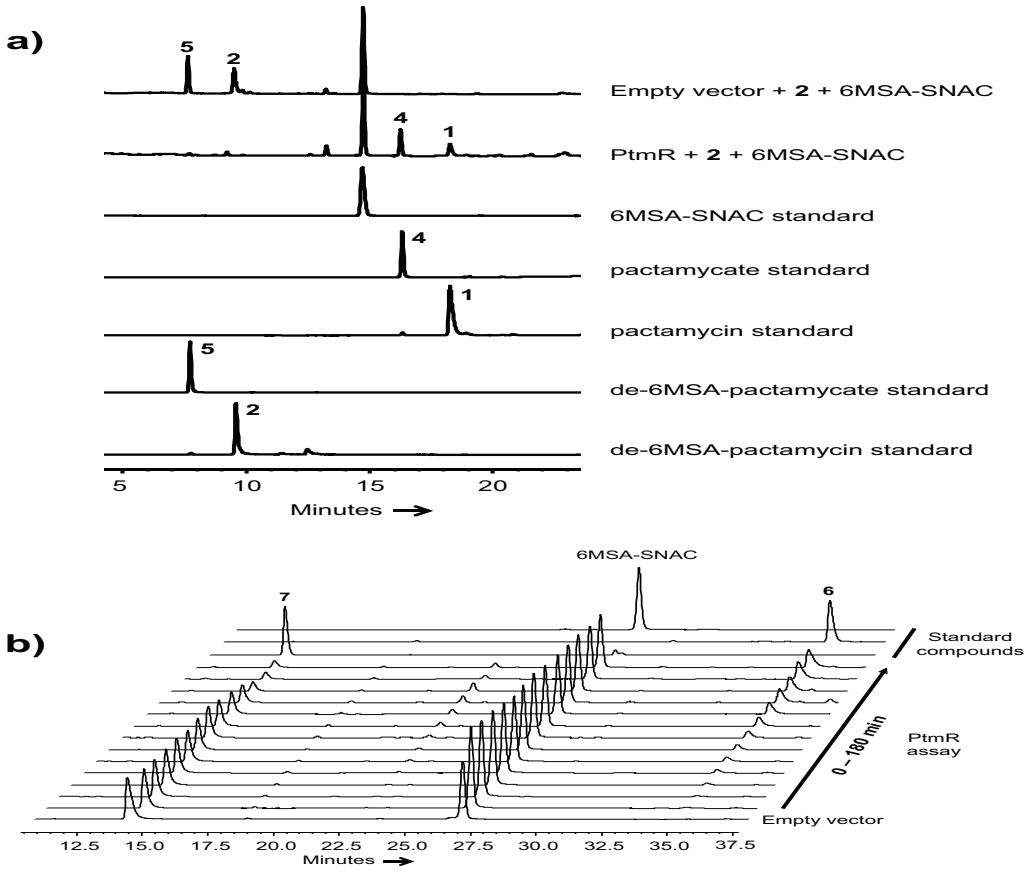

Figure 4.9. HPLC analyses of PtmR reactions. **a)** HPLC chromatograms of PtmR reaction using de-6MSA-pactamycin **(2)** and 6MSA-SNAC as substrates. Under the reaction conditions, a significant portion of **2** was converted to **5** non-enzymatically. **b)** HPLC chromatograms of PtmR reaction with TM-025 **(7)** and 6MSA-SNAC as substrates monitored at different time points.

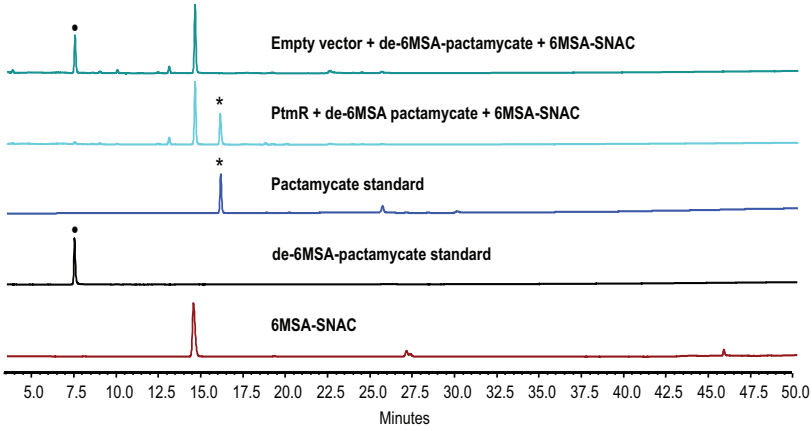

Figure 4.10 HPLC profile of PtmR enzymatic reaction using de-6MSA-pactamycate and 6MSA-SNAC. Filled circles represent de-6MSA-pactamycate and stars represent pactamycate.

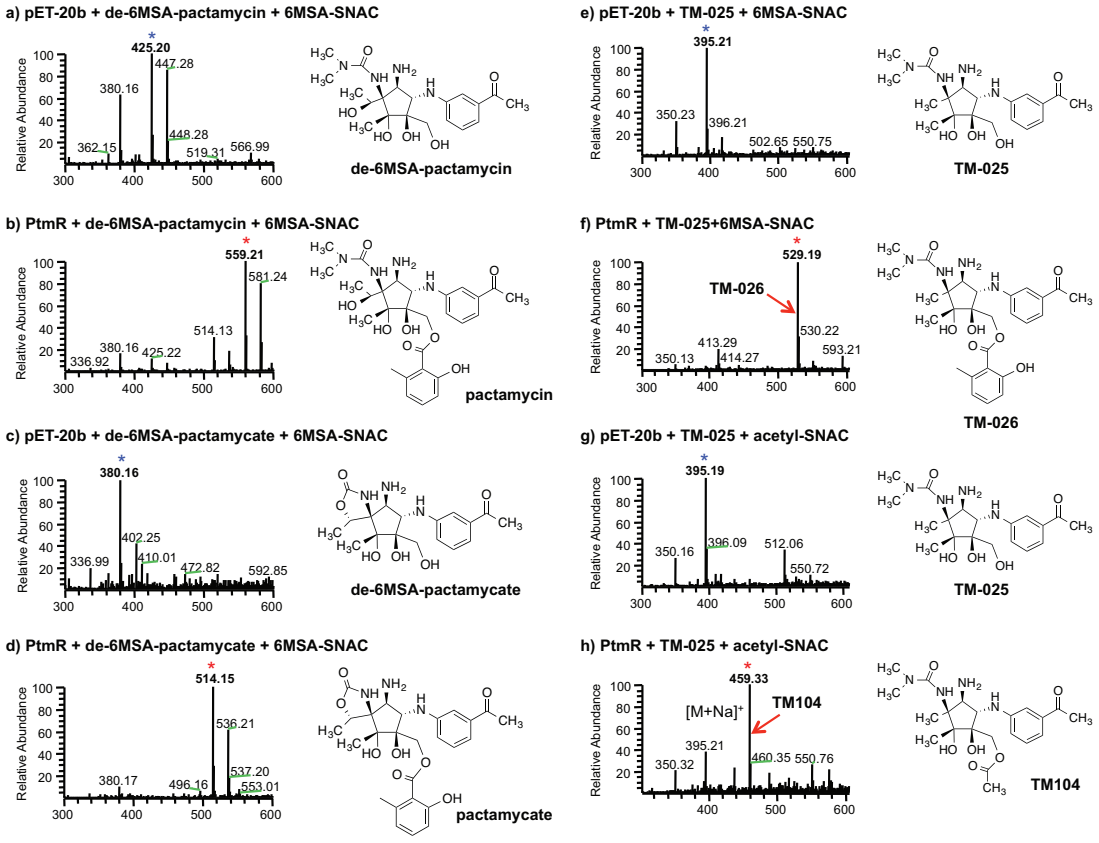

Figure 4.11 ESI-MS spectra of de-6MSA-pactamycin, de-6MSA-pactamycate, and TM-025 incubated with cell free extracts of cultures of *E. coli* harboring empty vector pET-20b(+) and that harboring *ptmR* in the presence of 6MSA-SNAC or acetyl-SNAC. Blue stars represent the substrates and red stars represent the products.

4.4.4 PtmR Transfers Activated 6MSA units onto Pactamycin Core

Incubations of the enzyme and TM-025 with 6MSA free acid as substrate did not give any products, indicating that PtmR only recognizes activated substrate. As no apparent CHIB3 homologue (a second KAS III) can be found in the pactamycin pathway, and given that PtmK (KAS I) and PtmI (ACP) are involved in the early steps of the pathway, it is conceivable that 6MSA is directly transferred from PtmQ to the aminocyclopentitol unit by PtmR (Figure 4.1 d). This is consistent with and also substantiates an earlier suggestion that the orsellinic acid moiety resulting from the iterative type I PKS in the avilamycin and calicheamicin pathways is directly transferred onto the designated sugar moieties of those compounds (He et al., 2009). Interestingly, in saphenamycin biosynthesis, it is proposed that 6MSA is first activated by a 6MSA adenylase (EsmD2) to its AMP derivative and loaded onto a 6MSA carrier protein (EsmD3) before being transferred to saphenic acid by a ChlB6 homologue, EsmD1 (Rui et al., 2012). However, incubation of 6MSA with the *ΔptmQ* and *ΔptmQ/ΔptmH* strains of *S. pactum* did not give pactamycin or TM-26, (Figure 4.12), suggesting that free 6MSA is not involved in the pathway.

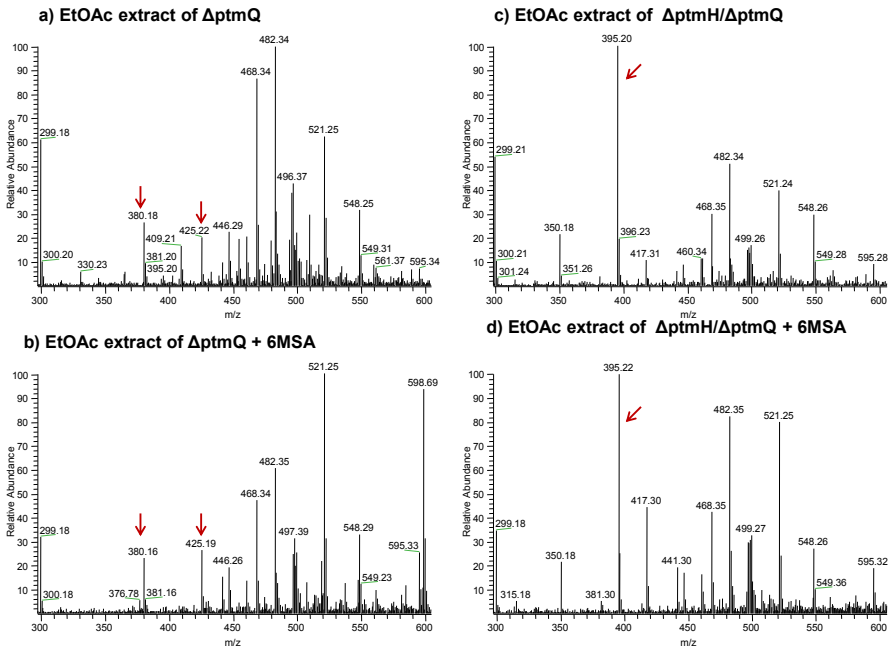

Figure 4.12 Feeding experiments with 6MSA to the *ΔptmQ* and *ΔptmQ/ΔptmH* strains of *S. pactum*. **a)** ESI-MS spectra of EtOAc extract of *ΔptmQ* without feeding. **b)** ESI-MS spectra of EtOAc extract of *ΔptmQ* fed with 6MSA. **c)** ESI-MS spectra of EtOAc extract of *ΔptmQ/ΔptmH* without feeding. **d)** ESI-MS spectra of EtOAc extract of *ΔptmQ/ΔptmH* fed with 6MSA.

4.4.5 The KAS III-like Protein PtmR is Responsible for a Direct transfer of 6MSA to Pactamycin core

A gene encoding a putative AMP-forming acyl-CoA synthetase is present in the pactamycin cluster. The gene product (PtmS) has been proposed to catalyze the activation of 3ABA, the precursor of the 3AAP moiety of pactamycin. Nonetheless, its role in the pactamycin pathway has yet to be experimentally established. To investigate the function of PtmS, we inactivated the gene in *S. pactum* by in frame-deletion and analyzed the products by ESI-MS. Similar to the *ΔptmI*, *ΔptmK*, and *ΔptmO* mutants; the *ΔptmS* strain was not able to produce pactamycin or its analogs

(Figure 4.3 g and Figure 4.13 d). This is consistent with the notion that it is involved in an early step of the pathway. However, the results cannot rule out the possibility of PtmS playing a dual role in the pathway – that is activating both 3ABA and 6MSA. This may also be the case with the discrete ACP PtmI. To test this possibility, we carried out co-culture experiments using *ΔptmQ/ΔptmH* + *ΔptmI* and *ΔptmQ/ΔptmH* + *ΔptmS*. Co-cultures of *ΔptmQ/ΔptmH* + *ΔptmJ* (which lacks the glycosyltransferase activity) (Ito et al., 2009) were used as a positive control. It is expected that the *ΔptmQ/ΔptmH* mutant product TM-025 will be taken up by the *ΔptmJ* strain and converted to TM-026. The same phenomenon should occur in the *ΔptmQ/ΔptmH* + *ΔptmI* and *ΔptmQ/ΔptmH* + *ΔptmS* cultures. However, if PtmI and/or PtmS are involved in the 6MSA attachment, no conversion from TM-025 to TM-026 should be observed in these cultures. As expected, ESI-MS analysis of the products of the *ΔptmQ/ΔptmH* + *ΔptmJ* co-cultures revealed the production of TM-026 as a major metabolite (Figure 4.13). Additionally, 7-deoxypactamycin and pactamycin were also detected in these cultures, suggesting to some extent that TM-025 and/or TM-026 are also modified by a radical SAM-dependent methyltransferase and a hydroxylase in the *ΔptmJ* strain. Similarly, the cultures of *ΔptmQ/ΔptmH* + *ΔptmI* and *ΔptmQ/ΔptmH* + *ΔptmS* also produced TM-026, 7-deoxypactamycin, and pactamycin indicating that both PtmI and PtmS do not play a role in the attachment of 6MSA to the cyclopentitol unit. All together, the results showed that the KAS III-like protein PtmR is responsible for a direct transfer of the 6MSA moiety from the iterative type I PKS PtmQ to the aminocyclopentitol unit in pactamycin biosynthesis (Figure 4.1 d).

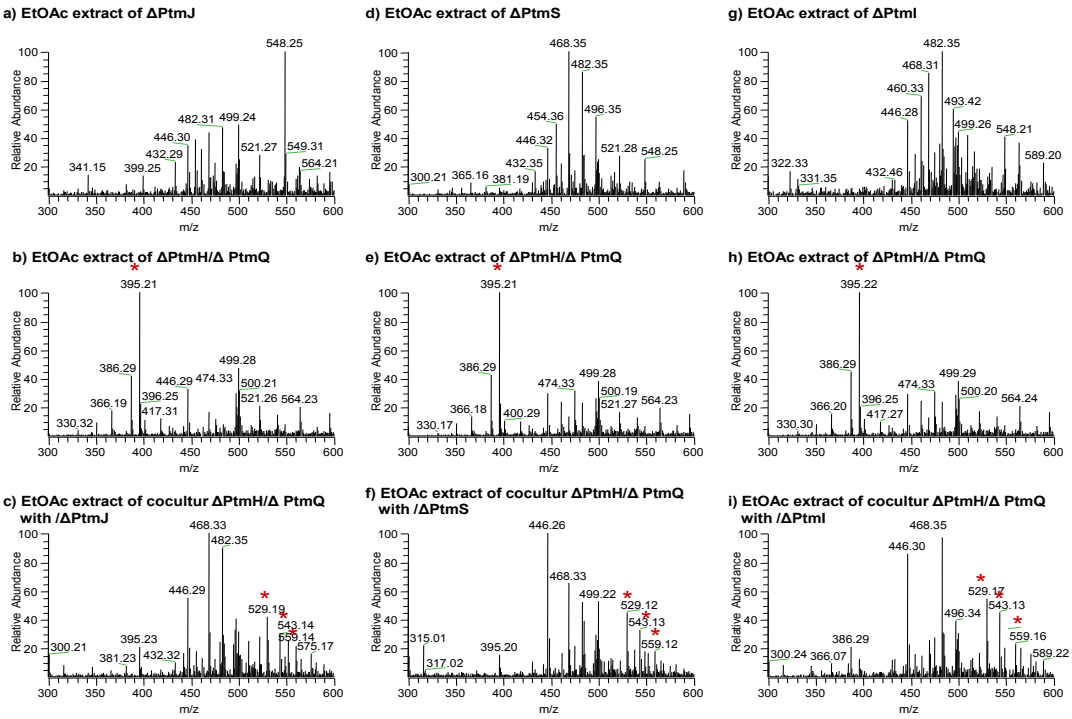

Figure 4.13 Co-culture experiments of *ΔptmQ/ΔptmH* with *ΔptmJ*, *ΔptmS*, and *ΔptmI* strains of *S. pactum.* **a)** ESI-MS spectra of EtOAc extract of *ΔptmJ*. **b)** ESI-MS spectra of EtOAc extract of *ΔptmQ/ΔptmH* strain. **c)** ESI-MS spectra of EtOAc extract of co-culture of *ΔptmQ/ΔptmH* with *ΔptmJ* strain. **d)** ESI-MS spectra of EtOAc extract of *ΔptmS* strain. **e)** ESI-MS spectra of EtOAc extract of *ΔptmQ/ΔptmH* strain. **f)** ESI-MS spectra of EtOAc extract of co-culture of *ΔptmQ/ΔptmH* with *ΔptmS* strain. **g)** ESI-MS spectra of EtOAc extract of ΔptmI strain. **h)** ESI-MS spectra of EtOAc extract of *ΔptmQ/ΔptmH* strain and **i)** ESI-MS spectra of EtOAc extract of co-culture of *ΔptmQ/ΔptmH* with *ΔptmI* strain. Red stars indicate the substrates and the products.

4.4.6 PtmR Displays Broad Substrate Specificity

The fact that PtmR does not only process de-6MSA-pactamycin but also de-6MSA-7-deoxypactamycin, de-6MSA-pactamycate, and TM-025 is consistent with our previous observations that some tailoring enzymes in pactamycin biosynthesis, including the enzyme that catalyzes 6MSA attachment, have relaxed substrate specificity (Lu et al., 2011). To explore if PtmR can also transfer acyl groups other than 6MSA, we

synthesized an additional 13 NAC thioesters with a variety of alkyl and aromatic features ranging from acetyl-SNAC to 3-aminobenzoyl-SNAC to cycloheptanecarbonyl-SNAC (Table 4.4), and incubated them with TM-025 and a cell-free extract of *E. coli* containing PtmR. A cell-free extract of *E. coli* harboring an empty pET20b(+) vector was used as a negative control. ESI-MS analysis of the enzymatic reactions revealed the ability of PtmR to use all 13 NAC thioesters, resulting in a suite of new pactamycin analogs with diverse functionalities (Table 4.4, Figures 4.11, Figure 4.14, Figure 4.15, and Figure 4.16).

Table 4.4 Conversion of TM-025 to various pactamycin analogs by PtmR.

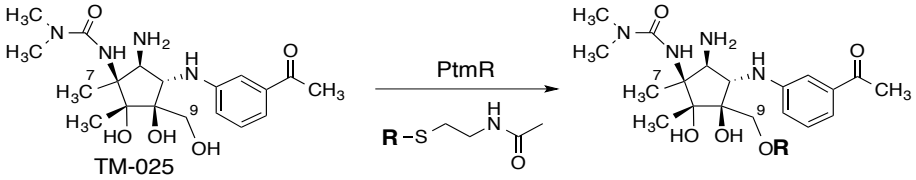

R	Product	HR ESI-MS *(m/z)*		Molecular Formula
		Calcd.	Observed	
	TM-026	529.26568 $[M+H]^+$	529.26635 $[M+H]^+$	$C_{27}H_{36}N_4O_7$
	TM-104	437.23946 $[M+Na]^+$	437.23960 $[M+Na]^+$	$C_{21}H_{32}N_4O_6$
	TM-105	473.23706 $[M+Na]^+$	473.23827 $[M+Na]^+$	$C_{22}H_{34}N_4O_6$
	TM-106	465.27076 $[M+H]^+$	465.27183 $[M+H]^+$	$C_{23}H_{36}N_4O_6$
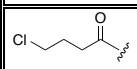	TM-107	499.23179 $[M+H]^+$	499.23272 $[M+H]^+$	$C_{23}H_{35}ClN_4O_6$
	TM-108	465.27076 $[M+H]^+$	465.27183 $[M+H]^+$	$C_{23}H_{36}N_4O_6$
	TM-109	479.28641 $[M+H]^+$	479.28735 $[M+H]^+$	$C_{24}H_{38}N_4O_6$

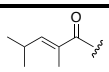	TM-110	505.30206 $[M+H]^+$	505.30253 $[M+H]^+$	$C_{26}H_{40}N_4O_6$
	TM-111	479.28641 $[M+H]^+$	479.28717 $[M+H]^+$	$C_{24}H_{38}N_4O_6$
	TM-112	499.25511 $[M+H]^+$	499.25584 $[M+H]^+$	$C_{26}H_{34}N_4O_6$
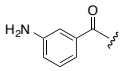	TM-113	514.26601 $[M+H]^+$	514.26902 $[M+H]^+$	$C_{26}H_{35}N_5O_6$
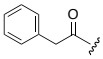	TM-114	513.27076 $[M+H]^+$	513.27376 $[M+H]^+$	$C_{27}H_{36}N_4O_6$
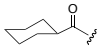	TM-115	505.30206 $[M+H]^+$	505.30220 $[M+H]^+$	$C_{26}H_{40}N_4O_6$
	TM-116	519.31771 $[M+H]^+$	519.31819 $[M+H]^+$	$C_{27}H_{42}N_4O_6$

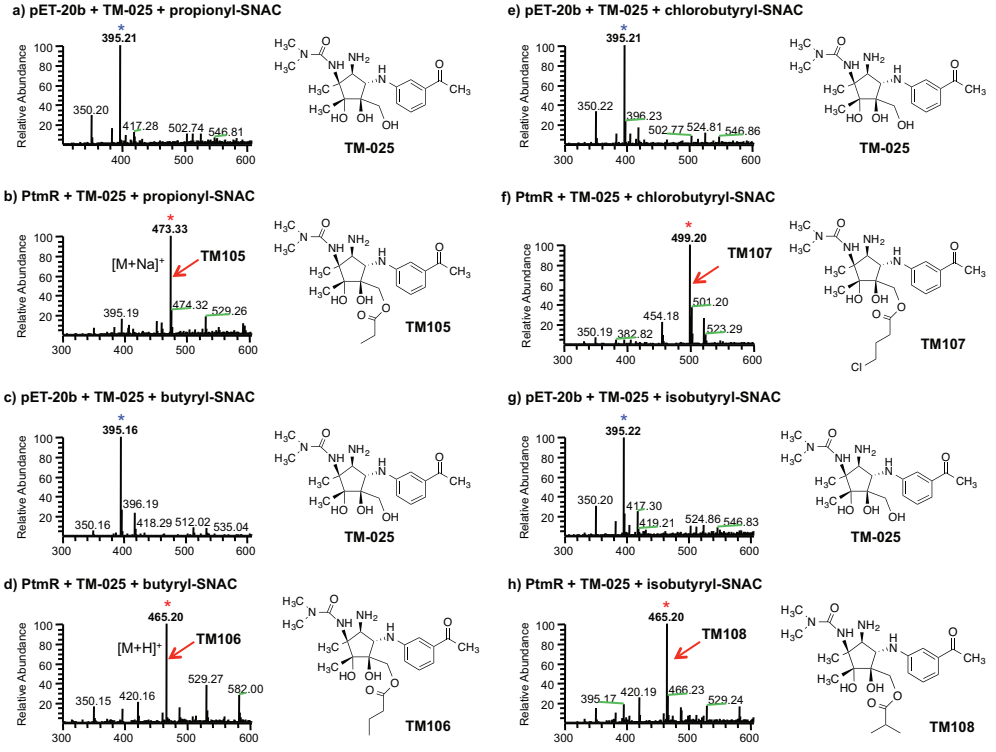

Figure 4.14 ESI-MS spectra of TM-025 incubated with cell free extracts of cultures of *E. coli* harboring empty vector pET-20b(+) and that harboring *ptmR* in the presence of propionyl-, butyryl-, chlorobutyryl-, or isobutyryl-SNAC. Blue stars represent the substrates and red stars represent the products.

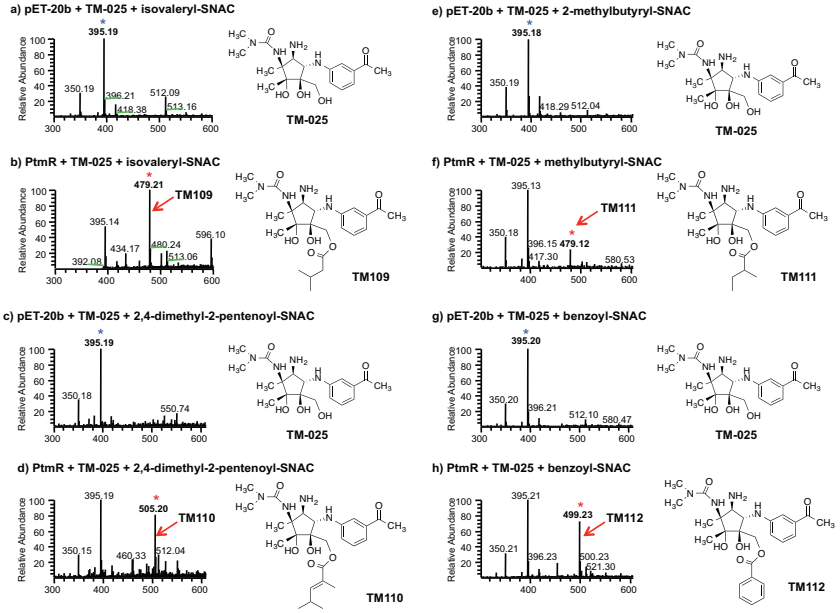

Figure 4.15 ESI-MS spectra of TM-025 incubated with cell free extracts of cultures of *E. coli* harboring empty vector pET-20b(+) and that harboring *ptmR* in the presence of isovaleryl-, 2,4-dimethyl-2-pentenoyl-, 2-methylbytyryl-, or benzoyl-SNAC. Blue stars represent the substrates and red stars represent the products.

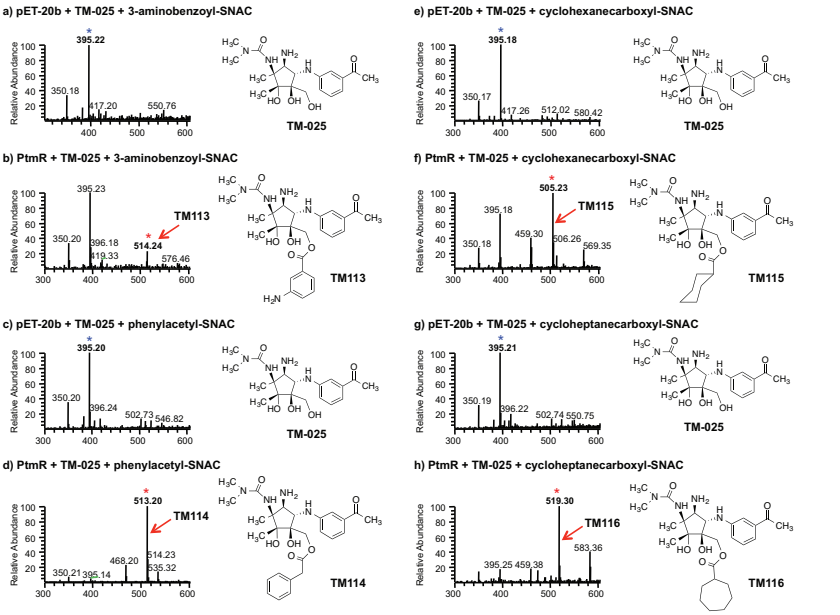

Figure 4.16 ESI-MS spectra of TM-025 incubated with cell free extracts of cultures of *E. coli* harboring empty vector pET-20b(+) and that harboring *ptmR* in the presence of 3-aminobenzoyl-, phenylacetyl-, cyclohexanecarboxylyl-, or cycloheptanecarboxylyl-SNAC. Blue stars represent the substrates and red stars represent the products.

Parallel experiments with benzoyl-CoA, acetyl-CoA, propionyl-CoA, and butyryl-CoA did not give any products, (Figure 4.17), indicating that PtmR does not recognize CoA esters as substrates.

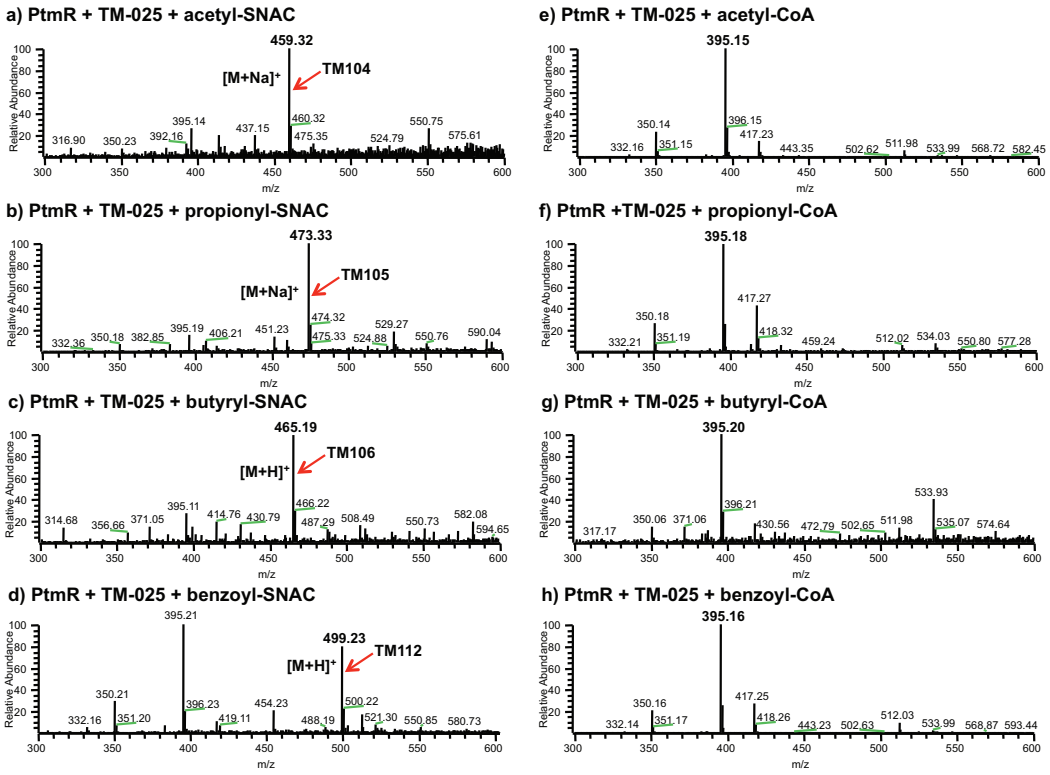

Figure 4.17 ESI-MS spectra of TM-025 (*m/z* 395) incubated with cell free extracts of cultures of *E. coli* harboring empty vector pET-20b(+) and that harboring *ptmR* in the presence of NAC and CoA esters of acetate, propionate, butyrate, and benzoate.

4.4.7 Phylogenetic Analysis of PtmR and Homologous Proteins

The ability of PtmR to utilize a broad range of substrates is somewhat surprising, as so far KAS III-like proteins, e.g., CloN2, ChlB6, CalO4, AviN, and EvrI, have only been associated with the transfer of an aryl or pyrrolylcarbonyl group to a sugar moiety. A phylogenetic analysis of PtmR and homologous proteins showed that PtmR falls within a clade of KAS III-like enzymes, but it forms a separate sub-clade together with

EsmD1 and a hypothetical protein, WP_010359166 (83% identity with PtmR), from a plant pathogen, *Streptomyces acidiscabies* 84-104 (Figure 4.18) (Huguet-Tapia and Loria, 2012). The WP_010359166 gene is part of a gene cluster in this organism and interestingly, similar to *ptmR*, is also located next to a gene encoding an iterative type I PKS (6MSA synthase). Therefore, we predict that WP_010359166 is also responsible for the attachment of 6MSA or its analog to the corresponding natural product.

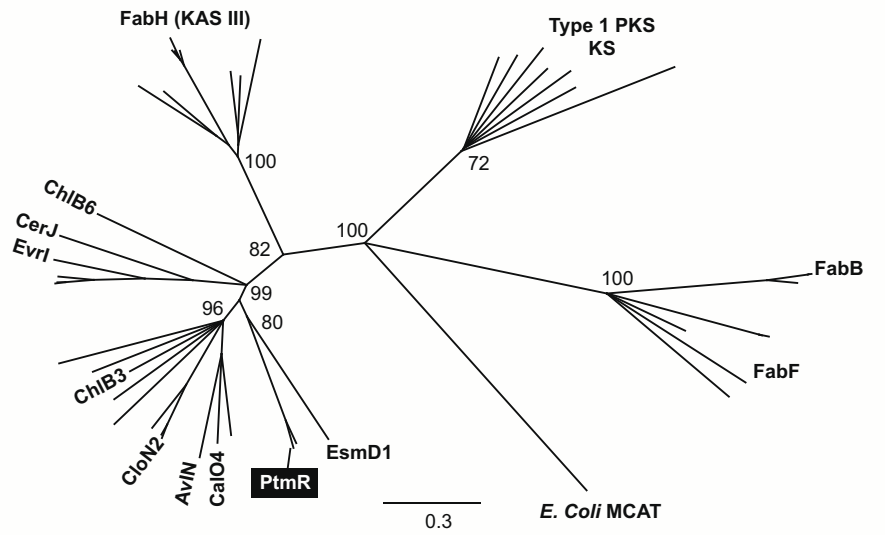

Figure 4.18 Phylogenetic analysis of PtmR and homologous proteins. A neighbor joining method was used for tree construction. The source and accession number of the proteins are listed in Table 4.5.

Although no biochemical studies have been reported for CalO4, AviN, and EvrI, on the basis of our results and those of others, it is conceivable that these enzymes are responsible for the transfer of 6MSA or orsellinic acid derivatives to their corresponding natural products. A careful inspection of the amino acid sequence alignment of these proteins revealed a conserved Cys-His-Asp catalytic triad (Table 4.6, Figure 4.19), suggesting their ability to perform an acyltransferase reaction similar

to CerJ, ChlB6, or PtmR. It is not implausible that they can also recognize various NAC thioesters as substrates to produce diverse and complex natural product derivatives. Therefore, our work not only provide new insight into KAS III-like enzymes but also serve as a starting point for their development as versatile tools for the creation of new libraries of complex natural products.

Table 4.5 Sources and accession numbers of KAS III homologues.

Species	Accession number	Protein
Streptomyces pactum	A8R0K3_9ACTO	KASIII/ACP-Shuttle AT-like, PtmR
Streptomyces acidiscabies	WP_010359166	KASIII/ACP-Shuttle AT-like
Streptomyces antibioticus	AFB35630	KASIII/ACP-Shuttle AT-like, EsmD1
Dactylosporangium aurantiacum subsp. *hamdenensis*	ADU85987.1	ACP-Shuttle AT, TiaF
Micromonospora echinospora	AAM70354.1	ACP-Shuttle AT CalO4
Nocardiopsis dassonvillei	ZP_04334033.1	ACP-Shuttle AT
Saccharopolyspora erythraea	YP_001107471.1	ACP-Shuttle AT
Stigmatella aurantiaca	ZP_01462124.1	ACP-Shuttle AT
Streptomyces antibioticus	AAZ77676.1	ACP-Shuttle AT, ChlB3
Streptomyces diastatochromogenes	ACN64832.1	ACP-Shuttle AT
Streptomyces rishiriensis	AAG29787.2	ACP-Shuttle AT
Streptomyces roseochromogenes	AAN65231.1	ACP-Shuttle AT, CloN2
Streptomyces sp. Tü6071	ABB69750.1	ACP-Shuttle AT
Streptomyces viridochromogenes Tü57	AF333038_20	ACP-Shuttle AT, AviN
Actinobacillus pleuropneumoniae	ZP_00134992.2	FabB
Citrobacter sp. 30_2	ZP_04562837.1	FabB
Escherichia coli	NP_416826.1	FabB
Shigella boydii	YP_001881145.1	FabB
Escherichia albertii	ZP_02902779.1	FabF
Escherichia coli	NP_415613.1	FabF
Staphylococcus aureus	NP_645683.1	FabF
Streptococcus pneumoniae	NP_344945.1	FabF
Thermus thermophilus	YP_143679.1	FabF
Streptomyces coelicolor	NP_626634.1	KAS III
Streptomyces echinatus	AAV84077.1	KAS III

Streptomyces glaucescens	Q54206.1	KAS III
Streptomyces griseus	AAQ08929.1	KAS III
Streptomyces griseus	YP_001826619.1	KAS III
Streptomyces roseofulvus	AAC18104.1	KAS III
Streptomyces sp. A2991200	CAM58805.1	KAS III
Streptomyces sp. CM020	ACI88883.1	KAS III
Streptomyces sp. R1128	AAG30195.1	KAS III
Streptomyces antibioticus	AAZ77679.1	KAS III-like, ChlB6
Streptomyces galilaeus	AAF70109.1	KAS III-like
Streptomyces galilaeus	BAB72048.1	KAS III-like
Streptomyces peucetius	AAA65208.1	KAS III-like, EviR
Streptomyces sp. SPB74	WP_008748182.1	KAS III-like
Streptomyces tendae	AEI91069.1	KAS III -like, CerJ
Escherichia coli	NP_415610.1	Malonyl-CoA-(ACP)-AT
Saccharopolyspora erythraea	YP_001102990.1	Type I PKS
Streptomyces antibioticus	AAF82408.1	Type I PKS
Streptomyces fradiae	AAB66504.1	Type I PKS
Streptomyces griseoruber	AAP85336.1	Type I PKS
Streptomyces nanchangensis	AAP42874.1	Type I PKS
Streptomyces sp. 307-9	ADC79637.1	Type I PKS
Streptomyces violaceusniger	ABJ97437.1	Type I PKS

Table 4.6 Proposed active site residue of selected KAS and KAS-like protein.

Protein	Residue 1	Residue 2	Residue 3	Residue 4
KAS III (FabH)	**Cys**	His	**Asn**	**Ser**
DpsC	**Ser**	His	**His**	**Asp**
ChlB6	**Cys**	His	**His**	**Asp**
CerJ	**Cys**	Val	**His**	**Asp**
CloN2	**Cys**	Ser	**His**	**Asp**
CouN2	**Cys**	Ser	**His**	**Asp**
AviN	**Cys**	Asn	**Thr**	**Asp**
EvrI	**Cys**	Asn	**His**	**Asp**
CalO4	**Cys**	Asn	**His**	**Asp**
PokM2	**Cys**	Asn	**His**	**Asp**
TiaF	**Cys**	Asn	**His**	**Asp**
ChlB3	**Cys**	Asn	**His**	**Asp**
PlaP2	**Cys**	Gly	**His**	**Asp**
EsmD1	**Cys**	Gly	**His**	**Asp**
PtmR	**Cys**	Gly	**His**	**Asp**

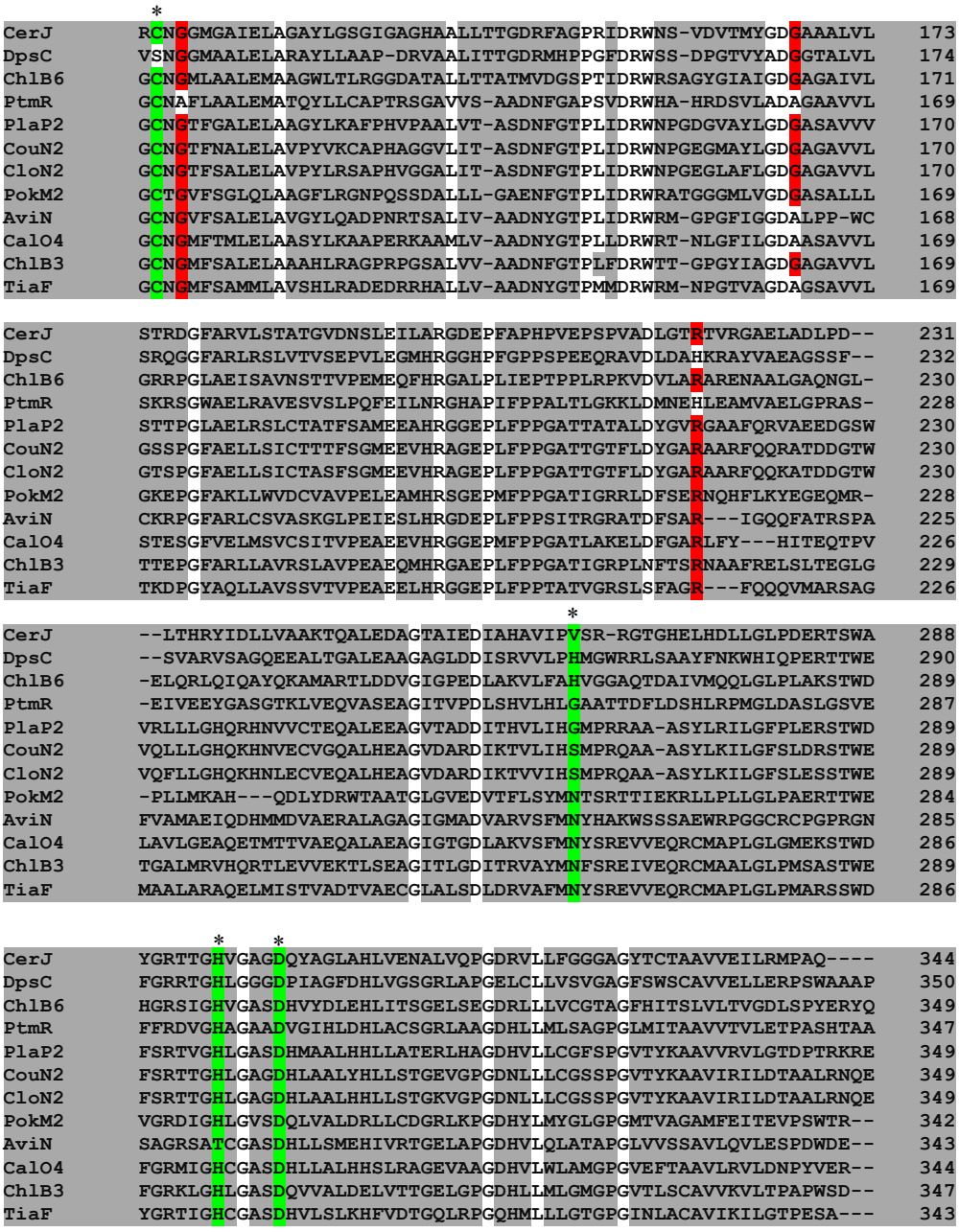

Figure 4.19 Multiple amino acid sequence alignment of KAS III homologues. CerJ, from the cervimycin pathway; DpsC, from the doxorubicin pathway; ChlB6 and ChlB3, from the chlorothricin pathway; PtmR, from the pactamycin pathway; PlaP2, from the phenalinolactone pathway; CouN2 and CloN2, from the clorobiocin pathway; PokM2, from the polyketomycin pathway; AviN, from the avilamycin pathway; and TiaF, from the tiacumicin pathway.

Chapter 5 : General Conclusion

Mostafa E. Abugrain

Despite progress made in recent years to understand how pactamycin is synthesized in nature, many aspects of its biosynthesis remained elusive. For example, it was unclear how 3-aminobenzoic acid (3ABA) is converted to 3-aminoacetophenone (3AAP); when the attachment of a sugar or a cyclopentitol moiety to the aromatic ring takes place; what is the sequence or the timing of the tailoring steps; and what gene is responsible for the attachment of 6-methylsalicylic (6MSA) acid to the aminocyclopentitol core. The studies presented in this dissertation were designed to address these questions. Specifically, we investigated both the early steps of the pathway, particularly the formation of 3AAP moiety, and the tailoring steps of pactamycin biosynthesis, including the enzyme that is responsible for the attachment of 6-methylsalicylyl (6MSA) moiety to the pactamycin core.

Using gene inactivation, chemical complementation, and biochemical studies, we demonstrated that the aminotransferase PtmT is responsible for the formation of 3ABA. The later compound is processed by a set of discrete polyketide synthase proteins (PKSs), i.e. an AMP-forming acyl-CoA synthetase (PtmS), an acyl carrier protein (ACP) (PtmI) and a β-ketoacyl-ACP synthase (PtmK), to produce 3-[3-aminophenyl]3-oxopropionyl-ACP (3AP-3OP). The hydrolase PtmO is responsible for the cleavage of a β-ketoacyl product from ACP, which then undergoes a spontaneous decarboxylation. This study also revealed that neither free 3AAP nor its glycosylated derivative are directly involved in the biosynthesis of pactamycin.

Although the mode of formation of the aminocyclopentitol moiety is unclear, it has been proposed that it is derived from a derivative of glucosamine catalyzed by a radical SAM-dependent enzyme, PtmC. The product is then modified by a number of tailoring enzymes. Some of them have previously been identified by gene inactivation and biochemical characterization. However, due to the promiscuity of some of those enzymes, the sequence or the timing of the tailoring processes were unclear.

Using double gene inactivation strategy, we were able to obtain new knowledge of the tailoring steps of pactamycin biosynthesis. Based on the results described in Chapter 3, we proposed that the *C*-methylations at C-1 and C-5 by PtmL and PtmM, as well as the urea formation by PtmG, take place early in the pathway, followed by the C-7 methylation by the radical SAM-dependent enzyme PtmH. The product is then *N*-methylated by PtmD, followed by the attachment of 6MSA, possibly by the KAS III-like protein PtmR. In addition, we were able to isolate two new pactamycin analogs, TM-101 and TM-102, with remarkable antimalarial activity, but in contrast to pactamycin, these new analogs have no significant antibacterial activity and reduced cytotoxicity against mammalian cells. The results suggest that either the compounds are highly selective towards plasmodial ribosomes, or they inhibit plasmodial growth by a different mechanism of action.

The catalytic function of the KAS III-like protein PtmR as an acyltransferase (AT) was confirmed by gene inactivation, both in the pactamycin producer *Streptomyces pactum*

and in the *ΔptmH* mutant, and by *in vitro* biochemical assay of the recombinant protein PtmR directly transfers 6MSA from an ACP to the aminocyclopentitol core of pactamycin. Interestingly, this enzyme is highly promiscuous, recognizing a wide array of synthetically prepared acyl-*N*-acetylcysteamine (acyl-NAC) derivatives as substrates to give a suite of new pactamycin analogs.

Our success in generating new pactamycin analogs via gene inactivation and chemoenzymatic reactions demonstrates the power of state-of-the-art biosynthetic approaches in drug discovery and development. A number of these new analogs have shown improved biological activities compared to the parent compound and some of them may be further developed as clinically useful drugs.

REFERENCE

Adams, E.S., and Rinehart, K.L. (1994). Directed Biosynthesis of 5"-Fluoropactamycin in Streptomyces-Pactum. Journal of Antibiotics *47*, 1456-1465.

Admiraal, S. J.; Khosla, C.; Walsh, C. T. (2003). A Switch for the transfer of substrate between nonribosomal peptide and polyketide modules of the rifamycin synthetase assembly line. J Am Chem Soc *125* (45), 13664-5.

Ahlert, J., Shepard, E., Lomovskaya, N., Zazopoulos, E., Staffa, A., Bachmann, B.O., Huang, K., Fonstein, L., Czisny, A., Whitwam, R.E.*, et al.* (2002). The calicheamicin gene cluster and its iterative type I enediyne PKS. Science (New York, NY *297*, 1173-1176.

Almabruk, K.H., Lu, W., Li, Y., Abugreen, M., Kelly, J.X., and Mahmud, T. (2013). Mutasynthesis of fluorinated pactamycin analogues and their antimalarial activity. Org Lett *15*, 1678-1681.

Altschul, S.F., Gish, W., Miller, W., Myers, E.W., and Lipman, D.J. (1990). Basic local alignment search tool. J Mol Biol *215*, 403-410.

Ankenbauer, R.G., Staley, A.L., Rinehart, K.L., and Cox, C.D. (1991). Mutasynthesis of siderophore analogues by Pseudomonas aeruginosa. Proc Natl Acad Sci U S A *88*, 1878-1882.

Arias, P., Fernandez-Moreno, M.A., and Malpartida, F. (1999). Characterization of the pathway-specific positive transcriptional regulator for actinorhodin biosynthesis in Streptomyces coelicolor A3(2) as a DNA-binding protein. J Bacteriol *181*, 6958-6968.

Austin, M.B., and Noel, J.P. (2003). The chalcone synthase superfamily of type III polyketide synthases. Nat Prod Rep *20*, 79-110.

Ballesta, J.P.G., and Cundliffe, E. (1991). Site-specific methylation of 16s ribosomal-rna caused by pct, a pactamycin resistance determinant from the producing organism, streptomyces-pactum. J Bacteriol *173*, 7213-7218.

Berdy, J. (2005). Bioactive microbial metabolites. J Antibiot (Tokyo) *58*, 1-26.

Bhuyan, B.K. (1962). Pactamycin production by Streptomyces pactum. Appl Microbiol *10*, 302-304.

Bhuyan, B.K., Dietz, A., and Smith, C.G. (1961). Pactamycin, a new antitumor antibiotic. I. Discovery and biological properties. Antimicrobial Agents and Chemotherapy, 184-190.

Bibb, M.J., Sherman, D.H., Omura, S., and Hopwood, D.A. (1994). Cloning, sequencing and deduced functions of a cluster of Streptomyces genes probably encoding biosynthesis of the polyketide antibiotic frenolicin. Gene *142*, 31-39.

Boddy, C.N., Hotta, K., Tse, M.L., Watts, R.E., and Khosla, C. (2004). Precursor-directed biosynthesis of epothilone in Escherichia coli. J Am Chem Soc *126*, 7436-7437.

Bormann, C., Kalmanczhelyi, A., Sussmuth, R., and Jung, G. (1999). Production of nikkomycins Bx and Bz by mutasynthesis with genetically engineered Streptomyces tendae Tu901. J Antibiot (Tokyo) *52*, 102-108.

Bretschneider, T., Zocher, G., Unger, M., Scherlach, K., Stehle, T., and Hertweck, C. (2012). A ketosynthase homolog uses malonyl units to form esters in cervimycin biosynthesis. Nature chemical biology *8*, 154-161.

Brodersen, D.E., Clemons, W.M., Jr., Carter, A.P., Morgan-Warren, R.J., Wimberly, B.T., and Ramakrishnan, V. (2000). The structural basis for the action of the antibiotics tetracycline, pactamycin, and hygromycin B on the 30S ribosomal subunit. Cell *103*, 1143-1154.

Calcutt, M.J., and Cundliffe, E. (1990). Resistance to pactamycin in clones of Streptomyces lividans containing DNA from pactamycin-producing Streptomyces pactum. Gene *93*, 85-89.

Carter, A.P., Clemons, W.M., Brodersen, D.E., Morgan-Warren, R.J., Wimberly, B.T., and Ramakrishnan, V. (2000). Functional insights from the structure of the 30S ribosomal subunit and its interactions with antibiotics. Nature *407*, 340-348.

Cohen, L.B., Goldberg, I.H., and Herner, A.E. (1969). Inhibition by pactamycin of the initiation of protein synthesis. Effect on the 30S ribosomal subunit. Biochemistry *8*, 1327-1335.

Coleman, R.S., and Lu, X. (2006). Total synthesis of strobilurin B using a hetero-bis-metallated pentadiene linchpin. Chem Commun, 423-425.

Daum , M., Peintner , I., Linnenbrink, A., Frerich, A., Weber, M., Paululat, T., and Bechthold, A. (2009). Organisation of the Biosynthetic Gene Cluster and Tailoring Enzymes in the Biosynthesis of the Tetracyclic Quinone Glycoside Antibiotic Polyketomycin. ChemBioChem *10*, 1073-1083.

Dawe, J.H., Porter, C.T., Thornton, J.M., and Tabor, A.B. (2003). A template search reveals mechanistic similarities and differences in beta-ketoacyl synthases (KAS) and related enzymes. Proteins *52*, 427-435.

Dias, D.A., Urban, S., and Roessner, U. (2012). A Historical Overview of Natural Products in Drug Discovery. Metabolites *2*, 303-336.

Dobashi, K., Isshiki, K., Sawa, T., Obata, T., Hamada, M., Naganawa, H., Takita, T., Takeuchi, T., Umezawa, H., Bei, H.S.*, et al.* (1986). 8"-Hydroxypactamycin and 7-Deoxypactamycin, New Members of the Pactamycin Group. J Antibiot *39*, 1779-1783.

Dunn, B.J., Watts, K.R., Robbins, T., Cane, D.E., and Khosla, C. (2014). Comparative analysis of the substrate specificity of trans- versus cis-acyltransferases of assembly line polyketide synthases. Biochemistry *53*, 3796-3806.

Fernandez-Moreno, M.A., Caballero, J.L., Hopwood, D.A., and Malpartida, F. (1991). The act cluster contains regulatory and antibiotic export genes, direct targets for translational control by the bldA tRNA gene of Streptomyces. Cell *66*, 769-780.

Flatt, P.M., and Mahmud, T. (2007). Biosynthesis of aminocyclitol-aminoglycoside antibiotics and related compounds. Nat Prod Rep *24*, 358-392.

Fujii, I., Watanabe, A., Sankawa, U., and Ebizuka, Y. (2001). Identification of Claisen cyclase domain in fungal polyketide synthase WA, a naphthopyrone synthase of Aspergillus nidulans. Chemistry & biology *8*, 189-197.

Goss, R.J., Shankar, S., and Fayad, A.A. (2012). The generation of "unnatural" products: synthetic biology meets synthetic chemistry. Nat Prod Rep *29*, 870-889.

Gregory, M.A., Petkovic, H., Lill, R.E., Moss, S.J., Wilkinson, B., Gaisser, S., Leadlay, P.F., and Sheridan, R.M. (2005). Mutasynthesis of rapamycin analogues through the manipulation of a gene governing starter unit biosynthesis. Angew Chem Int Ed Engl *44*, 4757-4760.

Gulick, A.M. (2009). Conformational dynamics in the Acyl-CoA synthetases, adenylation domains of non-ribosomal peptide synthetases, and firefly luciferase. ACS chemical biology *4*, 811-827.

Gummert, J.F., Ikonen, T., and Morris, R.E. (1999). Newer immunosuppressive drugs: a review. J Am Soc Nephrol *10*, 1366-1380.

Han, L., Lobo, S., and Reynolds, K.A. (1998). Characterization of beta-ketoacyl-acyl carrier protein synthase III from Streptomyces glaucescens and its role in initiation of fatty acid biosynthesis. J Bacteriol *180*, 4481-4486.

Hanessian, S., Vakiti, R.R., Chattopadhyay, A.K., Dorich, S., and Lavallee, C. (2013). Probing functional diversity in pactamycin toward antibiotic, antitumor, and antiprotozoal activity. Bioorg Med Chem *21*, 1775-1786.

Hanessian, S., Vakiti, R.R., Dorich, S., Banerjee, S., Lecomte, F., DelValle, J.R., Zhang, J., and Deschenes-Simard, B. (2011). Total synthesis of pactamycin. Angew Chem Int Ed Engl *50*, 3497-3500.

Hara, T., Niida, T., Sato, K., Kondo, S., Noguchi, T., and Kohmoto, K. (1964). A New Antibiotic, Cranomycin. The Journal of antibiotics *17*, 266.

Hart, G.W., Slawson, C., Ramirez-Correa, G., and Lagerlof, O. (2011). Cross talk between O-GlcNAcylation and phosphorylation: roles in signaling, transcription, and chronic disease. Annu Rev Biochem *80*, 825-858.

He, Y., Wang, Z., Bai, L., Liang, J., Zhou, X., and Deng, Z. (2010). Two pHZ1358-derivative vectors for efficient gene knockout in streptomyces. J Microbiol Biotechnol *20*, 678-682.

He, Q.L., Jia, X.Y., Tang, M.C., Tian, Z.H., Tang, G.L., and Liu, W. (2009). Dissection of two acyl-transfer reactions centered on acyl-S-carrier protein intermediates for incorporating 5-chloro-6-methyl-O-methylsalicyclic acid into chlorothricin. Chembiochem *10*, 813-819.

Hirayama, A., Eguchi, T., and Kudo, F. (2013). A single PLP-dependent enzyme PctV catalyzes the transformation of 3-dehydroshikimate into 3-aminobenzoate in the biosynthesis of pactamycin. Chembiochem *14*, 1198-1203.

Hosted, T.J., Wang, T.X., Alexander, D.C., and Horan, A.C. (2001). Characterization of the biosynthetic gene cluster for the oligosaccharide antibiotic, Evernimicin, in Micromonospora carbonacea var. africana ATCC39149. Journal of industrial microbiology & biotechnology *27*, 386-392.

Huguet-Tapia, J.C., and Loria, R. (2012). Draft genome sequence of Streptomyces acidiscabies 84-104, an emergent plant pathogen. J Bacteriol *194*, 1847.

Hunter, W.N. (2011). Isoprenoid precursor biosynthesis offers potential targets for drug discovery against diseases caused by apicomplexan parasites. Curr Top Med Chem *11*, 2048-2059.

Hurley, T.R., Smitka, T.A., Wilton, J.H., Bunge, R.H., Hokanson, G.C., and French, J.C. (1986). PD-113,618 AND PD-118,309, NEW PACTAMYCIN ANALOGS. J Antibiot *39*, 1086-1091.

Ishikawa, J., and Hotta, K. (1999). FramePlot: a new implementation of the frame analysis for predicting protein-coding regions in bacterial DNA with a high G + C content. FEMS microbiology letters *174*, 251-253.

Ito, T., Roongsawang, N., Shirasaka, N., Lu, W., Flatt, P.M., Kasanah, N., Miranda, C., and Mahmud, T. (2009). Deciphering pactamycin biosynthesis and engineered production of new pactamycin analogues. Chembiochem *10*, 2253-2265.

Iwatsuki, M., Nishihara-Tsukashima, A., Ishiyama, A., Namatame, M., Watanabe, Y., Handasah, S., Pranamuda, H., Marwoto, B., Matsumoto, A., Takahashi, Y.*, et al.* (2012). Jogyamycin, a new antiprotozoal aminocyclopentitol antibiotic, produced by Streptomyces sp. a-WM-JG-16.2. The Journal of antibiotics.

Jenner, M., Afonso, J.P., Bailey, H.R., Frank, S., Kampa, A., Piel, J., and Oldham, N.J. (2015). Acyl-Chain Elongation Drives Ketosynthase Substrate Selectivity in trans-Acyltransferase Polyketide Synthases. Angewandte Chemie (International ed *54*, 1817-1821.

Jia, X.Y., Tian, Z.H., Shao, L., Qu, X.D., Zhao, Q.F., Tang, J., Tang, G.L., and Liu, W. (2006). Genetic characterization of the chlorothricin gene cluster as a model for spirotetronate antibiotic biosynthesis. Chemistry & biology *13*, 575-585.

Kampfer, P. (2006) The Family Streptomycetaceae, Part I: Taxonomy. In: Dworkin, M., Falkow, S., Rosenberg, E., Schleifer, K.-H. and Stackebrandt, E., Eds., The Prokaryotes, 3rd Edition, Springer Science + Business Media, LLC, New York, 538-604.

Kato, J.Y., Funa, N., Watanabe, H., Ohnishi, Y., and Horinouchi, S. (2007). Biosynthesis of gamma-butyrolactone autoregulators that switch on secondary metabolism and morphological development in Streptomyces. Proc Natl Acad Sci U S A *104*, 2378-2383.

Kieser, T., Bibb, M.J., Buttner, M.J., Chater, K.F., and Hopwood, D.A. (2000). "Practical Streptomyces Genetics". The John Innes Foundation *Norwich*, England.

Kirkpatrick, P., Raja, A., LaBonte, J., and Lebbos, J. (2003). Daptomycin. Nat Rev Drug Discov *2*, 943-944.

Kondo, S.I., Shimura, M., Sezaki, M., Sato, K., and Hara, T. (1964). Isolation and Characterization of Cranomycin, a New Antibiotic. The Journal of antibiotics *17*, 230-233.

Kudo, F., Kasama, Y., Hirayama, T., and Eguchi, T. (2007a). Cloning of the pactamycin biosynthetic gene cluster and characterization of a crucial glycosyltransferase prior to a unique cyclopentane ring formation. The Journal of antibiotics *60*, 492-503.

Li, J.W., and Vederas, J.C. (2009). Drug discovery and natural products: end of an era or an endless frontier? Science (New York, NY *325*, 161-165.

Liu, G., Chater, K.F., Chandra, G., Niu, G., and Tan, H. (2013). Molecular regulation of antibiotic biosynthesis in streptomyces. Microbiol Mol Biol Rev *77*, 112-143.

Lu, W., Roongsawang, N., and Mahmud, T. (2011). Biosynthetic studies and genetic engineering of pactamycin analogs with improved selectivity toward malarial parasites. Chemistry & biology *18*, 425-431.

Malinowski, J.T., Sharpe, R.J., and Johnson, J.S. (2013). Enantioselective synthesis of pactamycin, a complex antitumor antibiotic. Science *340*, 180-182.

Mankin, A.S. (1997). Pactamycin resistance mutations in functional sites of 16S rRNA. J Mol Biol *274*, 8-15.

Manzoni, M., and Rollini, M. (2002). Biosynthesis and biotechnological production of statins by filamentous fungi and application of these cholesterol-lowering drugs. Appl Microbiol Biotechnol *58*, 555-564.

Mao, Y., Varoglu, M., and Sherman, D.H. (1999). Genetic localization and molecular characterization of two key genes (mitAB) required for biosynthesis of the antitumor antibiotic mitomycin C. Journal of bacteriology *181*, 2199-2208.

Miyadoh S (1993) Research on antibiotic screening in Japan over the last decade: A producing microorganisms approach. Actinomycetologica 9, 100-106.

Moore, B.S., and Hopke, J.N. (2001). Discovery of a new bacterial polyketide biosynthetic pathway. Chembiochem *2*, 35-38.

Newman, D.J., and Cragg, G.M. (2012). Natural products as sources of new drugs over the 30 years from 1981 to 2010. J Nat Prod *75*, 311-335.

Norris, K.L., Lee, J.Y., and Yao, T.P. (2009). Acetylation goes global: the emergence of acetylation biology. Sci Signal *2*, pe76.

Olano, C., Mendez, C., and Salas, J.A. (2009). Antitumor compounds from marine actinomycetes. Mar Drugs *7*, 210-248.

Onaka, H., Ando, N., Nihira, T., Yamada, Y., Beppu, T., and Horinouchi, S. (1995). Cloning and characterization of the A-factor receptor gene from Streptomyces griseus. J Bacteriol *177*, 6083-6092.

Ortholand, J.-Y., and Ganesan, A. (2004). Natural products and combinatorial chemistry: back to the future. Current Opinion in Chemical Biology *8*, 271-280.

Otoguro, K., Iwatsuki, M., Ishiyama, A., Namatame, M., Nishihara-Tukashima, A., Shibahara, S., Kondo, S., Yamada, H., and Omura, S. (2010). Promising lead compounds for novel antiprotozoals. The Journal of antibiotics *63*, 381-384.

Paget, M.S., Chamberlin, L., Atrih, A., Foster, S.J., and Buttner, M.J. (1999). Evidence that the extracytoplasmic function sigma factor sigmaE is required for normal cell wall structure in Streptomyces coelicolor A3(2). J Bacteriol *181*, 204-211.

Ramirez, M.S., and Tolmasky, M.E. (2010). Aminoglycoside modifying enzymes. Drug resistance updates : reviews and commentaries in antimicrobial and anticancer chemotherapy *13*, 151-171.

Rinehart, K.L. (1977). Mutasynthesis of new antibiotics. Pure and Appi Chem *49*, 1361-1384.

Rinehart, K.L., Jr., Potgieter, M., and Delaware, D.L. (1981). Direct evidence from multiple 13C labeling and homonuclear decoupling for the labeling pattern by glucose of the m-aminobenzoyl (C7N) unit of pactamycin. J Am Chem Soc *103*, 2099-2101.

Rinehart, K.L., Weller, D.D., and Pearce, C.J. (1980). Recent Biosynthetic-Studies on Antibiotics. J Nat Prod *43*, 1-20.

Roberts and M. Wink (1998) Alkaloids: biochemistry, ecology, and medicinal applications, 11–44. Plenum, New York, New York, USA.

Rui, Z., Ye, M., Wang, S., Fujikawa, K., Akerele, B., Aung, M., Floss, H.G., Zhang, W., and Yu, T.W. (2012). Insights into a divergent phenazine biosynthetic pathway governed by a plasmid-born esmeraldin gene cluster. Chemistry & biology *19*, 1116-1125.

Sacchettini, J.C., and Poulter, C.D. (1997). Creating isoprenoid diversity. Science (New York, NY *277*, 1788-1789.

Sambrook, J., and Russell, D.W. (2001). Molecular Cloning. A Laboratory Manual, Third edn (New York: Cold Spring Harbor Laboratory Press).

Saxena, P., Yadav, G., Mohanty, D., and Gokhale, R.S. (2003). A new family of type III polyketide synthases in Mycobacterium tuberculosis. J Biol Chem *278*, 44780-44790.

Seshime, Y., Juvvadi, P.R., Fujii, I., and Kitamoto, K. (2005). Discovery of a novel superfamily of type III polyketide synthases in Aspergillus oryzae. Biochem Biophys Res Commun *331*, 253-260.

Shier, W.T., Rinehart, K.L., Jr., and Gottlieb, D. (1969). Preparation of four new antibiotics from a mutant of Streptomyces fradiae. Proc Natl Acad Sci U S A *63*, 198-204.

Singh, B., Lee, C.B., and Sohng, J.K. (2010). Precursor for biosynthesis of sugar moiety of doxorubicin depends on rhamnose biosynthetic pathway in Streptomyces peucetius ATCC 27952. Appl Microbiol Biotechnol *85*, 1565-1574.

Sola-Landa, A., Moura, R.S., and Martin, J.F. (2003). The two-component PhoR-PhoP system controls both primary metabolism and secondary metabolite biosynthesis in Streptomyces lividans. Proc Natl Acad Sci U S A *100*, 6133-6138.

Staunton, J., and Wilkinson, B. (1997). Biosynthesis of Erythromycin and Rapamycin. Chem Rev *97*, 2611-2630.

Sun, Y., Zhou, X., Liu, J., Bao, K., Zhang, G., Tu, G., Kieser, T., and Deng, Z. (2002). 'Streptomyces nanchangensis', a producer of the insecticidal polyether antibiotic nanchangmycin and the antiparasitic macrolide meilingmycin, contains multiple polyketide gene clusters. Microbiology *148*, 361-371.

Taber, R., Rekosh, D., and Baltimore, D. (1971). Effect of pactamycin on synthesis of poliovirus proteins: a method for genetic mapping. J Virol *8*, 395-401.

Takeda, D., Okuno, S., Ohashi, Y., and Furumai, T. (1978). Mutational biosynthesis of butirosin analogs. I. Conversion of neamine analogs into butirosin analogs by mutants of Bacillus circulans. J Antibiot (Tokyo) *31*, 1023-1030.

Tian, F., Migaud, M.E., and Frost, J.W. (1999). myo-Inositol 1-Phosphate Synthase: Does a Single Active-Site Amino Acid Catalyze Multiple Proton Transfers? Journal of the American Chemical Society *121*, 5795-5796.

Trager, W., and Jensen, J.B. (1976). Human malaria parasites in continuous culture. Science *193*, 673-675.

Van Wezel, G.P., McKenzie, N.L., and Nodwell, J.R. (2009). Chapter 5. Applying the genetics of secondary metabolism in model actinomycetes to the discovery of new antibiotics. Methods Enzymol *458*, 117-141.

Vazquez, D. (1979). Inhibitors of protein biosynthesis. Mol Biol Biochem Biophys *30*, i-x, 1-312.

Weber, T., Charusanti, P., Musiol-Kroll, E.M., Jiang, X., Tong, Y., Kim, H.U., and Lee, S.Y. (2015). Metabolic engineering of antibiotic factories: new tools for antibiotic production in actinomycetes. Trends Biotechnol *33*, 15-26.

Weitnauer, G., Muhlenweg, A., Trefzer, A., Hoffmeister, D., Sussmuth, R.D., Jung, G., Welzel, K., Vente, A., Girreser, U., and Bechthold, A. (2001). Biosynthesis of the orthosomycin antibiotic avilamycin A: deductions from the molecular analysis of the avi biosynthetic gene cluster of Streptomyces viridochromogenes Tu57 and production of new antibiotics. Chemistry & biology *8*, 569-581.

Weller, D.D., Haber, A., Rinehart, K.L., and Wiley, P.F. (1978). C^{-13} Nuclear magnetic-resonance assignments of pactamycin and related compounds. J Antibiot *31*, 997-1006.

Weller, D.D., and Rinehart, K.L. (1978). Biosynthesis of the antitumor antibiotic pactamycin. A methionine-derived ethyl group and a C7N unit. J Am Chem Soc *100*, 6757-6760.

Wettenhall, R.E.H., and Wool, I.G. (1974). Reassociation of eukaryotic ribosomal-subunits - dependence of reassociation on formation of a 40s initiation complex - effects of aurintricarboxylic acid and pactamycin. Life Sci *14*, 1667-1677.

White, F.R. (1962). Pactamycin. Cancer chemotherapy reports *24*, 75-78.

Wiest, A., Grzegorski, D., Xu, B.W., Goulard, C., Rebuffat, S., Ebbole, D.J., Bodo, B., and Kenerley, C. (2002). Identification of peptaibols from Trichoderma virens and cloning of a peptaibol synthetase. J Biol Chem *277*, 20862-20868.

Wiley, P.F., Jahnke, H.K., Mackella.F, Kelly, R.B., and Argoudel.Ad (1970). Structure of pactamycin. journal of organic chemistry *35*, 1420-1425.

Wilson, D.N. (2014). Ribosome-targeting antibiotics and mechanisms of bacterial resistance. Nat Rev Microbiol *12*, 35-48.

Woodcock, J., Moazed, D., Cannon, M., Davies, J., and Noller, H.F. (1991). Interaction of antibiotics with a-site-specific and p-site-specific bases in 16S ribosomal-RNA. Embo J *10*, 3099-3103.

Xiao, Y., Li, S., Niu, S., Ma, L., Zhang, G., Zhang, H., Zhang, G., Ju, J., and Zhang, C. (2011). Characterization of tiacumicin B biosynthetic gene cluster affording diversified tiacumicin analogues and revealing a tailoring dihalogenase. Journal of the American Chemical Society *133*, 1092-1105.

Xu, H., Kahlich, R., Kammerer, B., Heide, L., and Li, S.M. (2003). CloN2, a novel acyltransferase involved in the attachment of the pyrrole-2-carboxyl moiety to the deoxysugar of clorobiocin. Microbiology *149*, 2183-2191.

Yu, T. W.; Bai, L.; Clade, D.; Hoffmann, D.; Toelzer, S.; Trinh, K. Q; XU, J.; Moss, S. J.; Leistner, E.; Floss, H. G. (2002). The biosynthetic gene cluster of the maytansinoid antitumor agent ansamitocin from Actinosynnema pretiosum. Proc Natl Acad Sci USA, *99* (12), 7968-73.

Ziegler, J., and Facchini, P.J. (2008). Alkaloid biosynthesis: metabolism and trafficking. Annu Rev Plant Biol *59*, 735-769.